

Evaluation of Corrosion Inhibitors

FINAL REPORT
October 1999

Submitted by
Dr. P. Balaguru
Professor

Center for Advanced Infrastructure & Transportation (CAIT)
Civil & Environmental Engineering
Rutgers, The State University
Piscataway, NJ 08854-8014



NJDOT Research Project Managers
Mr. Carey Younger & Mr. Robert Baker

In cooperation with

New Jersey
Department of Transportation
Division of Research and Technology
and
U.S. Department of Transportation
Federal Highway Administration

Disclaimer Statement

"The contents of this report reflect the views of the author(s) who is (are) responsible for the facts and the accuracy of the data presented herein. The contents do not necessarily reflect the official views or policies of the New Jersey Department of Transportation or the Federal Highway Administration. This report does not constitute a standard, specification, or regulation."

The contents of this report reflect the views of the authors, who are responsible for the facts and the accuracy of the information presented herein. This document is disseminated under the sponsorship of the Department of Transportation, University Transportation Centers Program, in the interest of information exchange. The U.S. Government assumes no liability for the contents or use thereof.

1. Report No. FHWA 2001-023	2. Government Accession No.	3. Recipient's Catalog No.	
4. Title and Subtitle Evaluation of Corrosion Inhibitors		5. Report Date October 1999	6. Performing Organization Code CAIT/Rutgers
		8. Performing Organization Report No. FHWA 2001-023	
7. Author(s) Dr. P. Balaguru	9. Performing Organization Name and Address New Jersey Department of Transportation CN 600 Trenton, NJ 08625		
12. Sponsoring Agency Name and Address Federal Highway Administration U.S. Department of Transportation Washington, D.C.		10. Work Unit No.	11. Contract or Grant No.
		13. Type of Report and Period Covered Final Report 06/27/1997 - 12/31/2000	
15. Supplementary Notes		14. Sponsoring Agency Code	
16. Abstract <p>Corrosion of reinforcement is a global problem that has been studied extensively. The use of good quality concrete and corrosion inhibitors seems to be an economical, effective, and logical solution, especially for new structures. A number of laboratory studies are available on the performance of various corrosion inhibiting admixtures. But studies on concrete used in the field are rare. A new bypass constructed by the New Jersey Department of Transportation provided a unique opportunity to evaluate the admixtures in the field. Five new bridge decks were used to evaluate four corrosion inhibiting admixtures.</p> <p>The concrete used in the four bridge decks had one of the following admixtures: DCI – S, XYPEX C-1000, Rheocrete 222+, Ferrogard901. All the admixtures are commercially available and used in the field. The fifth deck was used as a control. All the decks with admixtures had black steel where as the control deck had epoxy coated bars. Extra black steel bars were placed on the control deck.</p> <p>Both laboratory and field tests methods were used to evaluate the admixtures. The uniqueness of the study stems from the use of field concrete, obtained as the concrete for the individual bridge decks were placed. In addition to cylinder strength tests, minidecks were prepared for accelerated corrosion testing. The bridge decks were instrumented for long term corrosion monitoring. Tests to measure corrosion rate, corrosion potential, air permeability, and electrical resistance were used to determine the performance of the individual admixtures.</p> <p>The evaluation produced an overall best performing admixture though the differences in the overall performance of the admixtures were not significant. The admixtures were ranked from best to worst in corrosion protection for each test.</p> <p>In terms of scientific observations, xypex provides a denser concrete. If the concrete can be kept free of cracks this product will minimize the ingress of liquids reducing corrosion. The other three provides a protection to reinforcement by providing a barrier, reducing the effect of chlorides or both. In order to distinguish the differences the study should continue as explained in the following recommendation section.</p>			
17. Key Words corrosion, reinforcement, inhibitor, minideck, admixture, bridge deck, protection, chloride, barrier		18. Distribution Statement	
19. Security Classif (of this report) Unclassified	20. Security Classif. (of this page) Unclassified	21. No of Pages 163	22. Price

Executive Summary

Corrosion of reinforcement is a global problem that has been studied extensively. The use of good quality concrete and corrosion inhibitors seems to be an economical, effective, and logical solution, especially for new structures. A number of laboratory studies are available on the performance of various corrosion inhibiting admixtures. But studies on concrete used in the field are rare. A new bypass constructed by the New Jersey Department of Transportation provided a unique opportunity to evaluate the admixtures in the field. Five new bridge decks were used to evaluate four corrosion inhibiting admixtures.

The concrete used in the four bridge decks had one of the following admixtures: DCI - S, XYPEX C-1000, Rheocrete 222+, Ferrogard 901. All the admixtures are commercially available and used in the field. The fifth deck was used as a control. All the decks with admixtures had black steel where as the control deck had epoxy coated bars. Extra black steel bars were placed on the control deck.

Both laboratory and field tests methods were used to evaluate the admixtures. The uniqueness of the study stems from the use of field concrete, obtained as the concrete for the individual bridge decks were placed. In addition to cylinder strength tests, minidecks were prepared for accelerated corrosion testing. The bridge decks were instrumented for long term corrosion monitoring. Tests to measure corrosion rate, corrosion potential, air permeability, and electrical resistance were performed at regular periods throughout the year. Data obtained from the laboratory and field such as corrosion rate, corrosion potential, air permeability, and electrical resistance were used to determine the performance of the individual admixtures.

The evaluation produced an overall best performing admixture though the differences in the overall performances of the admixtures were not significant. The admixtures were ranked from best to worst in corrosion protection for each test.

In terms of scientific observations, xypex provides a denser concrete. If the concrete can be kept free of cracks this product will minimize the ingress of liquids reducing corrosion. The other three provides a protection to reinforcement by providing a barrier, reducing the effect of chlorides or both. In order to distinguish the differences the study should continue as explained in the following recommendation section.

Recommendations

Since the study was tied with the construction of 133, the time schedule had to be altered. The test samples were prepared using the field concrete and hence the start of the experiments were delayed more than 4 months. In order to obtain distinguishable differences the laboratory accelerated test should continue for at least another 6 months.

The instrumentation in the field is working well. The original proposal had a provision to continue the measurements by NJDOT. A proposal is written to facilitate the continuation of field measurements for at least 2 years. Note that the bridges are not open to traffic. At least two winters under loading are needed to obtain meaningful readings.

Acknowledgements

The authors gratefully acknowledges the support provided by NJDOT and the cooperation of Mr. Carey Younger and Mr. Robert Baker. The encouragement and contribution of Professor Ali Maher, Chairman and Director of CAIT are acknowledged with thanks.

The contribution of the following graduate students and Mr. Edward Wass are also acknowledged.

Mr. Nicholas Wong

Mr. Anand Bhatt

Mr. Hemal Shah

Mr. Yubun Auyeung

Table of Contents

	Page
Title Page	i
Abstract	ii
Acknowledgements	iv
Table of Contents	vi
List of Tables	viii
List of Figures	xi
1. Introduction	1
2. Background Information	3
3. Experimental Program	6
3.1 Test Variables	8
3.2 Test Methods	12
3.2.1 GECOR 6 Corrosion Rate Meter	12
3.2.2 Surface Air Flow Field Permeability Indicator	17
3.2.3 Electrical Resistance Test for Penetrating Sealers	25
3.2.4 Standard Test Method for Determining the Effects of Chemical Admixtures on the Corrosion of Embedded Steel Reinforcement in Concrete Exposed to Chloride Environments - ASTM G 109	28
3.3 Instrumentation for Field Tests	31
3.4 Specimen Preparation for Laboratory Tests	65
4. Results and Discussion	70
4.1.1 North Main Street Westbound: Laboratory Tests	71
4.1.2 North Main Street Westbound: Field Tests	74
4.2.1 North Main Street Eastbound: Laboratory Tests	82
4.2.2 North Main Street Eastbound: Field Tests	85
4.3.1 Wyckoff Road Westbound: Laboratory Tests	93
4.3.2 Wyckoff Road Westbound: Field Tests	96
4.4.1 Wyckoff Road Eastbound: Laboratory Tests	104

4.4.2 Wyckoff Road Eastbound: Field Tests	107
4.5.1 Route 130 Westbound: Laboratory Tests	115
4.5.2 Route 130 Westbound: Field Tests	118
4.6 Comparison of Corrosion Inhibiting Admixtures	127
5. Conclusions	143
6. Appendix	144
7. References	145

List of Tables

	Page
Table 3.1: Bridge Locations with Corresponding Corrosion Inhibiting Admixtures and Reinforcing Steel Type	8
Table 3.2: Mix Design of North Main Street – Westbound	9
Table 3.3: Mix Design of North Main Street – Eastbound	9
Table 3.4: Mix Design of Wyckoff Road – Westbound	10
Table 3.5: Mix Design of Wyckoff Road – Eastbound	10
Table 3.6: Mix Design of Route 130 – Westbound	11
Table 3.7: Interpretation of Corrosion Rate Data (Scannel, 1997)	16
Table 3.8: Interpretation of Half Cell (Corrosion) Potential Readings [ASTM C 876]	16
Table 3.9: Relative Concrete Permeability by Surface Air Flow	24
Table 3.10: Preliminary DC Testing of Gauge (Electrical Resistance Sealer Test)	27
Table 3.11: Minideck Sample Location, Admixture Type, and Designation.	69
Table 4.1: Fresh Concrete Properties	70
Table 4.2: Hardened Concrete Properties	70
Table 4.3: Minideck A - ASTM G 109 Corrosion Rate (A/cm^2)	71
Table 4.4: Minideck A - ASTM G 109 Corrosion Potential (mV)	71
Table 4.5: North Main Street Westbound GECOR 6 Corrosion Rate (A/cm^2)	74
Table 4.6: North Main Street Westbound GECOR 6 Corrosion Potential (mV)	75
Table 4.7: North Main Street Westbound GECOR 6 Electrical Resistance (K Ω)	75
Table 4.8: North Main Street Westbound Air Permeability Vacuum (mm Hg), SCCM (ml/min)	76
Table 4.9: North Main Street Westbound Electrical Resistance Sealer Test (K Ω)	76

Table 4.10: Minideck B - ASTM G 109 Corrosion Rate (A/cm^2)	82
Table 4.11: Minideck B - ASTM G 109 Corrosion Potential (mV)	82
Table 4.12: North Main Street Eastbound GECOR 6 Corrosion Rate (A/cm^2)	85
Table 4.13: North Main Street Eastbound GECOR 6 Corrosion Potential (mV)	86
Table 4.14: North Main Street Eastbound GECOR 6 Electrical Resistance (K Ω)	86
Table 4.15: North Main Street Eastbound Air Permeability Vacuum (mm Hg), SCCM (ml/min)	87
Table 4.16: North Main Street Eastbound Electrical Resistance Sealer Test (K Ω)	87
Table 4.17: Minideck C - ASTM G 109 Corrosion Rate (A/cm^2)	93
Table 4.18: Minideck C - ASTM G 109 Corrosion Potential (mV)	93
Table 4.19: Wyckoff Road Westbound GECOR 6 Corrosion Rate (A/cm^2)	96
Table 4.20: Wyckoff Road Westbound GECOR 6 Corrosion Potential (mV)	97
Table 4.21: Wyckoff Road Westbound GECOR 6 Electrical Resistance (K Ω)	97
Table 4.22: Wyckoff Road Westbound Air Permeability Vacuum (mm Hg), SCCM (ml/min)	98
Table 4.23: Wyckoff Road Westbound Electrical Resistance Sealer Test (K Ω)	98
Table 4.24: Minideck D - ASTM G 109 Corrosion Rate (A/cm^2)	104
Table 4.25: Minideck D - ASTM G 109 Corrosion Potential (mV)	104
Table 4.26: Wyckoff Road Eastbound GECOR 6 Corrosion Rate (A/cm^2)	107
Table 4.27: Wyckoff Road Eastbound GECOR 6 Corrosion Potential (mV)	108
Table 4.28: Wyckoff Road Eastbound GECOR 6 Electrical Resistance (K Ω)	108
Table 4.29: Wyckoff Road Eastbound Air Permeability Vacuum (mm Hg), SCCM (ml/min)	109
Table 4.30: Wyckoff Road Eastbound Electrical Resistance Sealer Test (K Ω)	109
Table 4.31: Minideck E - ASTM G 109 Corrosion Rate (A/cm^2)	115

Table 4.32: Minideck E - ASTM G 109 Corrosion Potential (mV)	115
Table 4.33: Route 130 Westbound GECOR 6 Corrosion Rate (A/cm ²)	118
Table 4.34: Route 130 Westbound GECOR 6 Corrosion Potential (mV)	119
Table 4.35: Route 130 Westbound GECOR 6 Electrical Resistance (KΩ)	120
Table 4.36: Route 130 Westbound Air Permeability Vacuum (mm Hg), SCCM (ml/min)	121
Table 4.37: Route 130 Westbound Electrical Resistance Sealer Test (KΩ)	121
Table 4.38: Ranked Results of Evaluation	140
Table 4.39: Points Evaluation of Corrosion Inhibiting Admixtures	141
Table 6.1: Interpretation of Corrosion Rate Data (Scannell, 1996)	144
Table 6.2: Interpretation of Half Cell (Corrosion) Potential Readings [ASTM C 876]	144
Table 6.3: Relative Concrete Permeability by Surface Air Flow (<u>Manual for the Operation of a Surface Air Flow Permeability Indicator</u> , 1994)	144

List of Figures

	Page
Fig. 3.1: Components of the GECOR 6 Corrosion Rate Meter	13
Fig. 3.2: GECOR 6 Corrosion Rate Meter Sensor with Sponge	13
Fig. 3.3: Surface Air Flow Field Permeability Indicator (Front View)	18
Fig. 3.4: Surface Air Flow Field Permeability Indicator (Front View)	19
Fig. 3.5: Surface Air Flow Field Permeability Indicator (Top View of Digital Displays)	20
Fig. 3.6: Drawing of Concrete Surface Air Flow Permeability Indicator	21
Fig. 3.7: Schematic of Concrete Surface Air Flow Permeability Indicator	22
Fig. 3.8: Strips of Silver Conductive Paint	25
Fig. 3.9: Equipment Required for Electrical Resistance Test for Penetrating Sealers	26
Fig. 3.10: View of Concrete Minideck	29
Fig. 3.11: Locations of GECOR 6 Corrosion Rate Meter Tests North Main Street Westbound	33
Fig. 3.12: Locations of GECOR 6 Corrosion Rate Meter Tests North Main Street Eastbound	34
Fig. 3.13: Locations of GECOR 6 Corrosion Rate Meter Tests Wyckoff Road Westbound	35
Fig. 3.14: Locations of GECOR 6 Corrosion Rate Meter Tests Wyckoff Road Eastbound	36
Fig. 3.15: Locations of GECOR 6 Corrosion Rate Meter Tests Route 130 Westbound	37
Fig. 3.16: Locations of Uncoated Steel Reinforcement Bars on Route 130 Westbound	38
Fig. 3.17: Insulated Copper Underground Feeder Cables	39
Fig. 3.18: Connection to North Main Street Westbound	40

Fig. 3.19: Connection to North Main Street Eastbound	41
Fig. 3.20: Connection to Wyckoff Road Westbound	42
Fig. 3.21: Connection to Wyckoff Road Eastbound	43
Fig. 3.22: Connection to Route 130 Westbound	44
Fig. 3.23: Conduits and Enclosure – North Main Street Westbound	45
Fig. 3.24: Conduits and Enclosure – North Main Street Eastbound	45
Fig. 3.25: Conduits and Enclosure – Wyckoff Road Westbound	46
Fig. 3.26: Conduits and Enclosure – Wyckoff Road Eastbound	46
Fig. 3.27: Conduits and Enclosure – Route 130 Westbound	47
Fig. 3.28: Vibrating of Fresh Concrete at North Main Street Eastbound	48
Fig. 3.29: Placement on Fresh Concrete at North Main Street Westbound	48
Fig. 3.30: View of Connections at North Main Street Westbound during Concrete Placement	49
Fig. 3.31: Bridge Deck over North Main Street Westbound near Completion	50
Fig. 3.32: Bridge Deck over North Main Street Eastbound near Completion	50
Fig. 3.33: Bridge Deck over Wyckoff Road Westbound near Completion	51
Fig. 3.34: Bridge Deck over Wyckoff Road Eastbound near Completion	51
Fig. 3.35: Bridge Deck over Route 130 Westbound near Completion	52
Fig. 3.36: Locations of Surface Air Flow Field Permeability Indicator Readings North Main Street Westbound	54
Fig. 3.37: Locations of Surface Air Flow Field Permeability Indicator Readings North Main Street Eastbound	55
Fig. 3.38: Locations of Surface Air Flow Field Permeability Indicator Readings Wyckoff Road Westbound	56

Fig. 3.39: Locations of Surface Air Flow Field Permeability Indicator Readings Wyckoff Road Westbound	57
Fig. 3.40: Locations of Surface Air Flow Field Permeability Indicator Readings Route 130 Westbound	58
Fig. 3.41: Locations of Electrical Resistance Tests North Main Street Westbound	60
Fig. 3.42: Locations of Electrical Resistance Tests North Main Street Eastbound	61
Fig. 3.43: Locations of Electrical Resistance Tests Wyckoff Road Westbound	62
Fig. 3.44: Locations of Electrical Resistance Tests Wyckoff Road Eastbound	63
Fig. 3.45: Locations of Electrical Resistance Tests Route 130 Westbound	64
Fig. 3.46: Prepared Minideck Mold	65
Fig. 3.47: Minideck after Removal from Mold	66
Fig. 3.48: View of Plexiglas Dam	67
Fig. 3.49: Poned Minideck Samples	68
Fig. 4.1: Minideck A - Average Corrosion Rate Macrocell Current (μA)	72
Fig. 4.2: Minideck A - Average Corrosion Potential (mV)	72
Fig. 4.3: North Main Street Westbound GECOR 6 Average Corrosion Rate Macrocell Current (μA)	77
Fig. 4.4: North Main Street Westbound GECOR 6 Average Corrosion Potential (mV)	78
Fig. 4.5: North Main Street Westbound GECOR 6 Average Electrical Resistance AC ($\text{K}\Omega$)	79
Fig. 4.6: North Main Street Westbound Average Air Flow Rate (ml/min)	80
Fig. 4.7: North Main Street Westbound Average Electrical Resistance AC ($\text{K}\Omega$)	81
Fig. 4.8: Minideck B - Average Corrosion Rate Macrocell Current (μA)	83
Fig. 4.9: Minideck B - Average Corrosion Potential (mV)	84

Fig. 4.10: North Main Street Eastbound Average Corrosion Rate Macrocell Current (μA)	88
Fig. 4.11: North Main Street Eastbound GECOR 6 Average Corrosion Potential (mV)	89
Fig. 4.12: North Main Street Eastbound GECOR 6 Average Electrical Resistance AC ($\text{K}\Omega$)	90
Fig. 4.13: North Main Street Eastbound Average Air Flow Rate (ml/min)	91
Fig. 4.14: North Main Street Eastbound Average Electrical Resistance AC ($\text{K}\Omega$)	92
Fig. 4.15: Minideck C - Average Corrosion Rate Macrocell Current (μA)	94
Fig. 4.16: Minideck C - Average Corrosion Potential (mV)	95
Fig. 4.17: Wyckoff Road Westbound GECOR 6 Average Corrosion Rate Macrocell Current (μA)	99
Fig. 4.18: Wyckoff Road Westbound GECOR 6 Average Corrosion Potential (mV)	100
Fig. 4.19: Wyckoff Road Westbound GECOR 6 Average Electrical Resistance AC ($\text{K}\Omega$)	101
Fig. 4.20: Wyckoff Road Westbound Average Air Flow Rate (ml/min)	102
Fig. 4.21: Wyckoff Road Westbound Average Electrical Resistance AC ($\text{K}\Omega$)	103
Fig. 4.22: Minideck D - Average Corrosion Rate Macrocell Current (μA)	105
Fig. 4.23: Minideck D - Average Corrosion Potential (mV)	106
Fig. 4.24: Wyckoff Road Eastbound GECOR 6 Average Corrosion Rate Macrocell Current (μA)	110
Fig. 4.25: Wyckoff Road Eastbound GECOR 6 Average Corrosion Potential (mV)	111
Fig. 4.26: Wyckoff Road Eastbound GECOR 6 Average Electrical Resistance AC ($\text{K}\Omega$)	112
Fig. 4.27: Wyckoff Road Westbound Average Air Flow Rate (ml/min)	113

Fig. 4.28: Wyckoff Road Eastbound Average Electrical Resistance AC ($K\Omega$)	114
Fig. 4.29: Minideck E - Average Corrosion Rate Macrocell Current (μA)	116
Fig. 4.30: Minideck E - Average Corrosion Potential (mV)	117
Fig. 4.31: Route 130 Westbound GECOR 6 Average Corrosion Rate Macrocell Current (μA)	122
Fig. 4.32: Route 130 Westbound GECOR 6 Average Corrosion Potential (mV)	123
Fig. 4.33: Route 130 Westbound GECOR 6 Average Electrical Resistance AC ($K\Omega$)	124
Fig. 4.34: Wyckoff Road Westbound Average Air Flow Rate (ml/min)	125
Fig. 4.35: Route 130 Westbound Average Electrical Resistance AC ($K\Omega$)	126
Fig. 4.36: Comparison of Corrosion Inhibitors Minideck Average Corrosion Rate Macrocell Current (μA)	128
Fig. 4.37: Comparison of Corrosion Inhibitors Minideck Average Corrosion Potential (mV)	129
Fig. 4.38: Comparison of Corrosion Inhibitors GECOR 6 Average Corrosion Rate Macrocell Current (μA)	130
Fig. 4.39: Comparison of Corrosion Inhibitors GECOR 6 Average Corrosion Potential (mV)	131
Fig. 4.40: Comparison of Corrosion Inhibitors GECOR 6 Average Electrical Resistance AC ($K\Omega$)	132
Fig. 4.41: Comparison of Corrosion Inhibitors Average Air Flow Rate (ml/min)	133
Fig. 4.42: Comparison of Corrosion Inhibitors Average Electrical Resistance AC ($K\Omega$)	134

1. Introduction

Corrosion of reinforcement is a global problem that has been studied extensively. Though the highly alkali nature of concrete normally protects reinforcing steel with the formation of a tightly adhering film which passivates the steel and protects it from corrosion, the harsh environment in the Northeastern United States and similar locations around the world accelerate the corrosion process. The major techniques used for reducing corrosion and preventing it to some extent are: (i) Use of concrete with least permeability, (ii) Use of corrosion inhibitors, (iii) Use of epoxy coated bars, (iv) Surface protection of concrete, and (v) Cathodic protection of reinforcement. Use of nonmetallic reinforcement is one more technique to reduce corrosion, which is still in development stage.

The use of inhibitors to control the corrosion of concrete is a well established technology. Inhibitors are in effect any materials that are able to reduce the corrosion rates when present at relatively small concentrations at or near the steel surface. When correctly specified and applied by experienced professionals, inhibitors can be effective for use in both the repair of deteriorating concrete structures and enhancing the durability of new structures.

The use of good quality concrete and corrosion inhibitors seems to be an economical, effective, and logical solution, especially for new structures. The objective of this study is to determine the effectiveness of four different corrosion inhibitors to reduce corrosion of the structural steel reinforcement in a structure. The data is compared with the data obtained from structural steel reinforcement not protected by a corrosion

inhibiting admixture. Five of the bridge decks in Route 133, constructed during 1998, were selected for this study, each of which has one specific corrosion inhibitor except one, which did not contain any corrosion inhibiting admixtures. This bridge deck was used as a controlled deck for the comparison. The bridges were instrumented to measure the corrosion rates.

Since corrosion may not initiate for 10 to 15 years, accelerated corrosion tests in the laboratory were also used to evaluate these inhibitors. The accelerated corrosion study conducted in the laboratory will be used to predict the behavior of the actual structures. The proposed study is unique due to the fact that all the samples for laboratory testing are prepared using concrete delivered at the site and used in the actual structures.

2. Background Information

Steel reinforced concrete is one of the most durable and cost effective construction materials. The alkaline environment of the concrete passivates the steel resulting in negligible corrosion activity. However, concrete is often utilized in extreme environments in which it is subjected to exposure to chloride ions, which disrupt the passivity (Berke, 1995). Though corrosion inhibitors is one of the most practical and effective means to arrest the corrosion process in old and new reinforced concrete, the use of good quality concrete is also very significant in inhibiting corrosion. Concrete with low water to cement ratios can lower the amount of chloride ingress. Pozzolans such as silica-fume increases concrete resistivity and permeability to chloride (Berke, 1995).

The principle of most inhibitors is to develop a thin chemical layer usually one or two molecules thick on the steel surface that inhibits the corrosion attack. Inhibitors can prevent the cathodic reaction, the anodic reaction, or both. They are consumed and will only work up to a given level of attack. The chloride content of the concrete determines the level of attack (Broomfield, 1997).

There are a number of inhibitors offered in the market. They have different effects on the steel or the concrete to enhance the alkalinity, block the chloride and reduce the corrosion rate. Some are true corrosion inhibitors, some are hybrid inhibitors, pore blockers and alkali generators (Broomfield, 1997).

There are a number of ways inhibitors can be applied. Corrosion inhibiting admixtures are added to fresh concrete during the batching process. Other inhibitors can

be applied to the surface of hardened concrete. These migrating inhibitors are called vapour phase inhibitors. These are volatile compounds that can be incorporated into a number of carriers such as waxes, gels, and oils. In principle their ability to diffuse as a vapour gives them an advantage over liquid inhibitors. However, they could also diffuse out of the concrete unless trapped in place (Broomfield, 1997).

DCI – S developed by W.R. Grace & Co., XYPEX C-1000 developed by Quick-Wright Associates, Inc., Rheocrete 222+ developed by Master Builders, Inc., and Ferrogard 901 developed by Sika Corporation are all corrosion inhibiting admixtures for concrete and represent the state of the art in technology. These admixtures were evaluated for their performance as a means to reduce corrosion in new structures.

DCI – S corrosion inhibitor is a calcium nitrite-based solution. It is added to concrete during the batching process and effectively inhibits the corrosion of reinforcing steel and prestressed strands. According to W.R. Grace & Co., the admixture chemically reacts with the embedded metal to form a "passivating" oxide layer, which inhibits chloride attack of the fortified reinforcing steel. The addition of DCI - S to concrete delays the onset of corrosion, and reduces the corrosion rate once it has begun. DCI - S is a neutral set (DCI – S Corrosion Inhibitor, 1997).

XYPEX C-1000 is a corrosion inhibitor, which is specially formulated as an additive for concrete at the time of batching. According to Quick-Wright Associates, Inc., the concrete itself becomes sealed against the penetration of water or liquid. The active chemicals in XYPEX C-1000 cause a catalytic reaction, which generates a non-soluble crystalline formation within the pores and capillary tracts of concrete preventing the penetration of water and liquids necessary to the corrosion process. XYPEX C-1000 may

delay the initial set time of the fresh concrete (XYPEX Concrete Waterproofing by Crystallization).

Rheocrete 222+ is a corrosion inhibiting admixture formulated to prevent the corrosion of steel reinforced concrete. According to Master Builders, Inc., Rheocrete 222+ can extend the service life of reinforced concrete in two ways. The admixture slows the ingress of chlorides and moisture, two elements involved in the corrosion process, by lining the pores of the concrete matrix. The admixture also slows the rate of corrosion by forming a protective film on the reinforcing steel depriving the corrosion process of oxygen and moisture. Rheocrete 222+ is added with the concrete batch water during the mixing process and does not require changes to the normal batching procedures (Rheocrete 222+: Organic Corrosion Inhibiting Admixture, 1995).

The Ferrogard 901 corrosion inhibitor admixture for fresh concrete, developed by the Sika Corporation, is based on an organic film forming amino compound that can diffuse through the pores of the concrete. The protective film that forms around the reinforcing steel is a protective layer that can protect the steel in both anodic and cathodic areas. According to Sika, this Ferrogard 901 suppresses the electrochemical corrosion reaction and shows no detrimental effects to the concrete (MacDonald, 1996).

3. Experimental Program

The primary objective of the research program is to evaluate the latest corrosion inhibiting admixtures for steel reinforced concrete using laboratory and field study. The accelerated corrosion study conducted in the laboratory will be used to predict the behavior of the actual structures. Data obtained during the first two to three years will be used to establish a correlation between laboratory and field performance.

The test variables are the four corrosion inhibiting admixtures used during the construction of the bridge decks on the Route 133 Hightstown Bypass and a control, which contained no corrosion inhibiting admixture.

The field evaluation consists of three tests: GECOR 6 Corrosion Rate Meter, Surface Air Flow Permeability Indicator, and Electrical Resistance Test for Penetrating Sealers. The results of these tests can be used to determine the physical characters as well as the corrosion protection provided by a particular admixture. The bridges were instrumented for corrosion testing and are periodically monitored for corrosion activity. The laboratory samples were tested using ASTM G 109. This accelerated process will give an early indication of the effectiveness of the admixtures. All the concrete samples were taken from the field as the concrete for the individual bridge decks was placed.

Fresh concrete was tested for workability and air content. Compressive strength was obtained at 28 days. The variables studied were corrosion rate, corrosion potential, air permeability, and electrical resistance.

An arbitrary point system will be used to determine the overall best performer. Each admixture including the control will be ranked from the best to worst in

performance in each test and given 5, 4, 3, 2, or 1 point, respectively. The resulting sum of all points will produce the best overall performer in corrosion protection.

3.1 Test Variables

During the course of this research program, four types of corrosion inhibiting admixtures as well as control specimens, with no corrosion inhibiting admixtures, were evaluated in laboratory and field tests. Table 3.1 lists the bridge locations on the new Route 133 Hightstown Bypass and the corresponding admixtures used on each bridge deck.

Table 3.1: Bridge Locations with Corresponding Corrosion Inhibiting Admixtures and Reinforcing Steel Type

Bridge Location	Corrosion Inhibiting Admixture	Type of Reinforcing Steel
North Main Street - Westbound	W.R. Grace: DCI - S	Black
North Main Street - Eastbound	Quick Wright Associates, Inc.: XYPEX C-1000	Black
Wyckoff Road - Westbound	Master Builders, Inc.: Rheocrete 222+	Black
Wyckoff Road - Eastbound	Sika Corporation: Ferrogard 901	Black
Route 130 - Westbound	Control: none	Epoxy Coated

The control concrete did not contain any corrosion inhibiting admixture. Epoxy coated steel was used in the reinforcement of the concrete deck unlike the other bridges tested which used uncoated black reinforcing steel.

The mix proportions for the five types of concrete used are presented in Tables 3.2, 3.3, 3.4, 3.5, and 3.6. The proportions were developed by the New Jersey Department of Transportation in accordance with ASTM C 94. From the Tables 3.2 to 3.6, it can be seen that the cement and aggregate contents remained the same for all the mixes. The water content was adjusted to account for water present in the admixtures.

Table 3.2: Mix Design of North Main Street - Westbound

Bridge Deck over North Main Street - Westbound	
Date of Deck Pour: May 6, 1998	
Cement (lbs)	700
Sand (lbs)	1346
¾ in. Aggregate (lbs)	1750
Water (gal)	29.3
W/C Ratio	0.38
Sika Corporation AER Air-Entraining Admixture ASTM C-150 (oz)	6.3
Sika Corporation Plastocrete 161 Water reducing Admixture Type "A" ASTM C 494 (oz)	21
W.R. Grace: DCI - S (gal)	3
Slump (inches)	3 ± 1
Air (%)	6 ± 1.5

Table 3.3: Mix Design of North Main Street - Eastbound

Bridge Deck over North Main Street - Eastbound	
Date of Deck Pour: May 14, 1998	
Cement (lbs)	700
Sand (lbs)	1346
¾ in. Aggregate (lbs)	1750
Water (gal)	31.8
W/C Ratio	0.38
Sika Corporation AER Air-Entraining Admixture ASTM C-150 (oz)	4.2
Sika Corporation Plastocrete 161 Water reducing Admixture Type "A" ASTM C 494 (oz)	21
Quick Wright Associates, Inc.: XYPEX C-1000 (lbs)	12
Slump (inches)	3 ± 1
Air (%)	6 ± 1.5

Table 3.4: Mix Design of Wyckoff Road - Westbound

Bridge Deck over Wyckoff Road- Westbound	
Date of Deck Pour: May 21, 1998	
Cement (lbs)	700
Sand (lbs)	1346
$\frac{3}{4}$ in. Aggregate (lbs)	1750
Water (gal)	31.8
W/C Ratio	0.38
Sika Corporation AER Air-Entraining Admixture ASTM C-150 (oz)	8.4
Sika Corporation Plastocrete 161 Water reducing Admixture Type "A" ASTM C 494 (oz)	21
Master Builders, Inc.: Rheocrete 222+ (gal)	1
Slump (inches)	3 \pm 1
Air (%)	6 \pm 1.5

Table 3.5: Mix Design of Wyckoff Road - Eastbound

Bridge Deck over Wyckoff Road - Eastbound	
Date of Deck Pour: May 27, 1998	
Cement (lbs)	700
Sand (lbs)	1346
$\frac{3}{4}$ in. Aggregate (lbs)	1750
Water (gal)	29.1
W/C Ratio	0.38
Sika Corporation AER Air-Entraining Admixture ASTM C-150 (oz)	4.2
Sika Corporation Plastocrete 161 Water reducing Admixture Type "A" ASTM C 494 (oz)	21
Sika Corporation: Ferrogard 901 (gal)	2
Slump (inches)	3 \pm 1
Air (%)	6 \pm 1.5

Table 3.6: Mix Design of Route 130 - Westbound

Bridge Deck over Route 130- Westbound	
Date of Deck Pour: May 29, 1998	
Cement (lbs)	700
Sand (lbs)	1346
¾ in. Aggregate (lbs)	1750
Water (gal)	31.8
W/C Ratio	0.38
Sika Corporation AER Air-Entraining Admixture ASTM C-150 (oz)	4.2
Sika Corporation Plastocrete 161 Water reducing Admixture Type "A" ASTM C 494 (oz)	21
Slump (inches)	3 ± 1
Air (%)	6 ± 1.5

3.2 Test Methods

The test procedures used are described in the following sections. The first three tests were conducted in the field where as the fourth one was conducted in the laboratory.

3.2.1 GECOR 6 Corrosion Rate Meter

The GECOR 6 Corrosion Rate Meter provides valuable insight into the kinematics of the corrosion process. Based on a steady state linear polarization technique it provides information on the rate of the deterioration process. The meter monitors the electrochemical process of corrosion to determine the rate of deterioration. This nondestructive technique works by applying a small current to the reinforcing bar and measuring the change in the half cell potential. The corrosion rate, corrosion potential, and electrical resistance are provided by the corrosion rate meter.

The GECOR 6 Corrosion Rate Meter has three major components, the rate meter and two separate sensors. Only the larger sensor was used during this project. The sensor is filled with a saturated Cu/CuSO₄ solution for the test for half cell potential. The main components of this device can be seen in Fig. 3.1. A wet sponge is used between the probe and the concrete surface as seen in Fig. 3.2. Long lengths of wire are also provided to connect the sensor to the rate meter and to connect the rate meter to the reinforcing bar mat of the bridge deck, a necessary step for the operation of the meter.



Fig. 3.1: Components of the GECOR 6 Corrosion Rate Meter

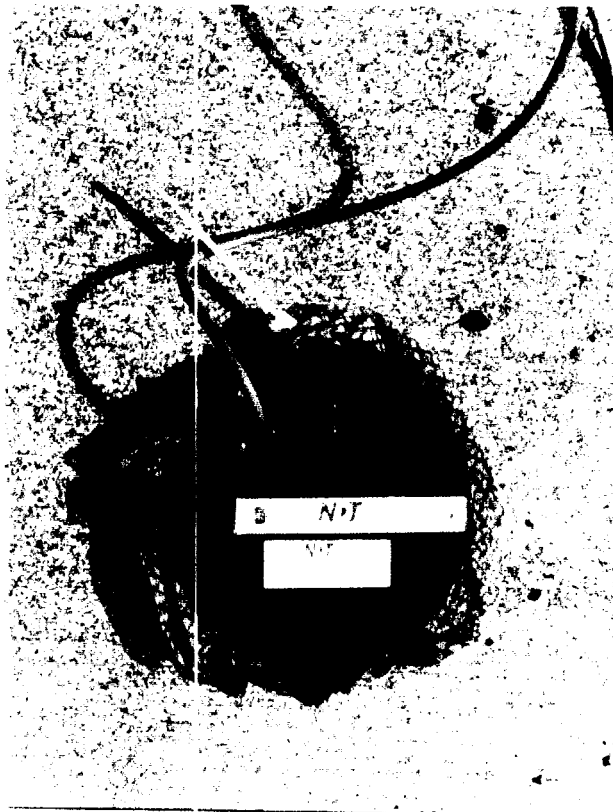


Fig. 3.2: GECOR 6 Corrosion Rate Meter Sensor with Sponge

The procedure for the operation of the GECOR 6 Corrosion Rate Meter is as follows (Scannell, 1996):

1. The device should not be operated at temperatures below 0 °C (32 °F) or above 50 C (122 °F). The relative humidity within the unit should not exceed 80%.
2. Use a reinforcing steel locator to define the layout at the test location. Mark the bar pattern on the concrete surface at the test location.
3. Place a wet sponge and the sensor over a single bar or over the point where the bars intersect perpendicularly if the diameter of both bars are known.
4. Connect the appropriate lead to an exposed bar. The leads from the sensor and exposed reinforcing steel are then connected to the GECOR device.
5. Turn on the unit. The program version appears on the display screen.

“LG-ECM-06 V2.0
© GEOCISA 1993”

6. A help message appears on the screen momentarily. This message advises the operator to use the arrows for selecting an option and C.R. to activate an option. The various options are:
 - “CORROSION RATE MEASUREMENT”
 - “REL.HUMIDITY AND TEMPERATURE”
 - “RESISTIVITY MEASUREMENT”
 - “EDIT MEASUREMENT PARAMETERS”
 - “DATAFILE SYSTEM EDITING”
 - “DATE AND TIME CONTROL”
7. Select the option CORROSION RATE MEASUREMENT and press the C.R. key.
8. The screen prompts the user to input the area of steel. Calculate the area of steel using the relationship, $\text{Area} = 3.142 \times D \times 10.5 \text{ cm}$. D is the diameter of the bar in centimeters and 10.5 cm (4 in.) is the length of the bar confined by the guard ring. Key in the area to one decimal space. In case of an error, use the B key to delete the previous character. Press the C.R. key to enter the area.
9. The next screen displays;

“ADJUSTING
OFFSET, WAIT”

No operator input is required at this stage. The meter measures the half cell potential and then nulls it out to measure the potential shift created by the current applied from the sensor.

10. The next screen displays:

“Er	mV OK”
“Vs	mV OK”

E_r (E_{CORR}) is the static half-cell potential versus CSE and V_s is the difference in potential between the reference electrodes which control the current confinement. Once the E_r and the V_s values are displayed. No input is required from the operator.

11. The meter now calculates the optimum applied current I_{CE} . This current is applied through the counter electrode at the final stage of the measurement. The optimum I_{CE} value is displayed. No input is required from the operator.
12. The next screen displays the polarized potential values. No input is required from the operator.
13. The meter now calculates the “balance constant” in order to apply the correct current to the guard ring. It is displayed on the next screen. No input is required from the operator.
14. The meter now calculates the corrosion rate using the data collected from the sensor and input from the operator. The corrosion rate is displayed in $\mu A/cm^2$. Associated parameters including corrosion potential, mV and electrical resistance $k\Omega$ can be viewed using the cursor keys.
15. Record the corrosion rate, corrosion potential, electrical resistance.
16. Press the B key to reset the meter for the next reading. The screen will return to CORROSION RATE MEASUREMENT. Repeat the procedure for the next test location.

The corrosion rate and corrosion potential data can be interpreted using Table 3.7 and 3.8, and Tables 6.1 and 6.2 in the Appendix, respectively. As also explained in the Chapter 3.2.3 for the Electrical Resistance Test for Penetrating Sealers, the higher the resistance the less potential for corrosion in the embedded steel due to the higher density of the concrete and improved insulation against the electrochemical process of corrosion.

Unlike the Electrical Resistance Test for Penetrating Sealers, the GECOR 6 penetrates the concrete surface for a greater area of measurement.

Table 3.7: Interpretation of Corrosion Rate Data (Scannell, 1997)

I_{CORR} ($\mu A/cm^2$)	Corrosion Condition
Less than 0.1	Passive Condition
0.1 to 0.5	Low to Moderate Corrosion
0.5 to 1.0	Moderate to High Corrosion
Greater than 1.0	High Corrosion

Table 3.8: Interpretation of Half Cell (Corrosion) Potential Readings (ASTM C 876)

Half Cell Potential (mV)	Corrosion Activity
-200 >	90% Probability of No Corrosion Occurring
-200 to -350	Corrosion Activity Uncertain
< -350	90% Probability of Corrosion Occurring

3.2.2 Surface Air Flow Field Permeability Indicator

The Concrete Surface Air Flow (SAF) Permeability Indicator is a nondestructive technique designed to give an indication of the relative permeability of flat concrete surfaces. The SAF can be utilized to determine the permeability of concrete slabs, support members, bridge decks, and pavement (Manual for the Operation of a Surface Air Flow Field Permeability Indicator, 1994). The concrete permeability is based on air flow out of the concrete surface under an applied vacuum. The depth of measurement was determined to be approximately 0.5 in. below the concrete surface. A study between the relationships between SAF readings and air and water permeability determined that there is good correlation in the results. As stated in the Participant's Workbook: FHWA – SHRP Showcase, (Scannell, 1996) the SAF should not be used as a substitute for actual laboratory permeability testing. Cores tested under more standardized techniques will provide a more accurate value for permeability due the fact that the effects of surface texture and microcracks have not been fully studied for the SAF.

The SAF can determine permeability of both horizontal surfaces, by use of an integral suction foot, and vertical surfaces, by use of external remote head. The remote head was not used for this project. A picture of the device and its accessories can be seen in Fig. 3.3 and Fig. 3.4. For transportability the device uses a rechargeable Ni-Cad battery. The suction foot is mounted using three centering springs to allow it to rotate and swivel in relation to the main body. A closed cell foam gasket is used between the foot and the testing surface to create an air tight seal. Two foot pads are threaded into the suction foot so the operator can apply pressure to compress the gasket. The switches to

open the solenoid and hold the current reading are located within easy reach at the base of the handles. Digital displays for the permeability readings and the time are located at the top of the device Fig. 3.5. Outline drawings of the device and its schematics can be seen on Fig. 3.6 and Fig. 3.7, respectively (Manual for the Operation of a Surface Air Flow Field Permeability Indicator, 1994)

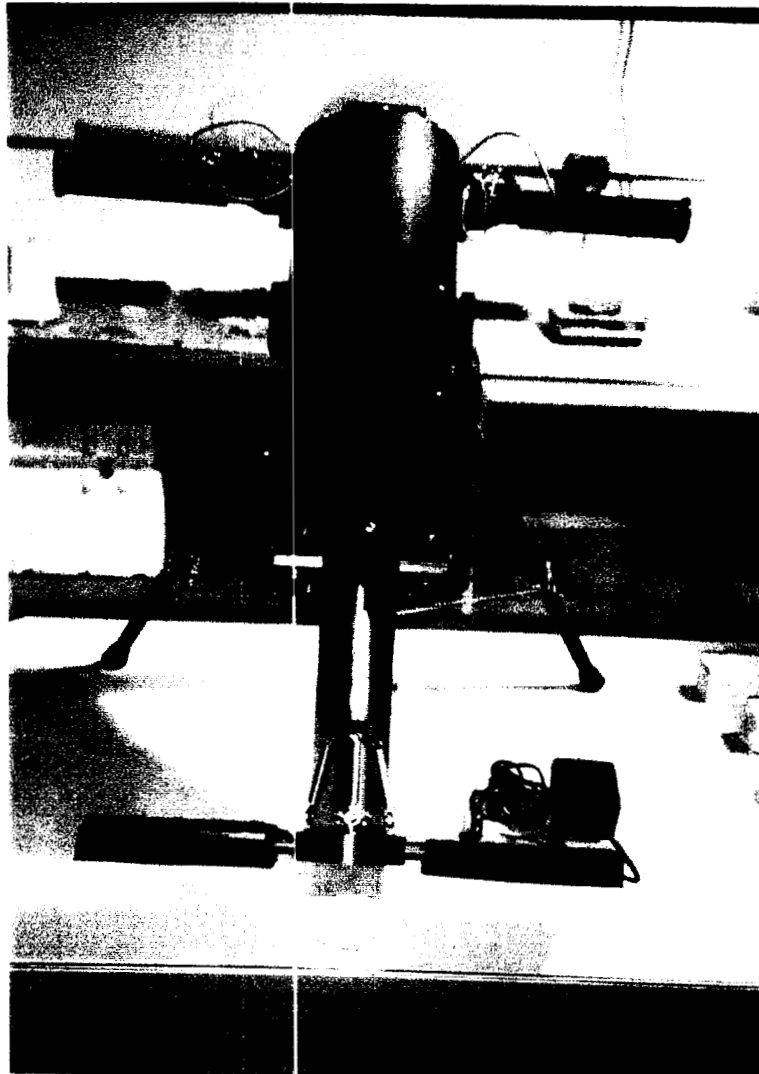


Fig. 3.3: Surface Air Flow Field Permeability Indicator (Front View)



Fig. 3.4: Surface Air Flow Field Permeability Indicator (Front View)

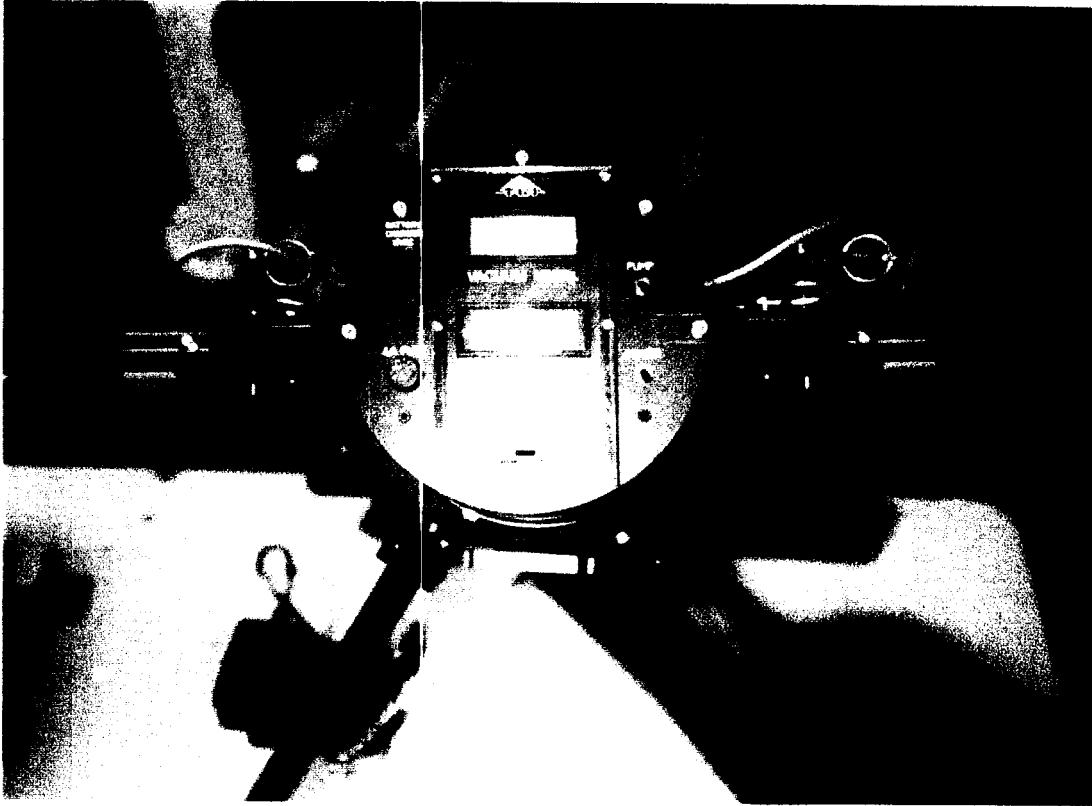


Fig. 3.5: Surface Air Flow Field Permeability Indicator
(Top View of Digital Displays)

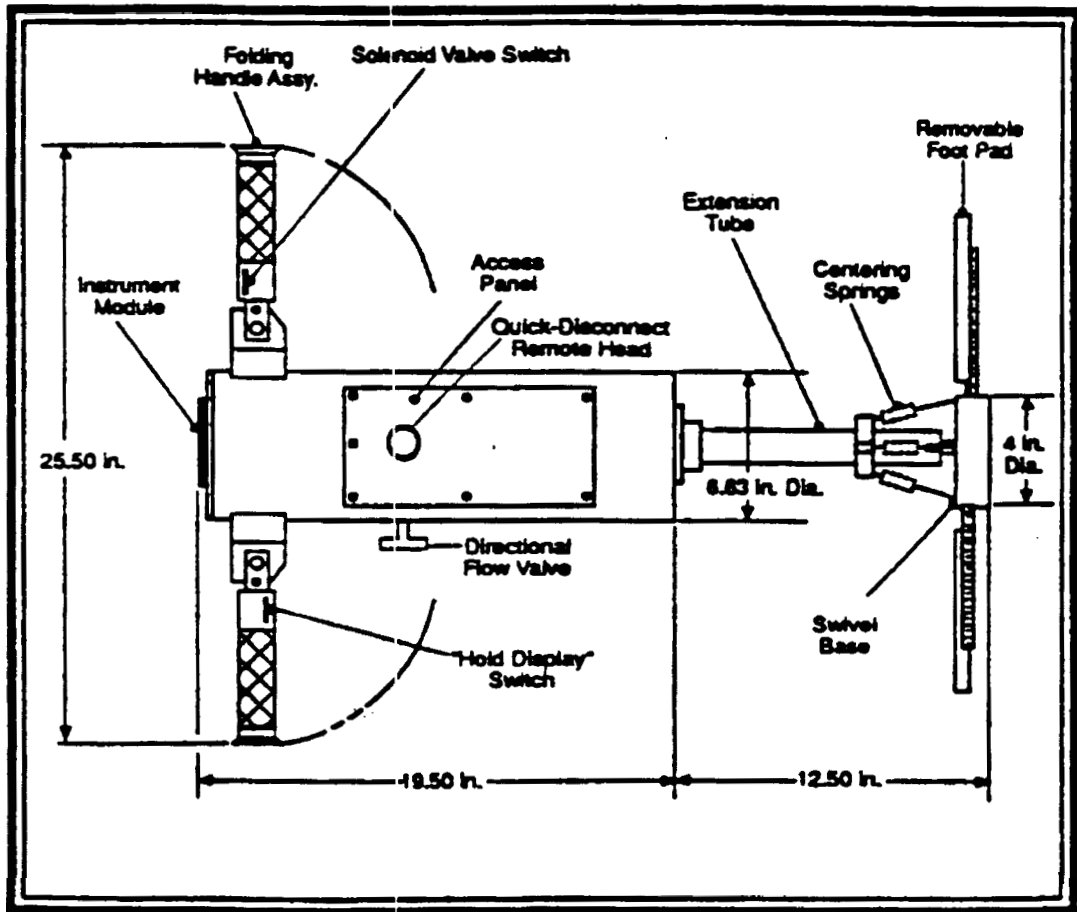


Fig. 3.6: Drawing of Concrete Surface Air Flow Permeability Indicator

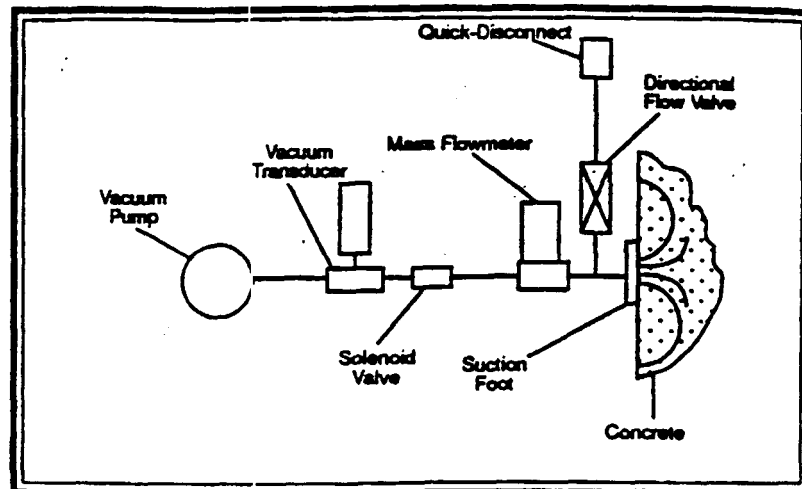


Fig. 3.7: Schematic of Concrete Surface Air Flow Permeability Indicator

The procedure for the operation of the SAF on horizontal surfaces is as follows
(Manual for the Operation of a Surface Air Flow Field Permeability Indicator, 1994).

1. Remove the instrument from its case and install the two foot pads. The foot pads should be screwed all the way into the tapped holes on the suction foot base and then backed out until the aluminum checkered plates are pointed to the top of the machine.
2. Unfold the two handles by pushing the buttons on either end of the "T" handle lock pins, and removing them. When the handles are horizontal, the lock pins are need to be reinserted the other holes in the handle brackets to lock the handles in the extended positions.
3. Make sure all the switches are in the off position and the left handle switch in the RELEASE position. Set the elapsed time indicator to zero by pushing the RESET switch. Ensure that the directional valve switch is in the down position.
4. Charge the battery at least for at least eighteen hours before testing.
5. Unplug the charger and turn on the power switch, and observe that the digital displays are activated. Turn ON the POWER switch. Wait ten minute for the device to warm up. The device should be tested before any field activities to make sure that it is operating correctly. To test the vacuum in a closed system, turn the PUMP in ON position. Wait thirty seconds. The readings should stabilize between 750 to 765 mm Hg. To test the device as an open system, leave the PUMP ON and turn ON the

solenoid switch. Wait thirty seconds. The readings should stabilize at a value of 29 to 31 SCCM.

6. To check the device on a reference plate, place the closed cell gasket on an impermeable metallic plate. Center the suction foot over the gasket.
7. Stand on the foot pads with the balls of your feet. About half of the body weight should be placed on the foot pads and the other half on the heels. This will compress the gasket and form an airtight seal.
8. Turn ON the PUMP. At this time both the flow and vacuum gages will display values and the elapsed time indicator will start. The vacuum should stabilize greater than 650 mm Hg., vacuum. The flow will have a high initial value due to air in the lines, but will stabilize after about fifteen to twenty seconds.
9. Turn On the solenoid switch.
10. When the elapsed time indicator reads 45 seconds, push the left handle switch to the hold position to freeze the reading. Record the reading at this point. The vacuum should read greater than 650 mm Hg, and the flow should be less than 1 SCCM (1 ml/min).
11. Turn off the vacuum PUMP. and the solenoid valve. Turn the switch on the left handle to the release position and push the reset button on the elapsed time indicator. The device is now ready to be moved to the next test spot.
12. Tests on actual concrete surfaces are performed in a manner identical to the initial check test. In some cases, however it may take longer than 45 seconds for the readings to stabilize. Surfaces should be dry, free of dirt or debris, and not cracked grooved or textured.

The permeability of concrete greatly contributes to the corrosion potential of the embedded steel bars due to water and chloride penetration. The lower the permeability the more resistant the concrete is to chloride and water penetration. The relative concrete permeability readings provided by SAF can be categorized into low, moderate, and high according to the air flow rate (ml/min) illustrated on Table 3.9 and Table 6.3 in the Appendix. The collected data and a discussion on the permeability indicated are presented and discussed in the Results and Discussions chapter.

Table 3.9: Relative Concrete Permeability by Surface Air Flow (Manual for the Operation of a Surface Air Flow Field Permeability Indicator, 1994).

Air Flow Rate (ml/minute)	Relative Permeability Indicated
0 to 30	Low
30 to 80	Moderate
80 >	High

3.2.3 Electrical Resistance Test for Penetrating Sealers

Although the main use of this testing method is to determine the effectiveness of concrete penetrating sealers, it can also indicate the resistance of unsealed concrete surfaces. The resistance measurement is tested on two strips of conductive paint sprayed onto the concrete surface to be tested by using a Nilsson 400, soil resistance meter. The spray pattern can be seen in Fig. 3.8.

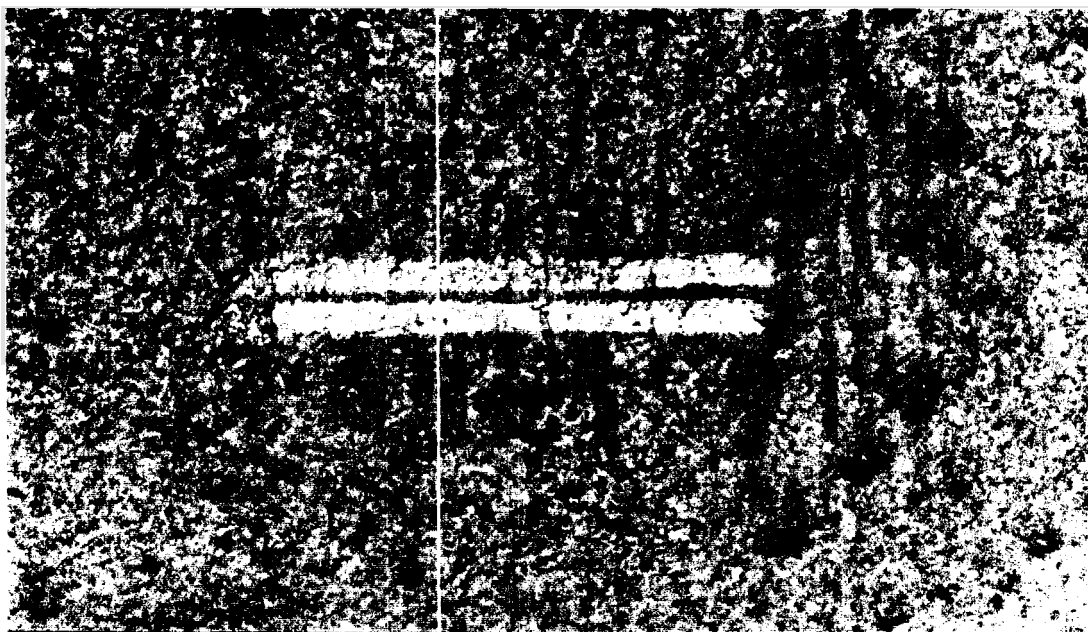


Fig. 3.8: Str ps of Silver Conductive Paint

The materials needed for this test are shown in Fig. 3.9 and are as follows:

- Fine line tape (1/8 in. wide)
- Metal mask (with 5/8in. wide and 4 in. long cutout)
- Conductive silver spray paint
- Duct tape
- Nilsson 400, soil resistance meter
- Multimeter
- Thermometer
- Infrared propane heater

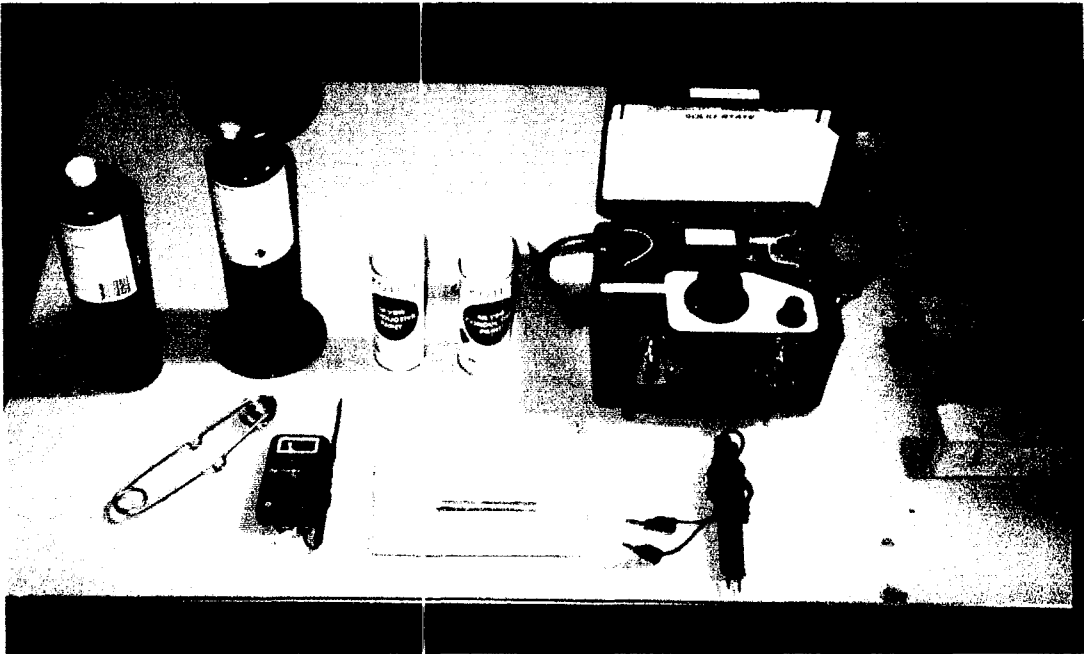


Fig. 3.9: Equipment Required for Electrical Resistance Test for Penetrating Sealers

The procedure for the performing the Electrical Resistance Test for Penetrating Sealers are as follows (Scannell, 1996)

1. Surface must be clean and dry with no grooves or cracks.
2. Apply the fine line tape to the test area.
3. Center metal mask over fine line tape.
4. Duct tape mask in place.
5. Spray paint lengthwise over slit six times.
6. Heat surface with infrared heater for five minutes keeping the temperature at 120 F.
7. Repeat steps 5 and 6 two additional times.
8. Remove the mask and the fine line tape.

9. Measure DC end to end resistance of both sides of the gage using the multimeter and record the readings.
10. Measure the DC resistance between the two sides of the gage using the multimeter and record the reading.
11. Compare the DC readings for the end to end resistance as well and the one taken between the two sides to the acceptance criteria in Table 3.10.
12. Lay wet sponge on gage and keep wet for five minutes.
13. Remove the sponge and press a folded paper towel against the gage for five seconds.
14. Gently wipe the gage with a crumpled paper towel in a lengthwise direction.
15. Place the probes on the soil resistance meter against the gage and record the AC resistance reading.

Table 3.10: Preliminary DC Testing of Gauge (Scannell, 1996)

Test	Acceptance Criteria
End-to-End Resistance	5 to 15 Ω – Very Good up to 125 Ω -- Acceptable
Insulation Resistance (Side-to-Side)	> 20 M Ω – Normal > 5 M Ω -- Acceptable

The higher the resistance the less potential for corrosion in the embedded steel due to the higher density of the concrete and improved insulation against the electrochemical process of corrosion. The collected data and a discussion on the resistance indicated are presented and discussed in the Test Results and Discussions chapter.

3.2.4 Standard Test Method for Determining the Effects of Chemical Admixtures on the Corrosion of Embedded Steel Reinforcement in Concrete Exposed to Chloride Environments -ASTM G 109

This test method is used to determine the effects of chemical admixtures on the corrosion of metals in concrete. The test method provides a reliable means to predict the inhibiting and corrosive properties of admixtures to be used in concrete. The method, in brief, tests minidecks, concrete specimens with known lengths of embedded steel reinforcing bars, in a chloride solution. The minidecks are tested periodically for corrosion rate and corrosion potential.

The 15 in. long embedded steel bars are wire brushed of all existing corrosion. The ends were wrapped in electroplated tape and wrapped in heat shrink tubing to prevent the unwanted corrosion of the ends of the bars during moist curing. The eleven inches of exposed bar are centered in the formwork and cast into the concrete. Three bars total are placed into each minideck. One bar is placed on top and two on the bottom. The dimensions of the concrete minideck can be seen in Fig. 3.10. Plexiglas dams are fabricated to hold the 3% NaCl solution. The dams are sealed to the top of the minidecks with silicon caulk. Concrete sealing epoxy is used to seal all four sides and the top of the minidecks except for the area inside the dam.

The specimens are tested on a four week cycle. The dams are filled with 1.5 in. of 3% NaCl solution for two weeks. The solution is then vacuumed out and the specimen is left to dry for an additional two. The specimens are tested for corrosion rate and corrosion potential after the first week of ponding with the NaCl solution.

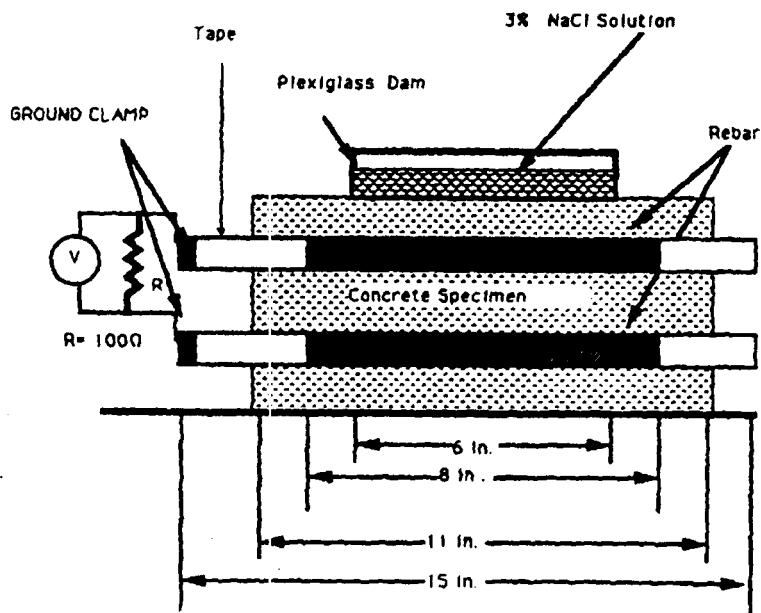
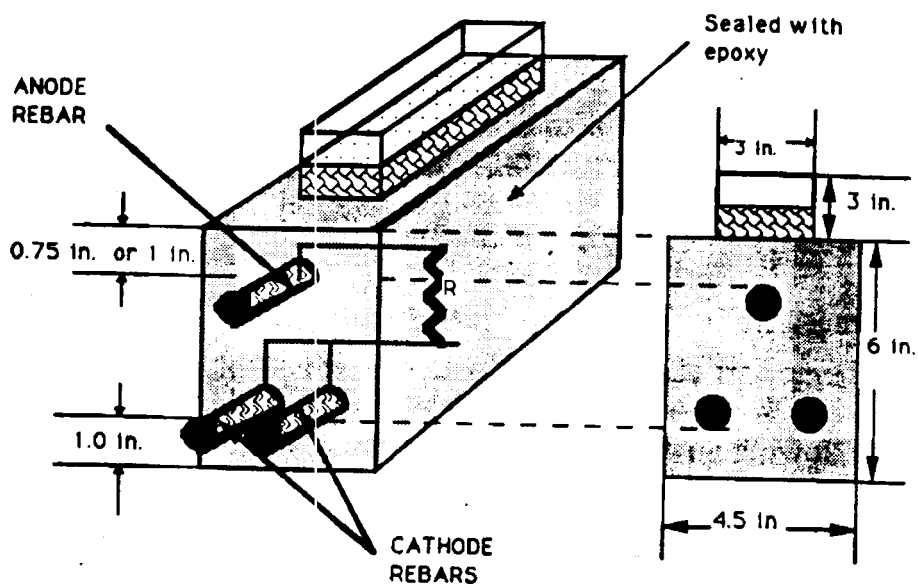


Fig. 3.10: View of Concrete Minideck (ASTM G 109)

The corrosion rate is tested using a high impedance voltmeter accurate up to 0.01 mV. The top bar is used as the anode while the bottom bars are used as the cathode. Voltage is measured across a 100Ω resistor. The current flowing, I_j , from the electrochemical process is calculated from the measured voltage across the 100Ω resistor, V_j , as:

$$I_j = V_j/100$$

The corrosion potential of the bars is measured against a reference electrode half cell. The electrode is placed in the dam containing the NaCl solution. The voltmeter is connected between the electrode and bars.

The current is monitored as a function of time until the average current of the control specimens is 10 μA or Greater, and at least half the samples show currents equal to or greater than 10 μA. The test is continued for a further three complete cycles to ensure the presence of sufficient corrosion for a visual evaluation. At the conclusion of the test, the minidecks are broken and the bars removed to assess the extent of corrosion and to record the percentage of corroded area.

The results are interpreted with Table 6.1 and Table 6.2 in the Appendix. The results of this test are presented in the Results and Discussion Chapter.

3.3 Instrumentation for Field Tests

Electrical connections were made to the top reinforcing mat of each bridge deck before the placement of the concrete. Five connections were made to Route 130 Westbound and four each on the remaining four bridges. A total of 105 readings were taken per cycle using the GECOR 6 Corrosion Rate Meter. Twenty five readings were taken at the bridge deck over RT130 West Bound. Twenty readings each were taken at the other four bridge decks tested. The locations of the tests are presented on Fig. 3.11, 3.12, 3.13, 3.14, and 3.15. Due to the use of epoxy coated reinforcing bars on the bridge deck over RT130 West Bound, it was necessary to place uncoated reinforcing bars into the top mat. The locations of these bars are presented in Fig. 3.16. Short lengths of uncoated reinforcing bars were welded to the existing reinforcement. The ends were tapped to accept stainless steel nuts and bolts to attach underground copper feeder cables seen in Fig. 3.17 that were used to connect the meter to the reinforcement in the bridge deck. To ensure accurate readings, the connecting lengths of reinforcing bars were wire brushed to remove the existing corrosion. They were then coated with epoxy and spray painted to seal out moisture. The details of the connections are presented in Fig 3.18, 3.19, 3.20, 3.21, and 3.22. The cables were passed through flexible steel conduits and into rain tight steel enclosure to protect them from the elements and from possible tampering Fig. 3.23, 3.24, 3.25, 3.26, and 3.27. A reinforcing steel locator was not needed because locations of reinforcement and connections were recorded before the placement of the concrete.

Connections were observed during the placement of concrete and were tested after the concrete had hardened to check for broken connections. Pictures of the connections during concrete placement can be seen in Fig. 3.28, 3.29, and 3.30. All connections survived and remained intact.

Photographs of the five bridge decks tested on the new Route 133 Hightstown Bypass can be seen in Fig. 3.31, 3.32, 3.33, 3.34, and 3.35.

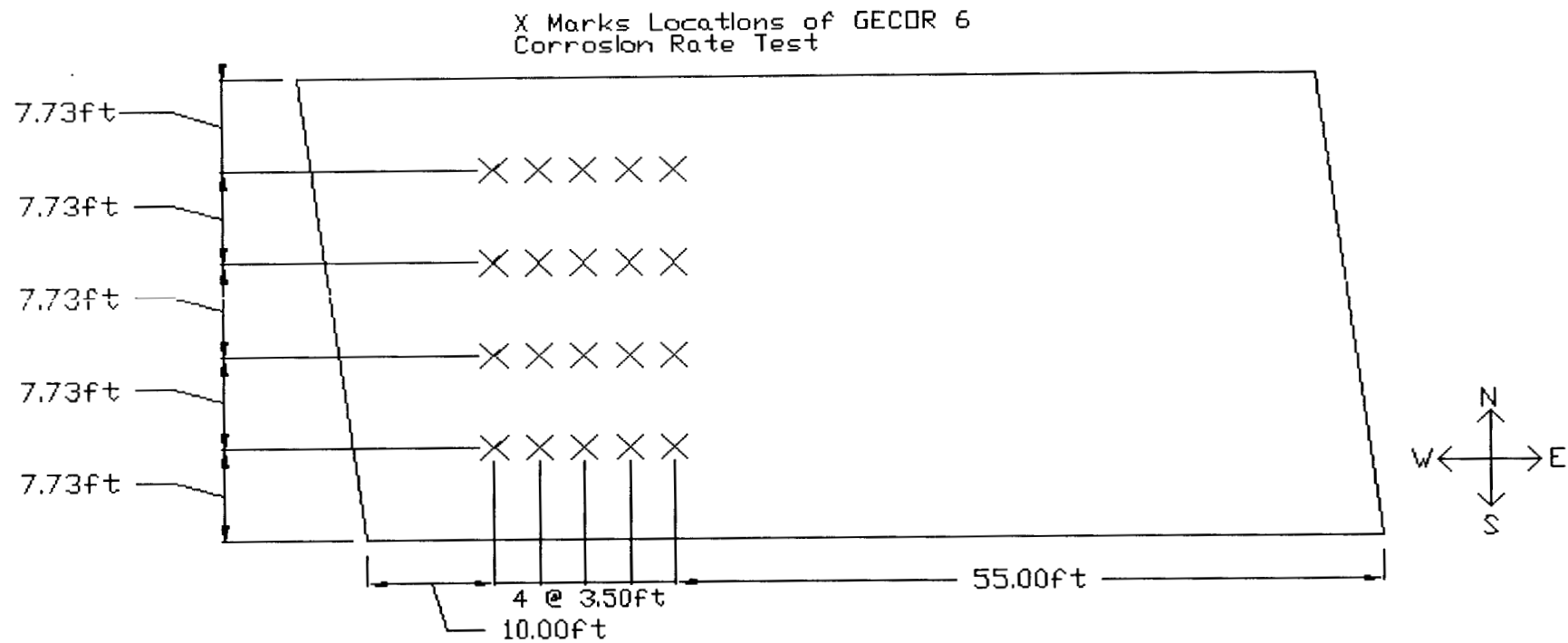


Fig. 3.11: Locations of GECOR 6 Corrosion Rate Meter Tests
North Main Street Westbound

X Marks Locations of GECOR 6
Corrosion Rate Test

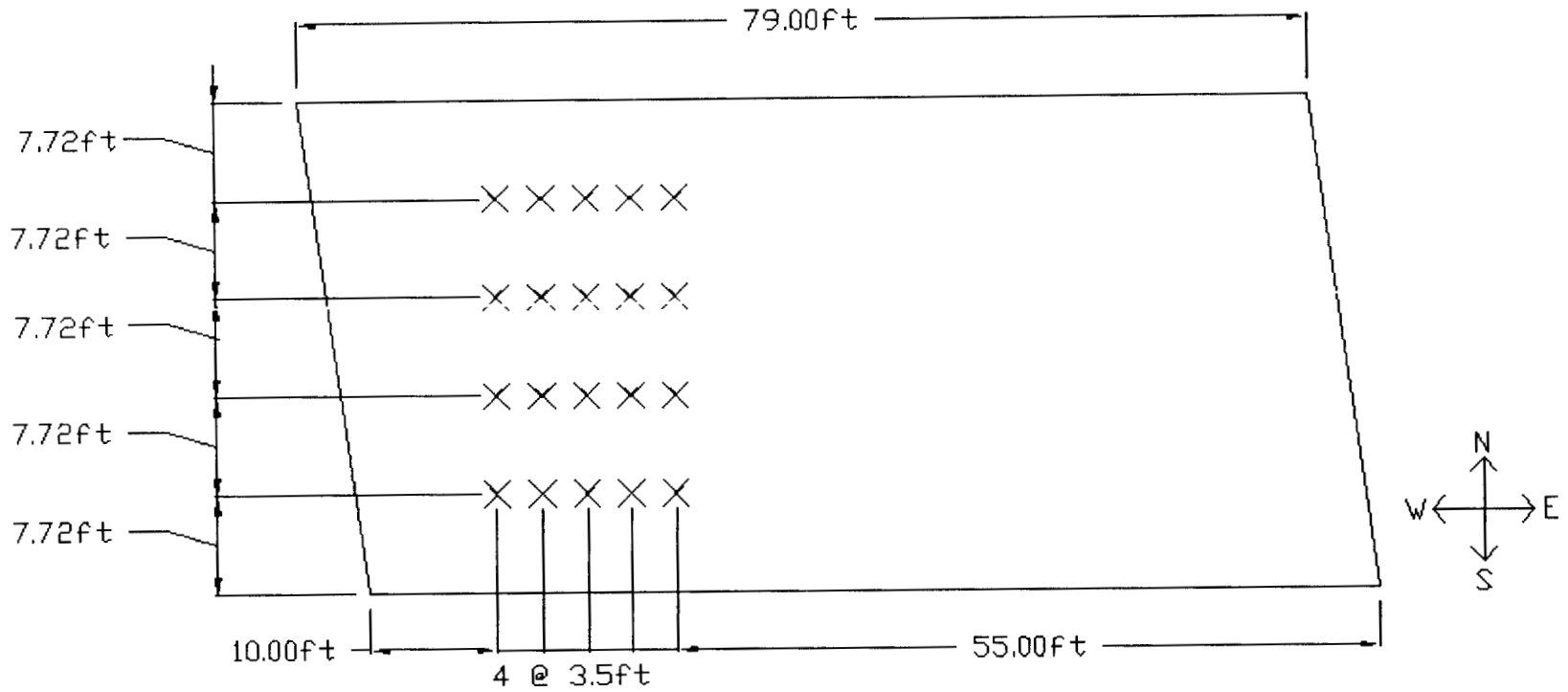


Fig. 3.12: Locations of GECOR 6 Corrosion Rate Meter Tests
North Main Street Eastbound

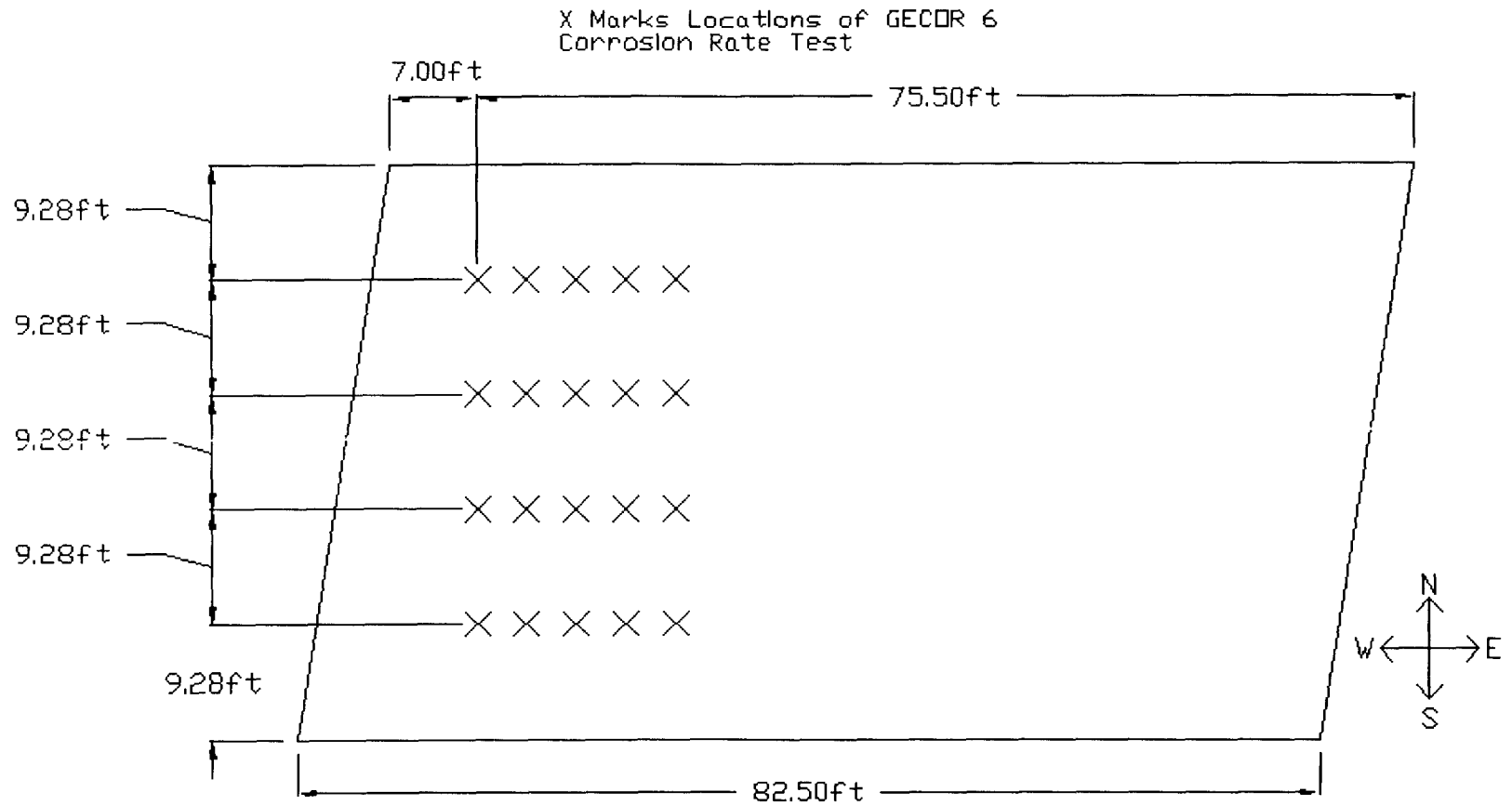


Fig. 3.13: Locations of GECOR 6 Corrosion Rate Meter Tests
Wyckoff Road Westbound

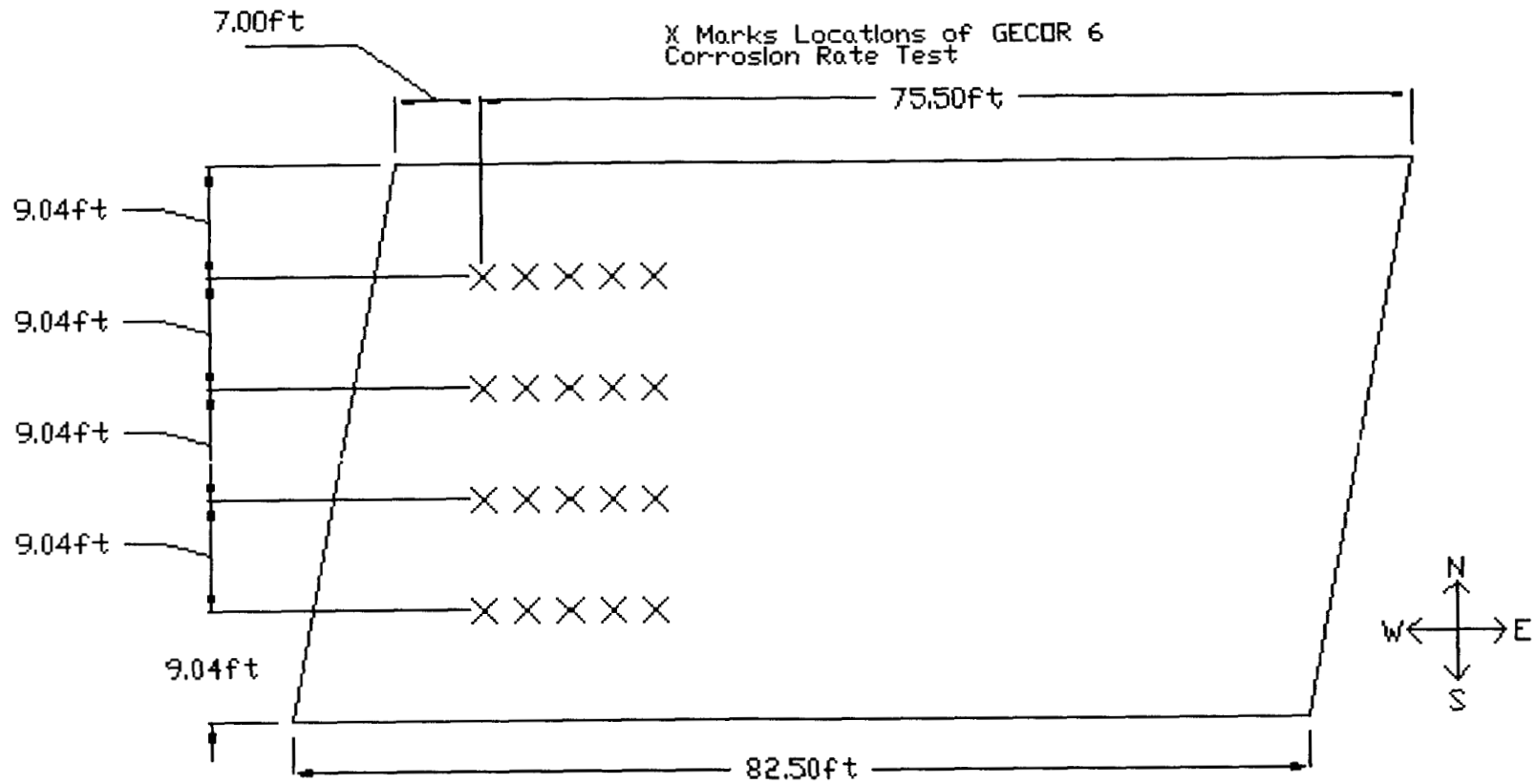


Fig. 3.14: Locations of GECOR 6 Corrosion Rate Meter Tests
Wyckoff Road Eastbound

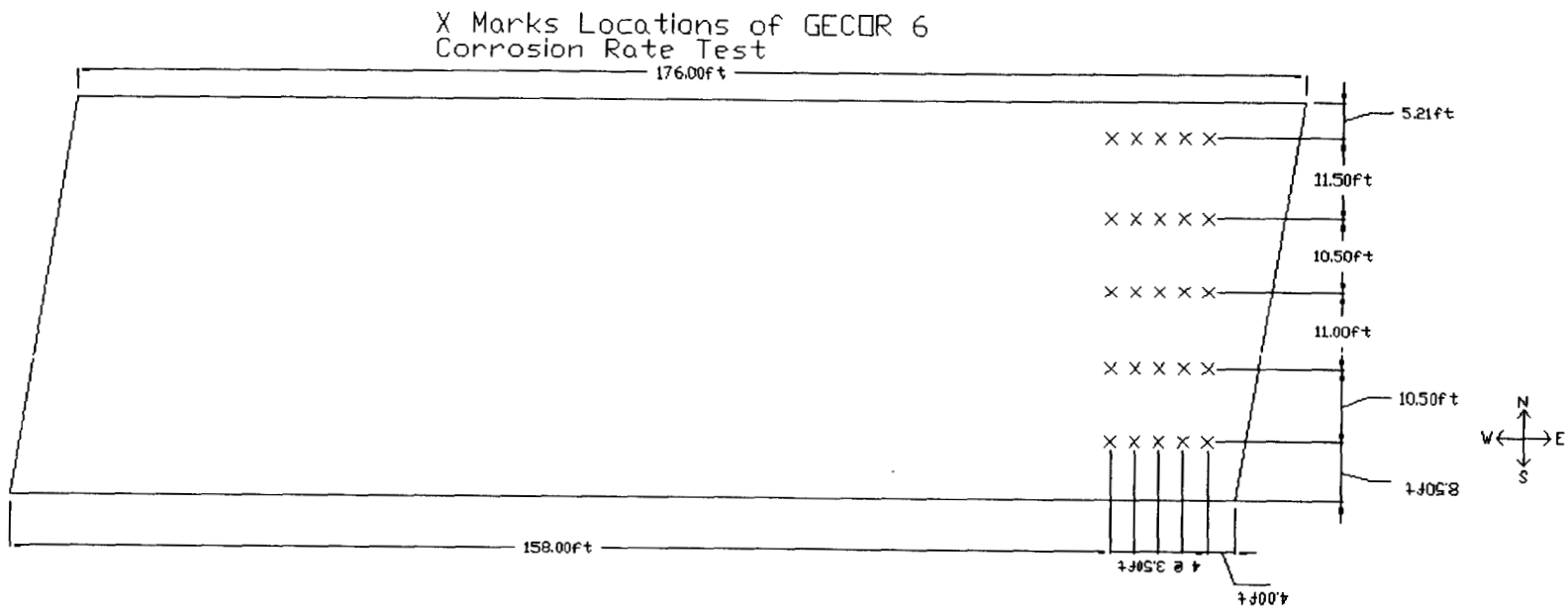


Fig. 3.15: Locations of GECOR 6 Corrosion Rate Meter Tests
Route 130 Westbound

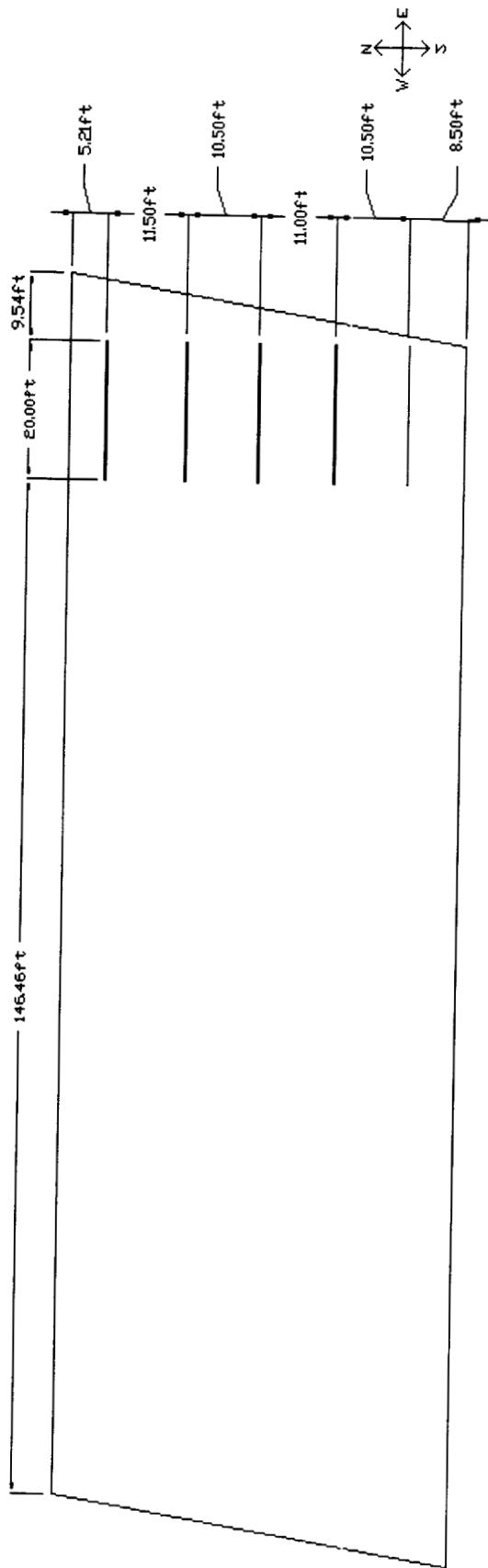


Fig. 3.16: Locations of Uncoated Steel Reinforcement Bars on Route 130 Westbound

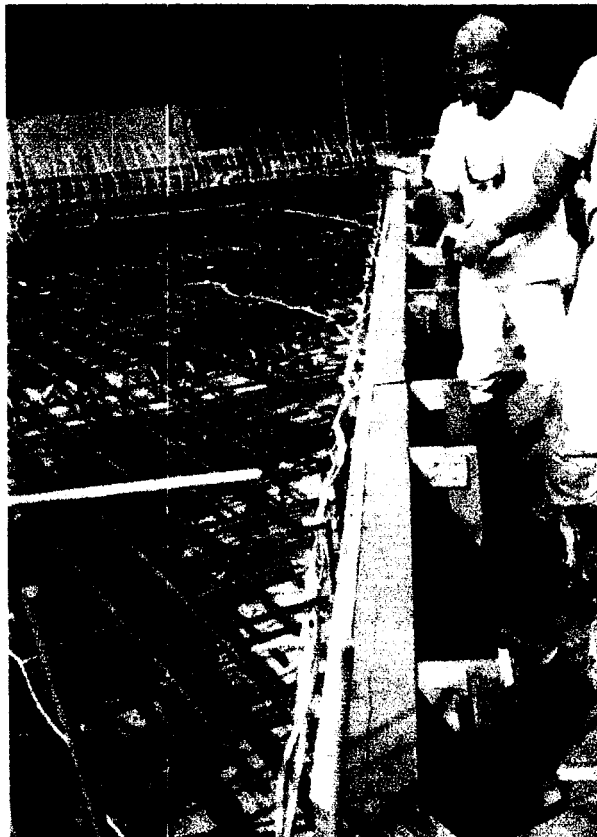
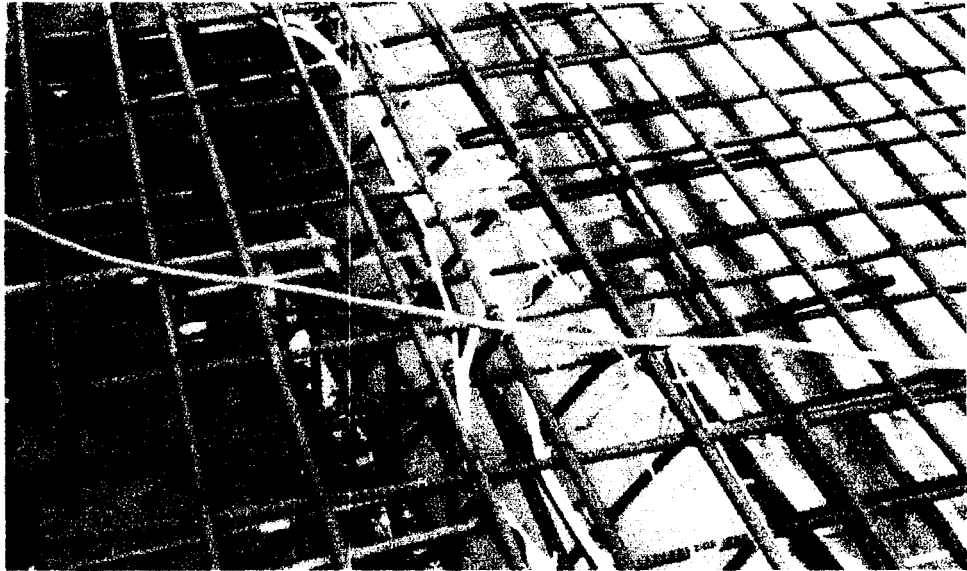


Fig. 3.17: Insulated Copper Underground Feeder Cables

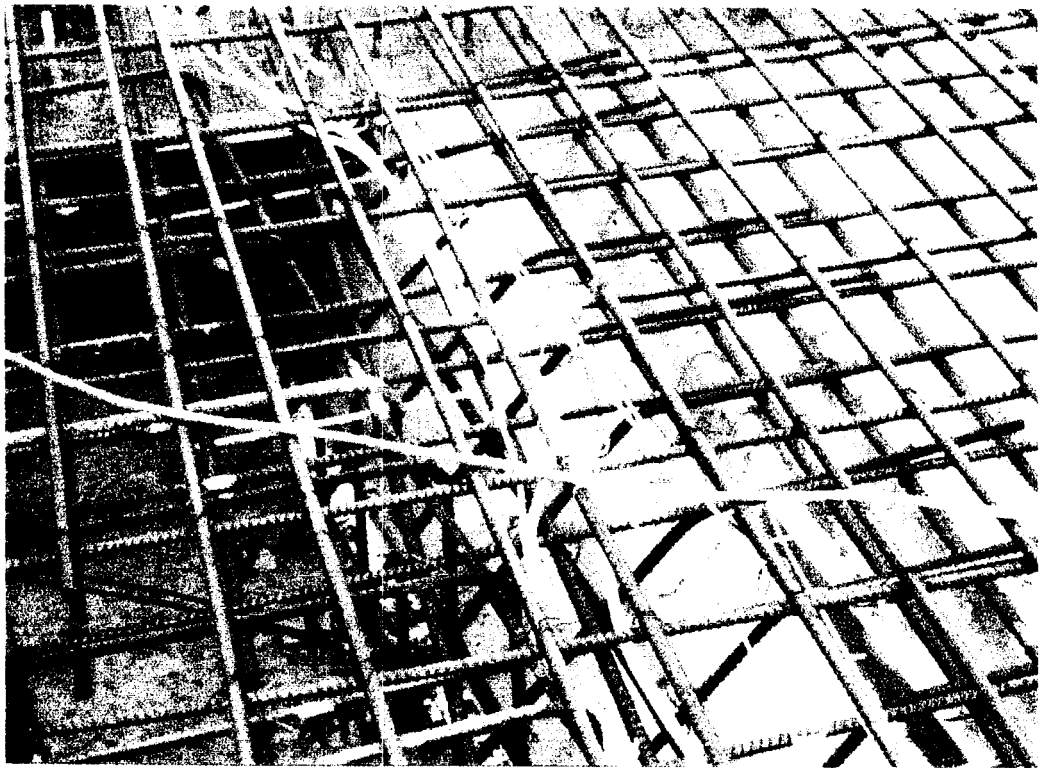
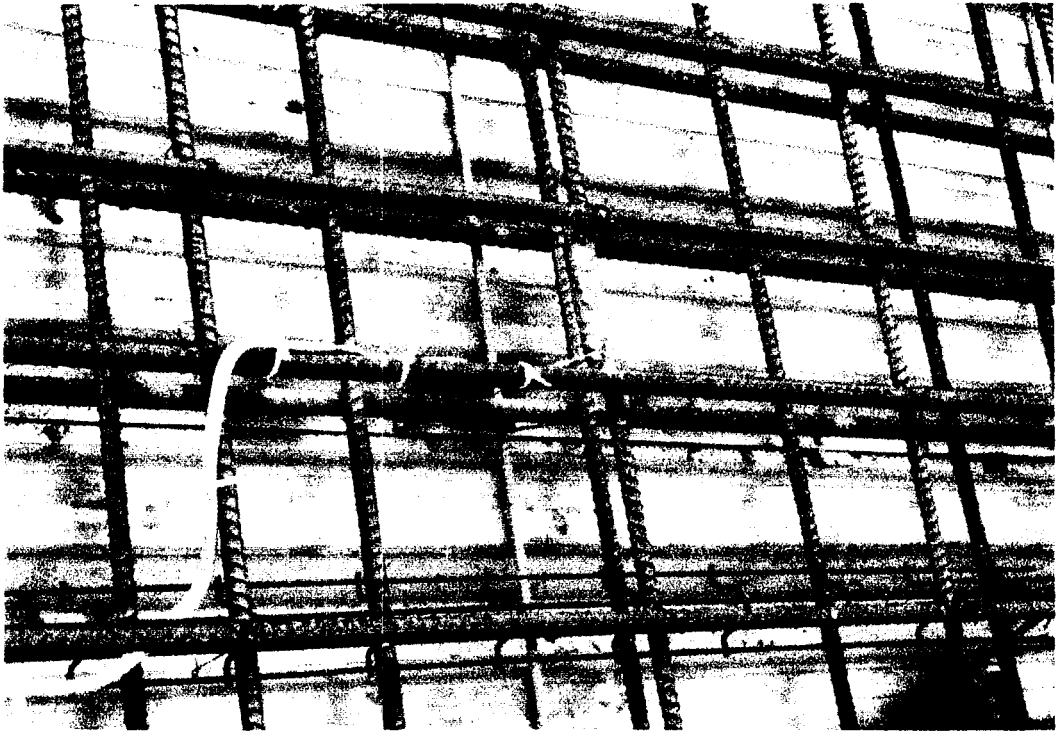


Fig. 3.18: Connection to North Main Street Westbound

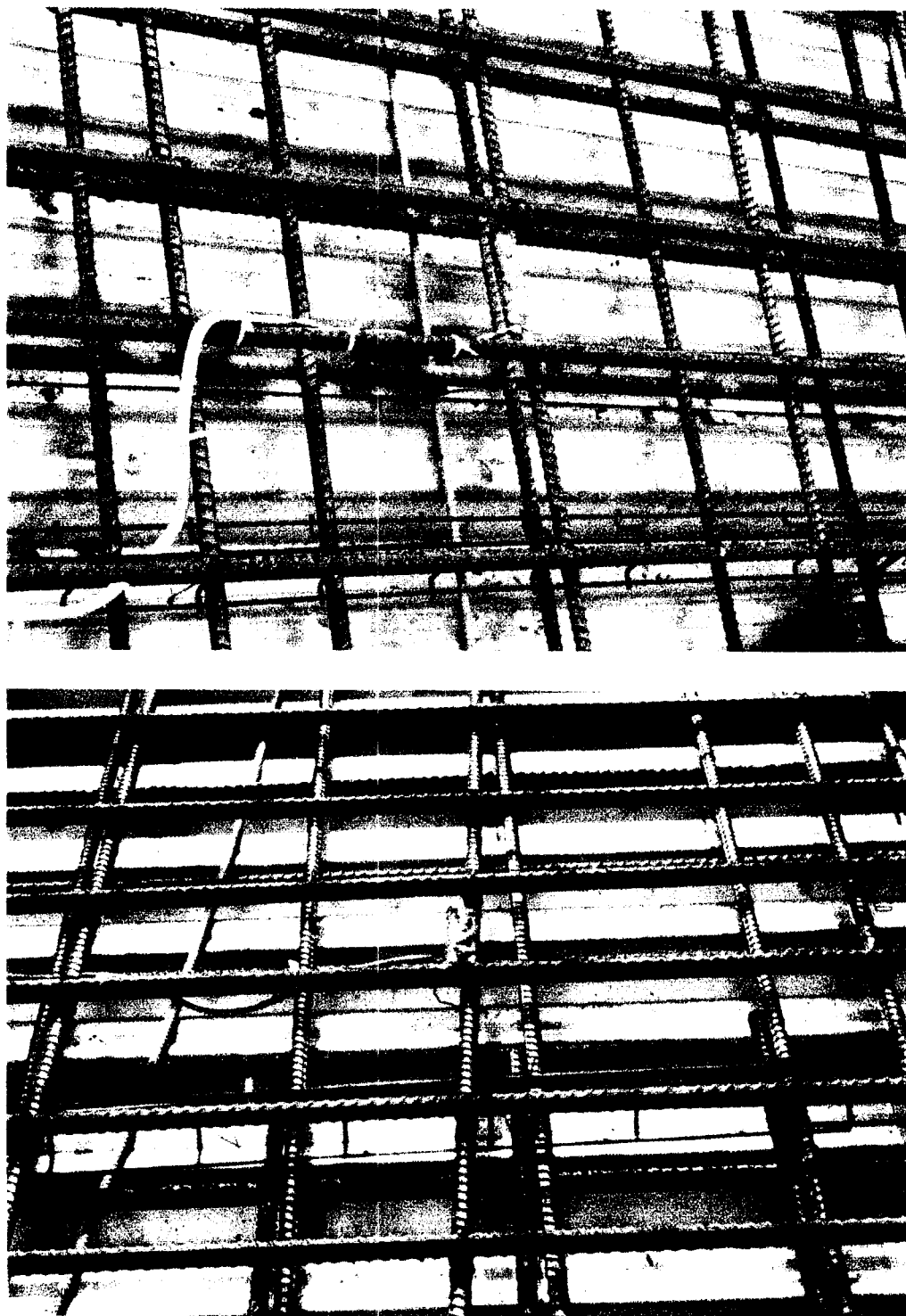


Fig. 3.19: Connection to North Main Street Eastbound

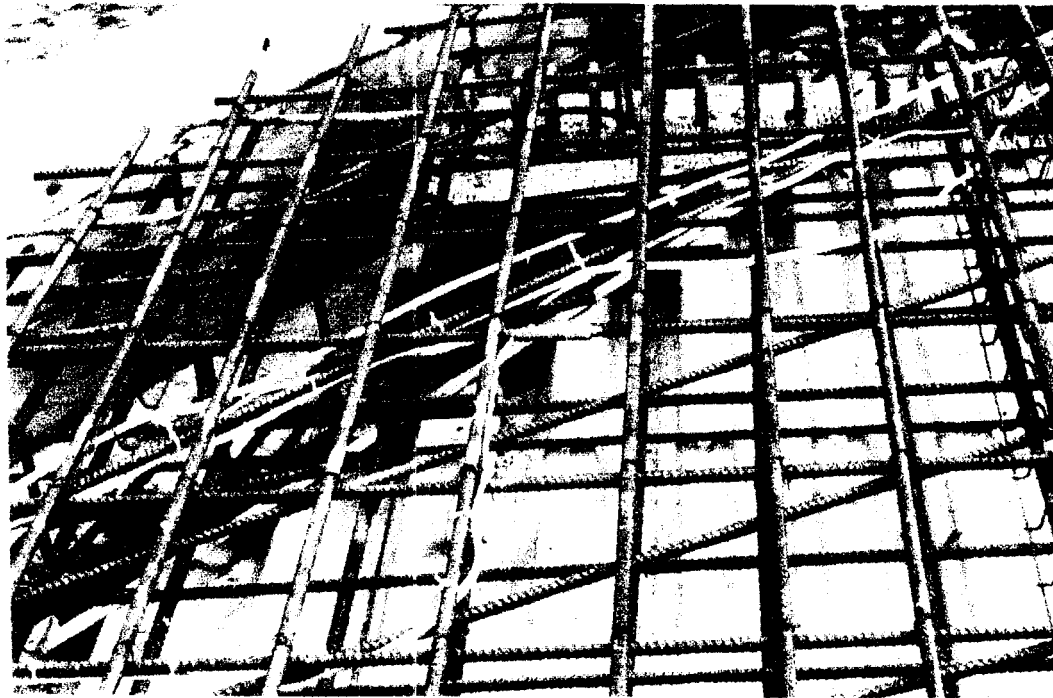
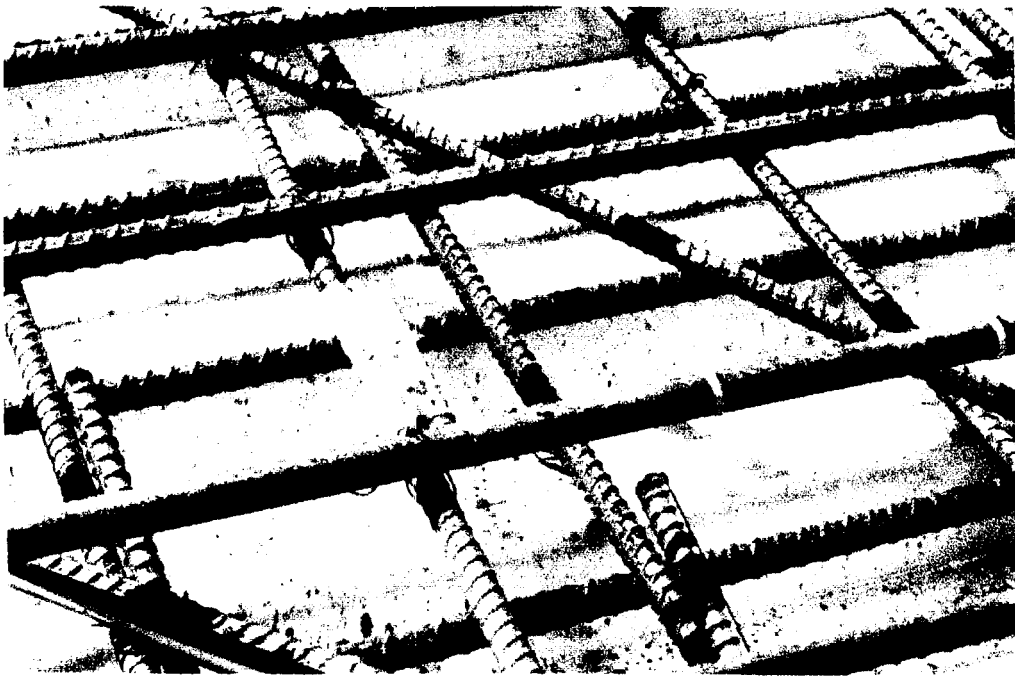


Fig. 3.20: Connection to Wyckoff Road Westbound

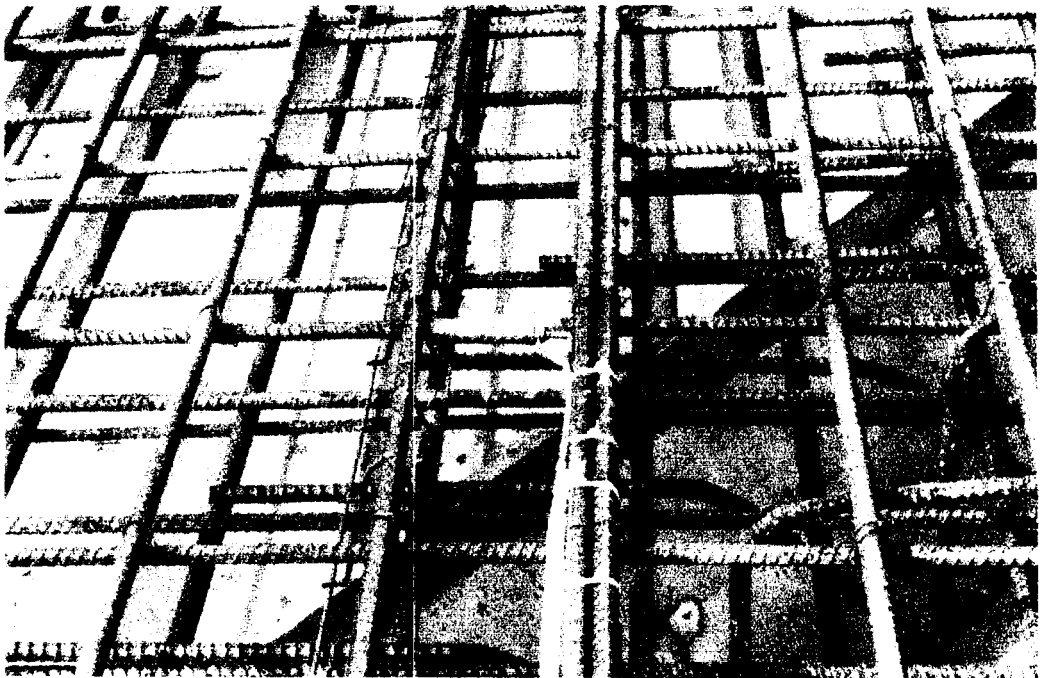
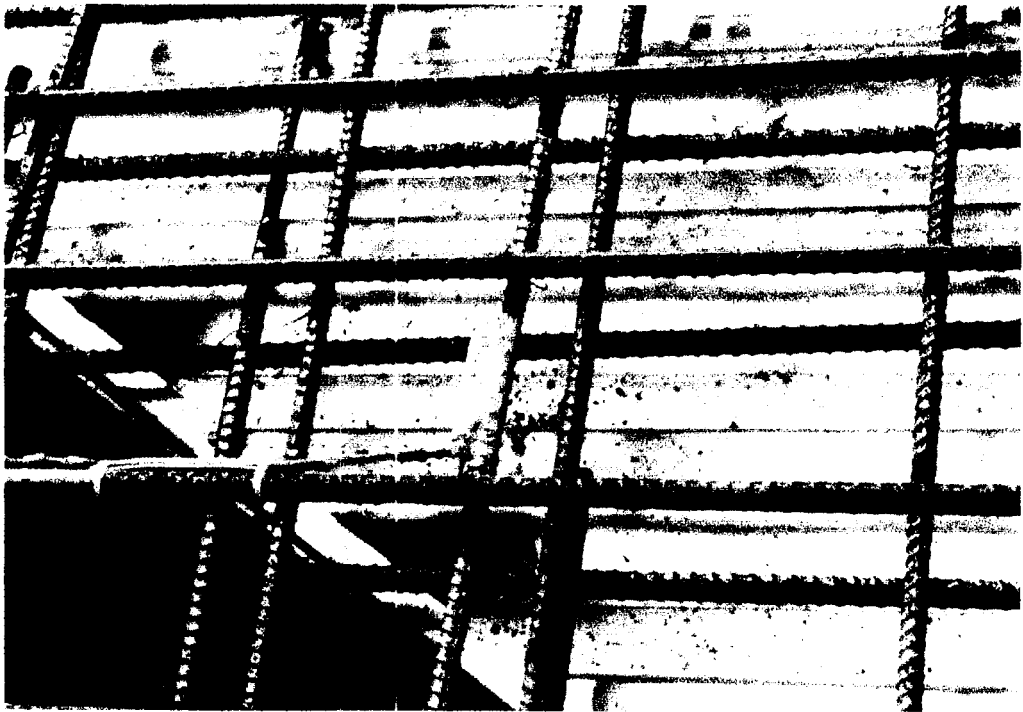


Fig. 3.21: Connection to Wyckoff Road Eastbound

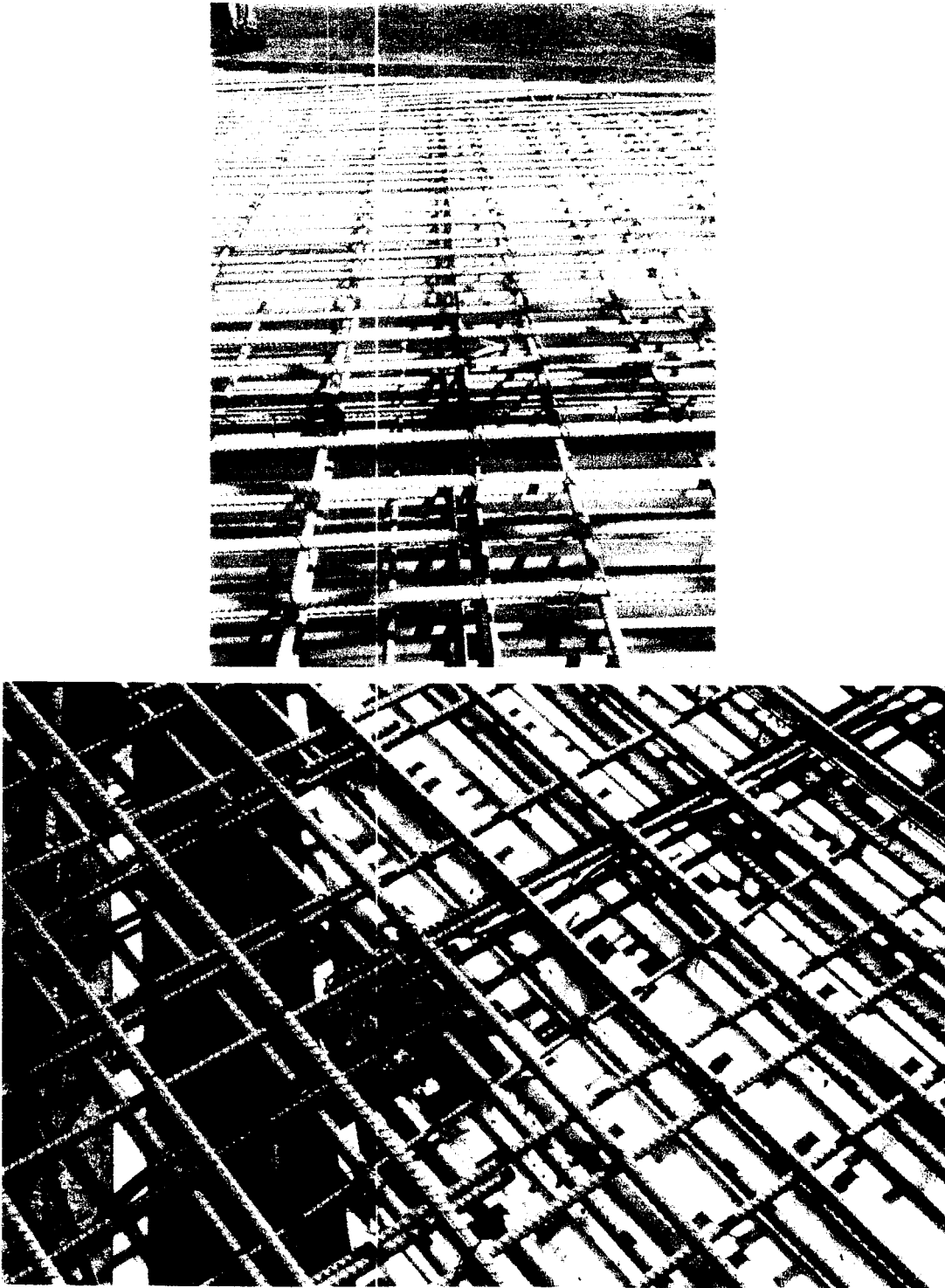


Fig. 3.22: Connection to Route 130 Westbound

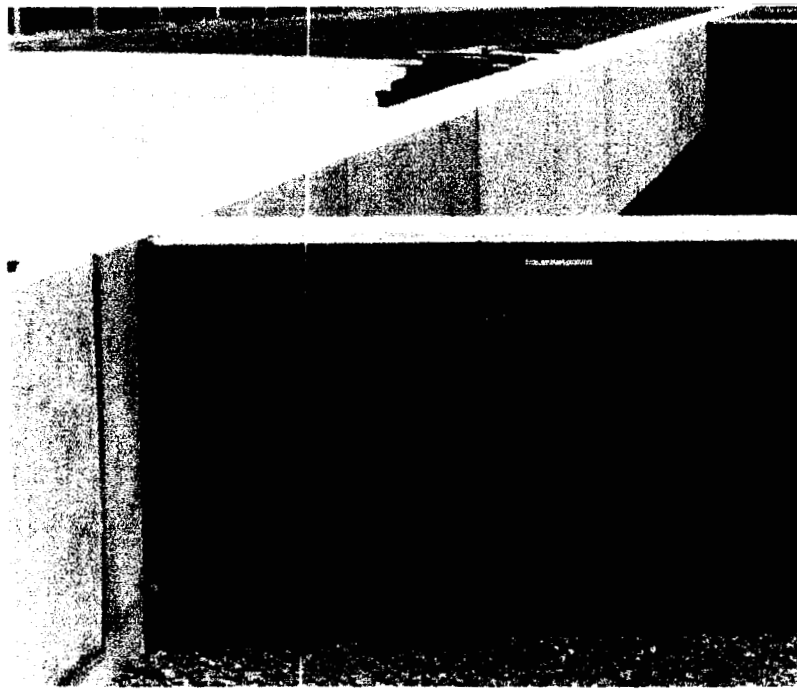


Fig. 3.23: Conduits and Enclosure – North Main Street Westbound

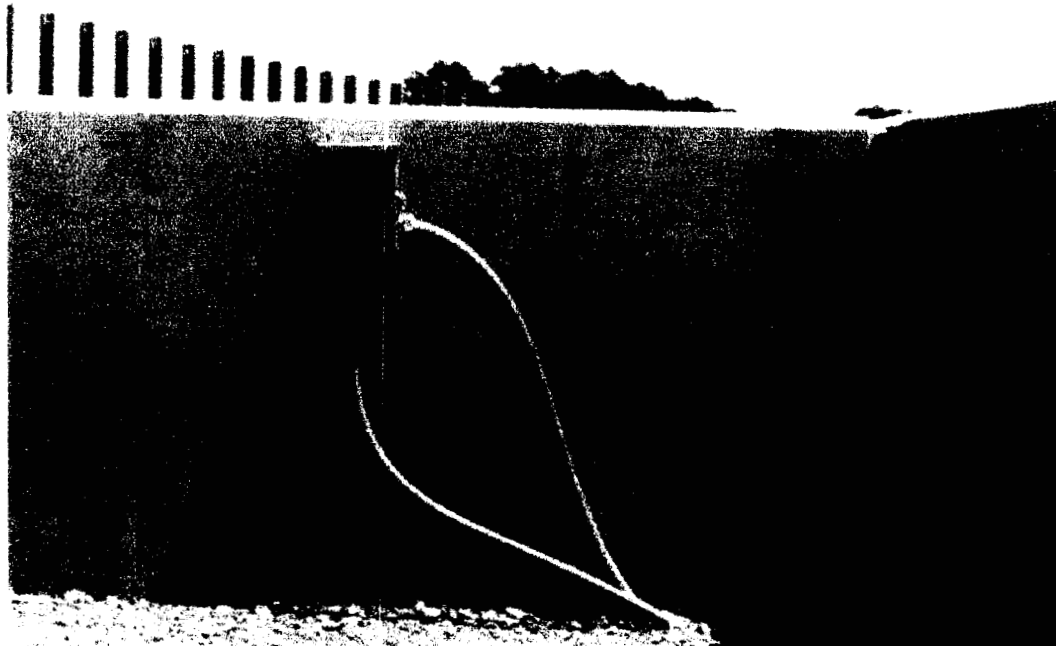


Fig. 3.24: Conduits and Enclosure – North Main Street Eastbound

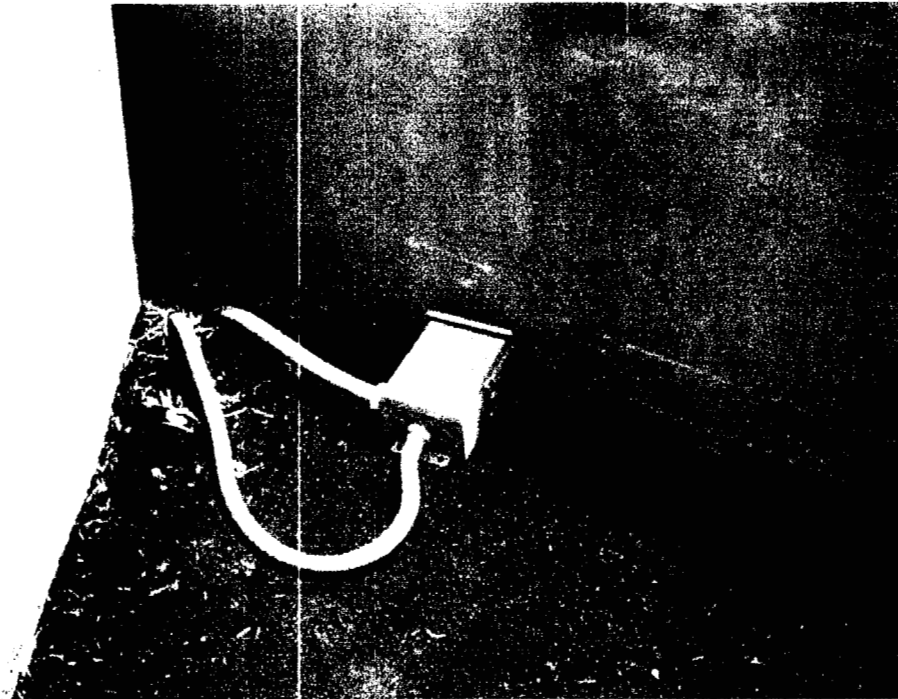


Fig. 3.25: Conduits and Enclosure – Wyckoff Road Westbound

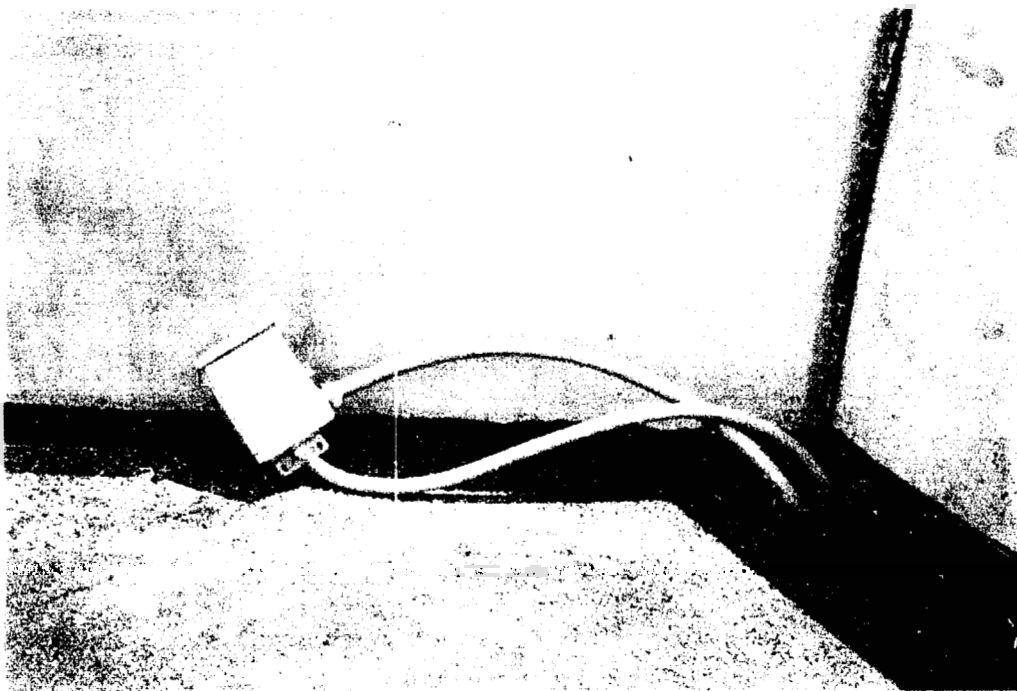


Fig. 3.26: Conduits and Enclosure – Wyckoff Road Eastbound

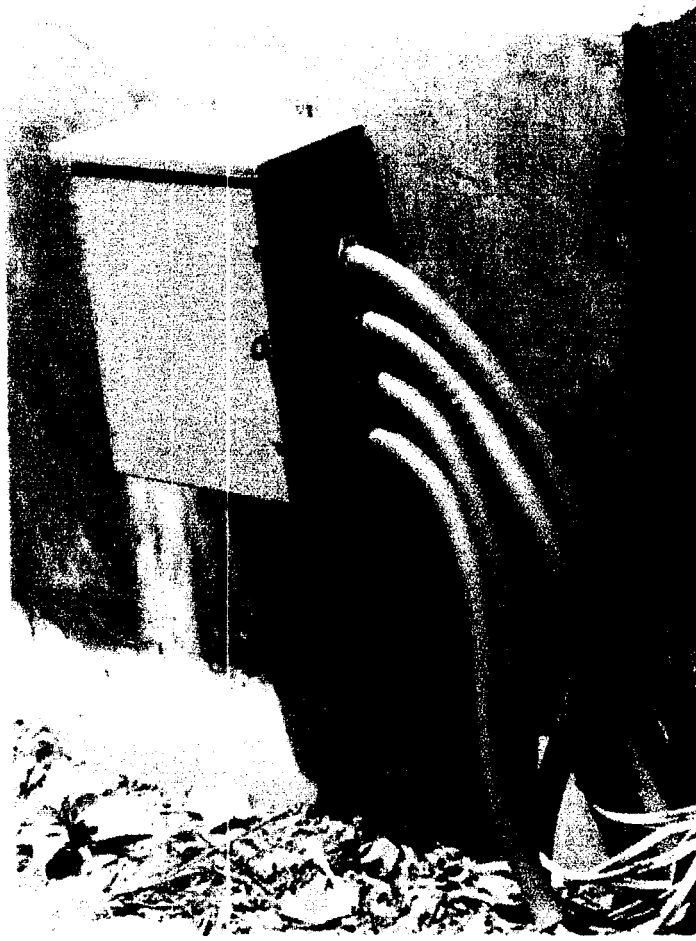


Fig. 3.27: Conduits and Enclosure – Route 130 Westbound



Fig. 3.28: Vibrating of Fresh Concrete at North Main Street Eastbound

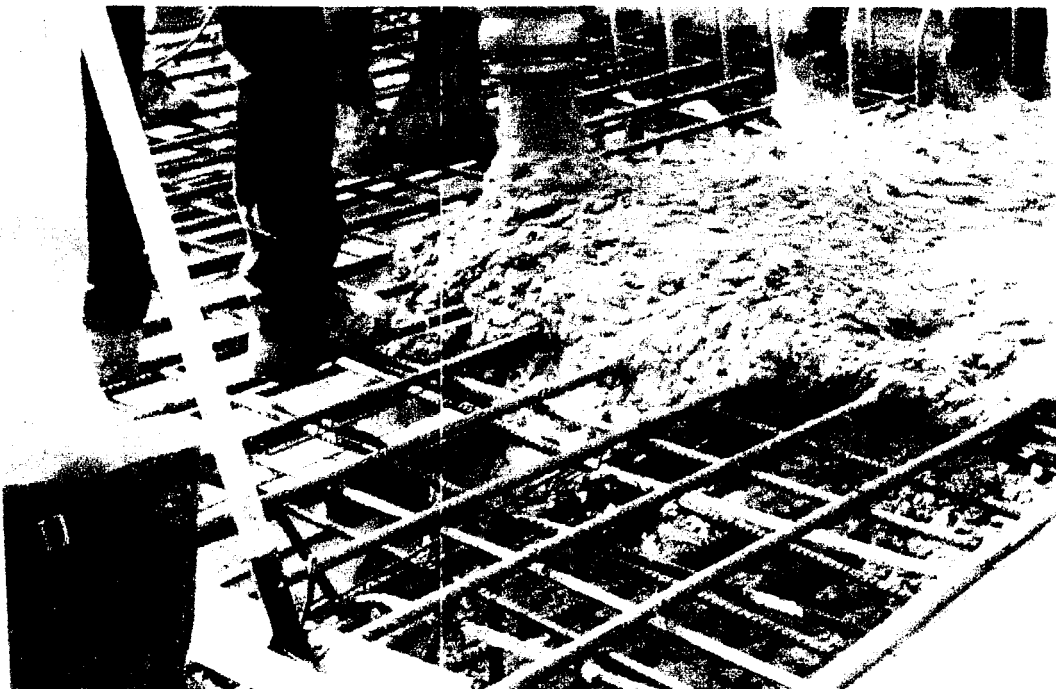


Fig. 3.29: Placement on Fresh Concrete at North Main Street Westbound

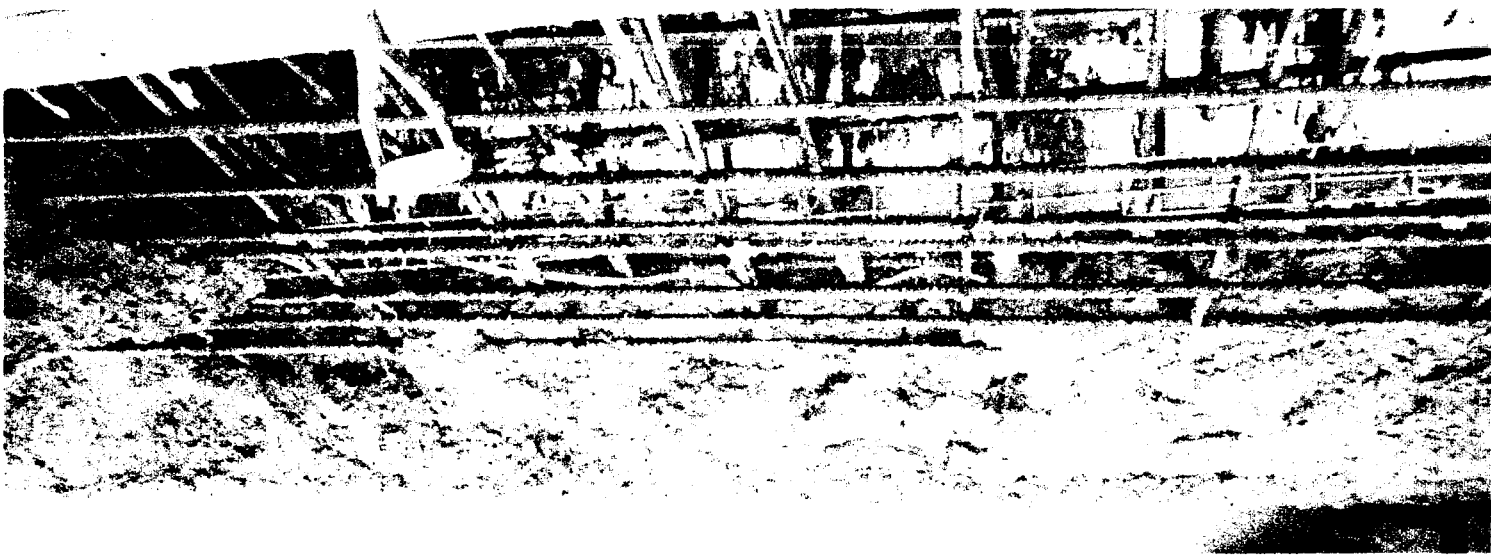


Fig. 3.30: View of Connections at North Main Street Westbound during Concrete Placement



Fig. 3.31: Bridge Deck over North Main Street Westbound near Completion

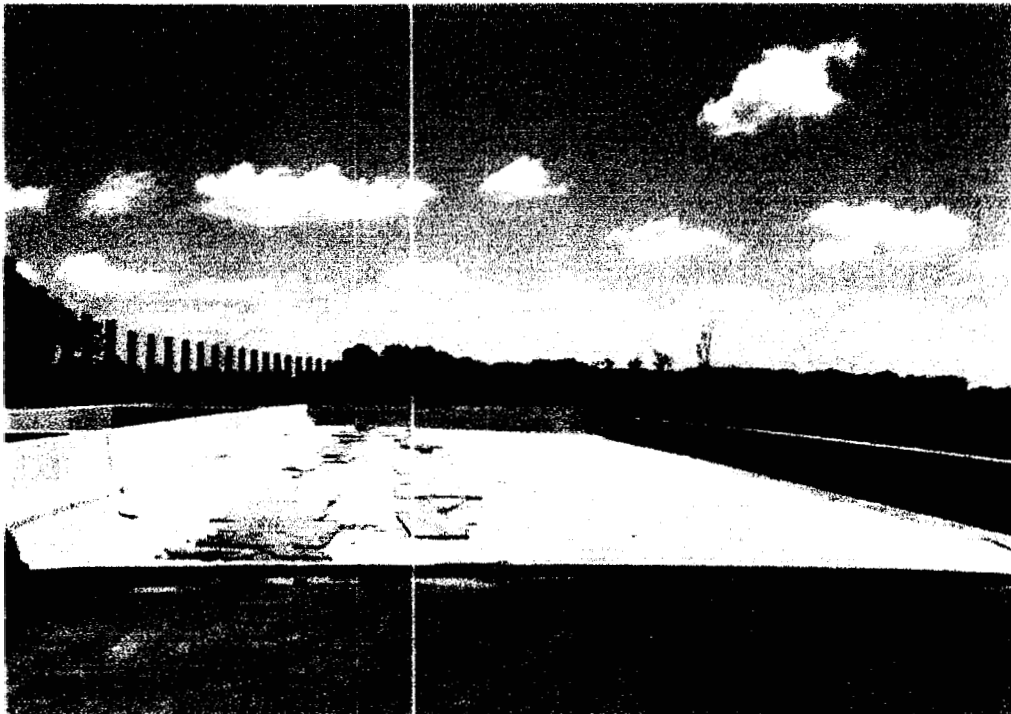


Fig. 3.32: Bridge Deck over North Main Street Eastbound near Completion



Fig. 3.33: Bridge Deck over Wyckoff Road Westbound near Completion

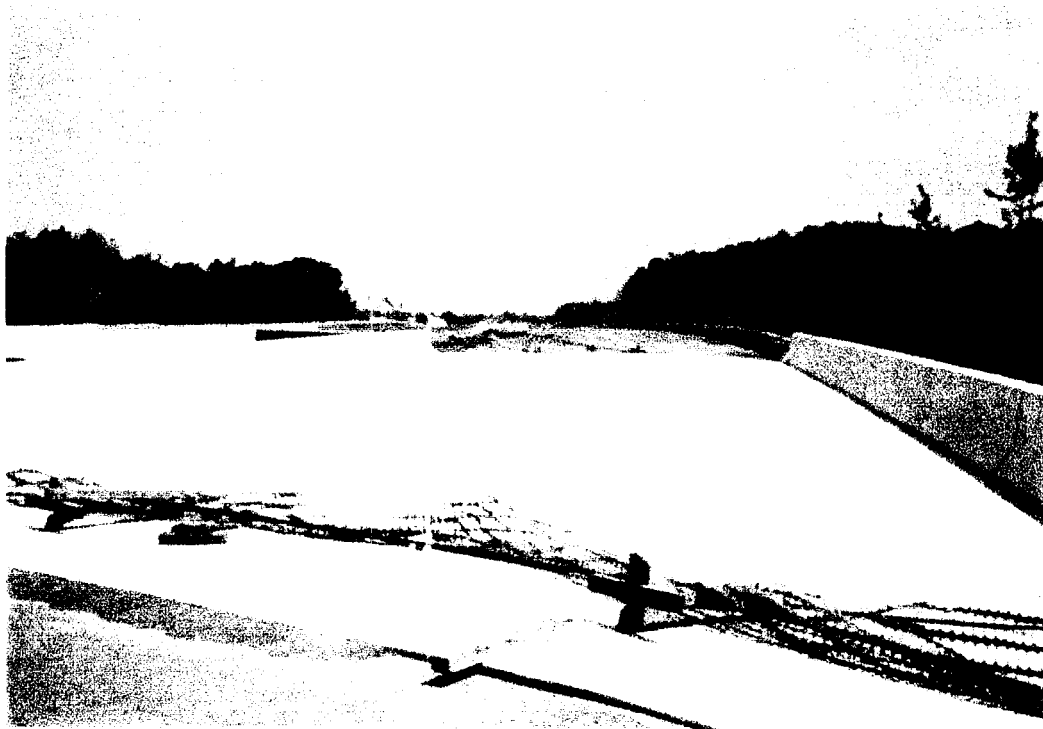


Fig. 3.34: Bridge Deck over Wyckoff Road Eastbound near Completion



Fig. 3.35: Bridge Deck over Route 130 Westbound near Completion

A total of fifteen readings were recorded per cycle using the Surface Air Flow Field Permeability Indicator. Three readings were taken transversely across the concrete deck at either end and at midspan. The locations of the readings can be seen on Fig. 3.36, 3.37, 3.38, 3.39, and 3.40. The readings provide an indication of effect of a particular corrosion inhibiting admixture on permeability.

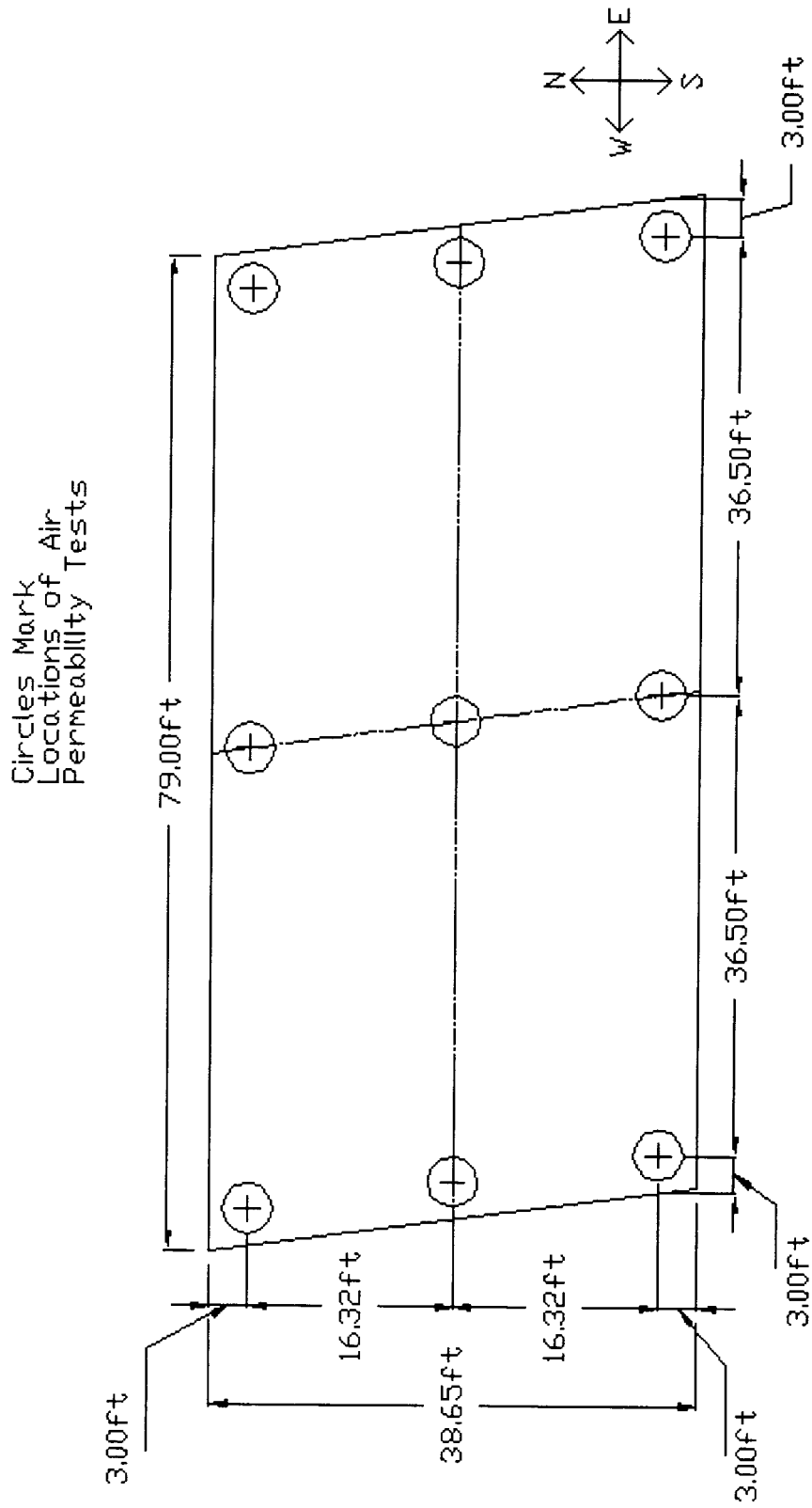


Fig. 3.36: Locations of Surface Air Flow Field Permeability Indicator Readings
North Main Street Westbound

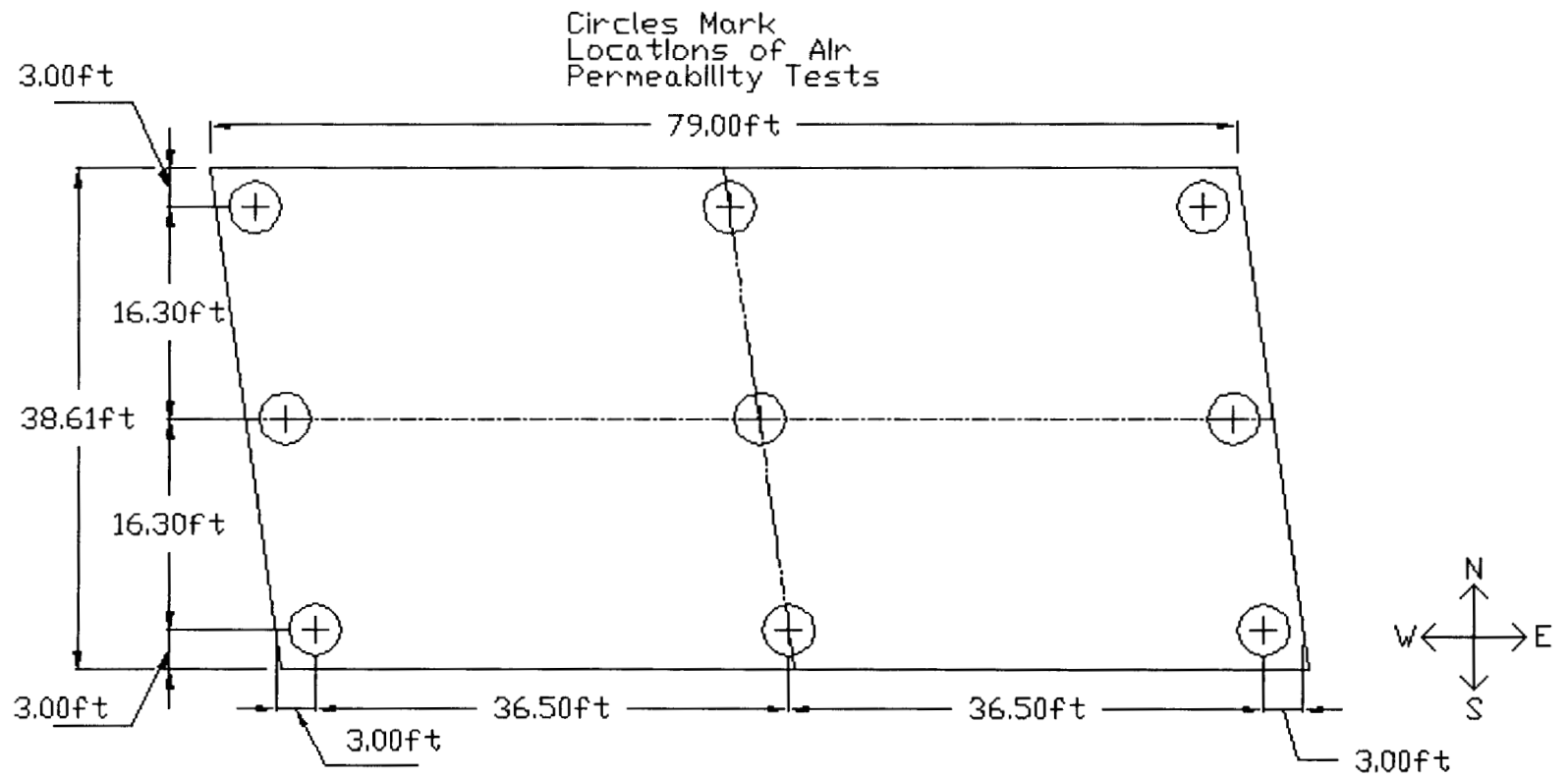


Fig. 3.37: Locations of Surface Air Flow Permeability Indicator Readings
North Main Street Eastbound

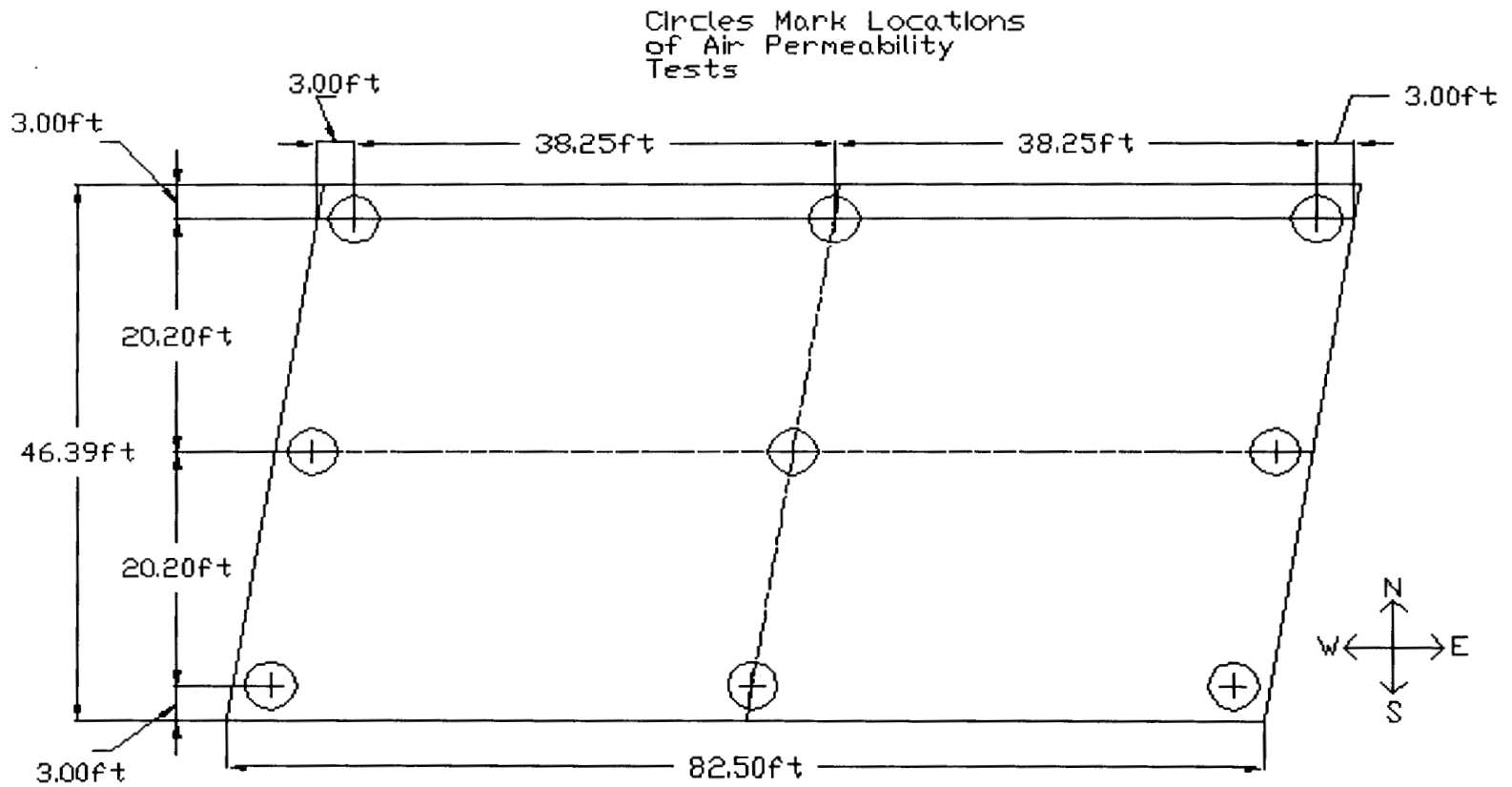


Fig. 3.38: Locations of Surface Air Flow Permeability Readings
Wyckoff Road Westbound

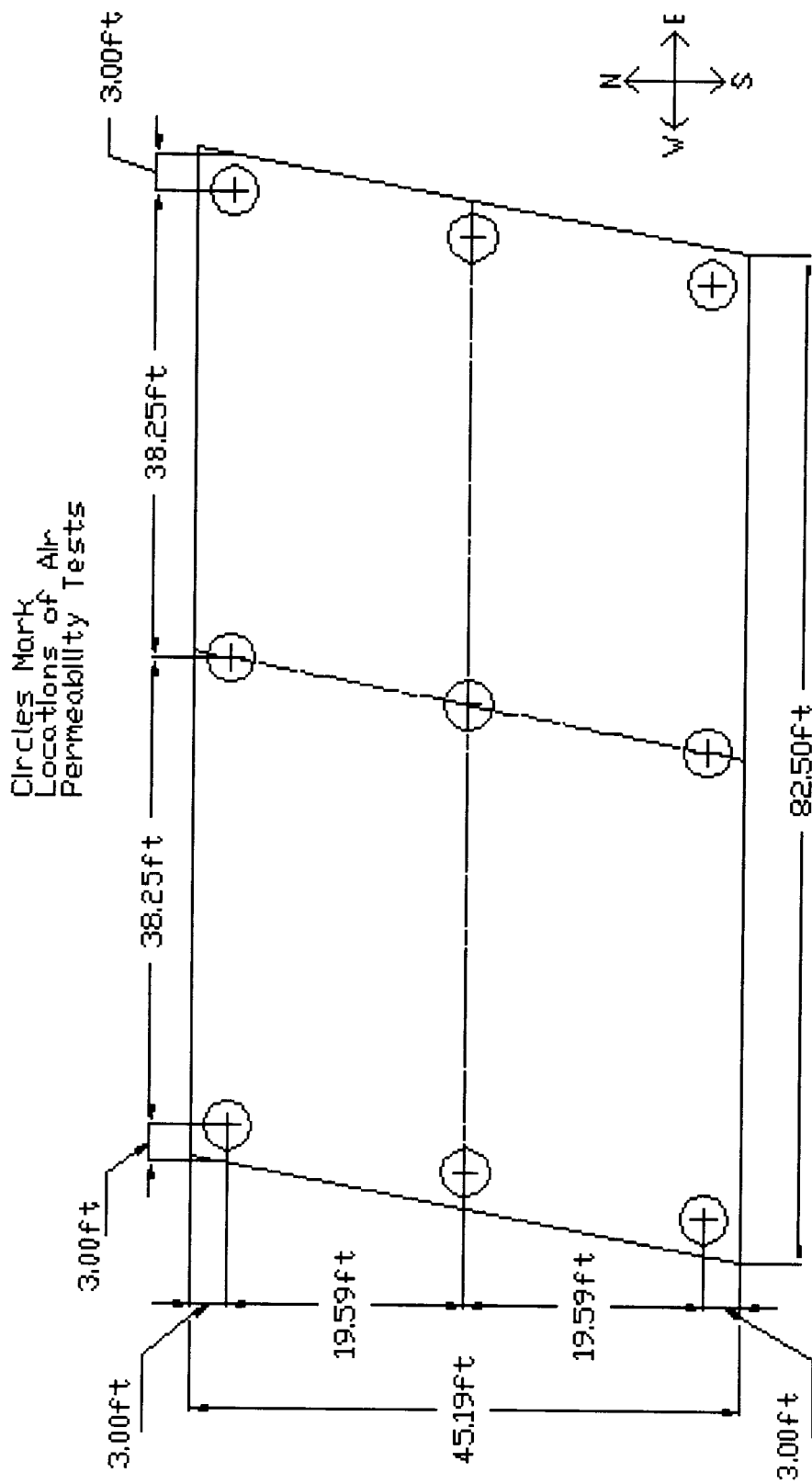


Fig. 3.39: Locations of Surface Air Flow Permeability Readings
Wyckoff Road Eastbound

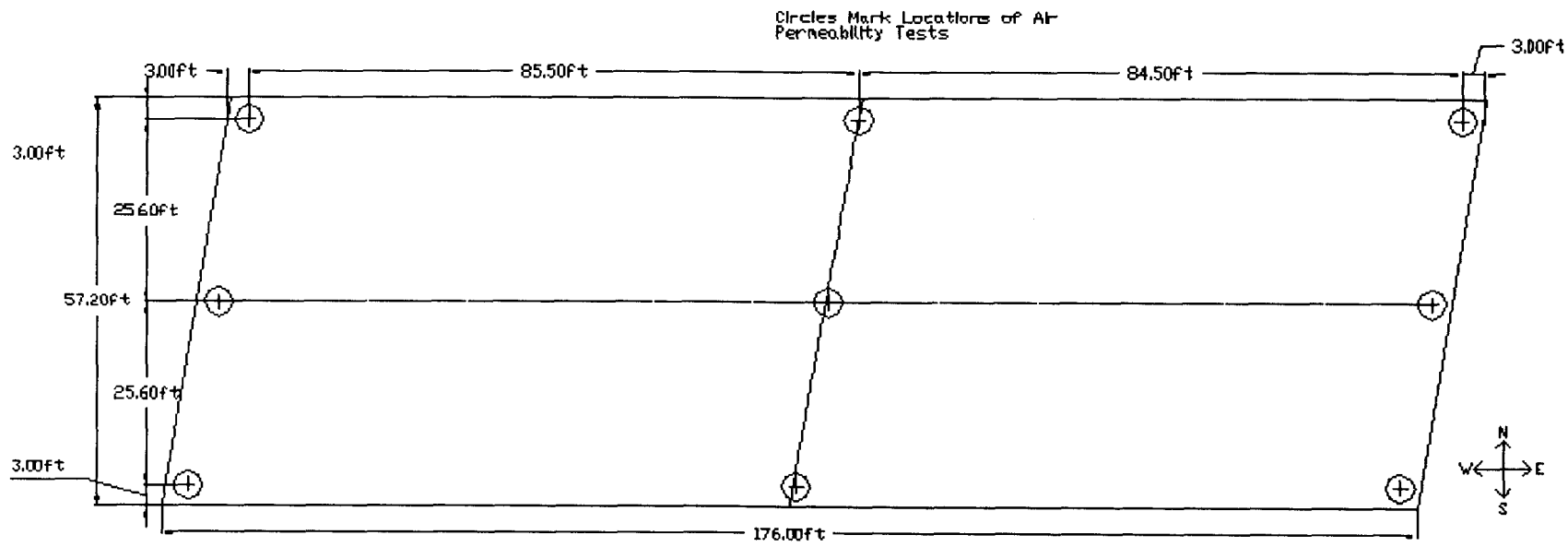


Fig. 3.40: Locations of Surface Air Flow Permeability Indicator Readings
Route 130 Westbound

A total of fifteen readings were taken per cycle using the Electrical Resistance Test for Penetrating Sealers. Three resistance readings were taken on each bridge deck at midspan. The locations of the readings can be seen on Fig. 3.41, 3.42, 3.43, 3.44, and 3.45. Due to the difficulty in creating an adequate gage using the fine line tape and the metal mask, an aluminum mask with a rubber gasket was fabricated. The stiff aluminum mask fabricated with the correct dimensions eliminated the need for the fine line tape and mask as well as producing a better gage according to the acceptance criteria. Though a formal determination has not been made for categorizing unsealed concrete effectiveness against corrosive effects using this testing method, a comparison of the various bridge decks and admixtures in relation to each other can determine which is most effective.

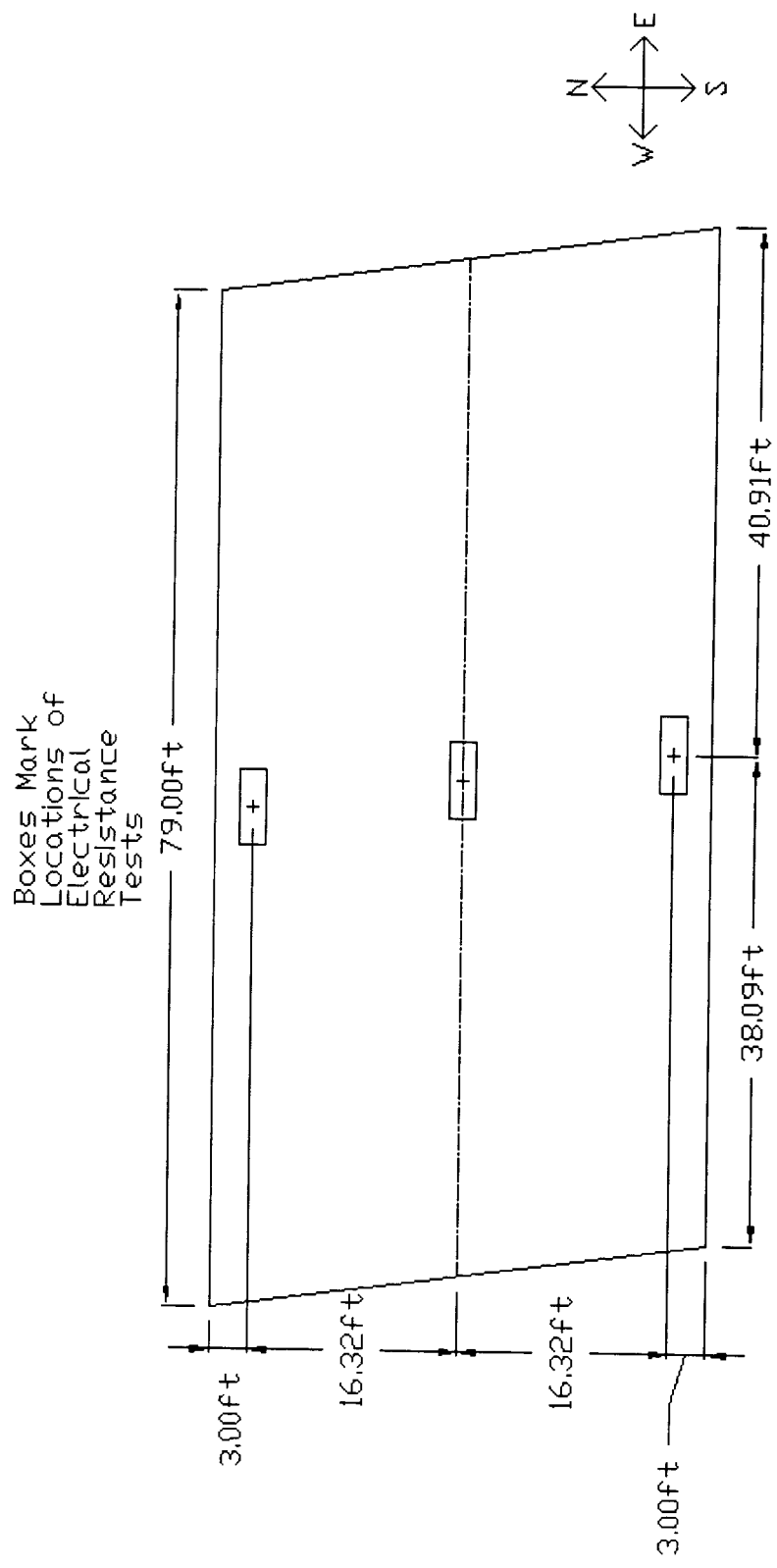


Fig. 3.41: Locations of Electrical Resistance Tests
North Main Street Westbound

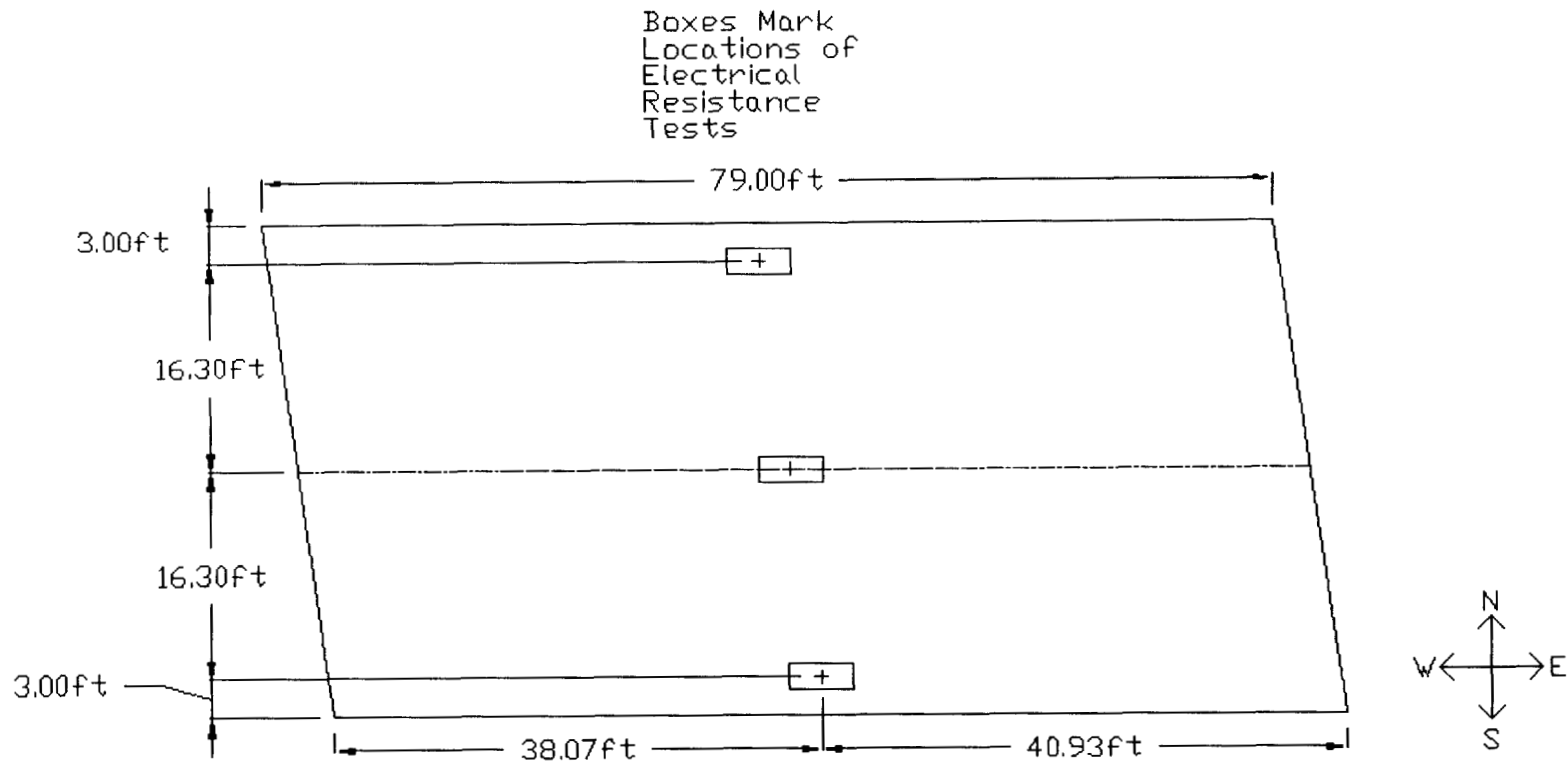


Fig. 3.42: Locations of Electrical Resistance Tests
North Main Street Eastbound

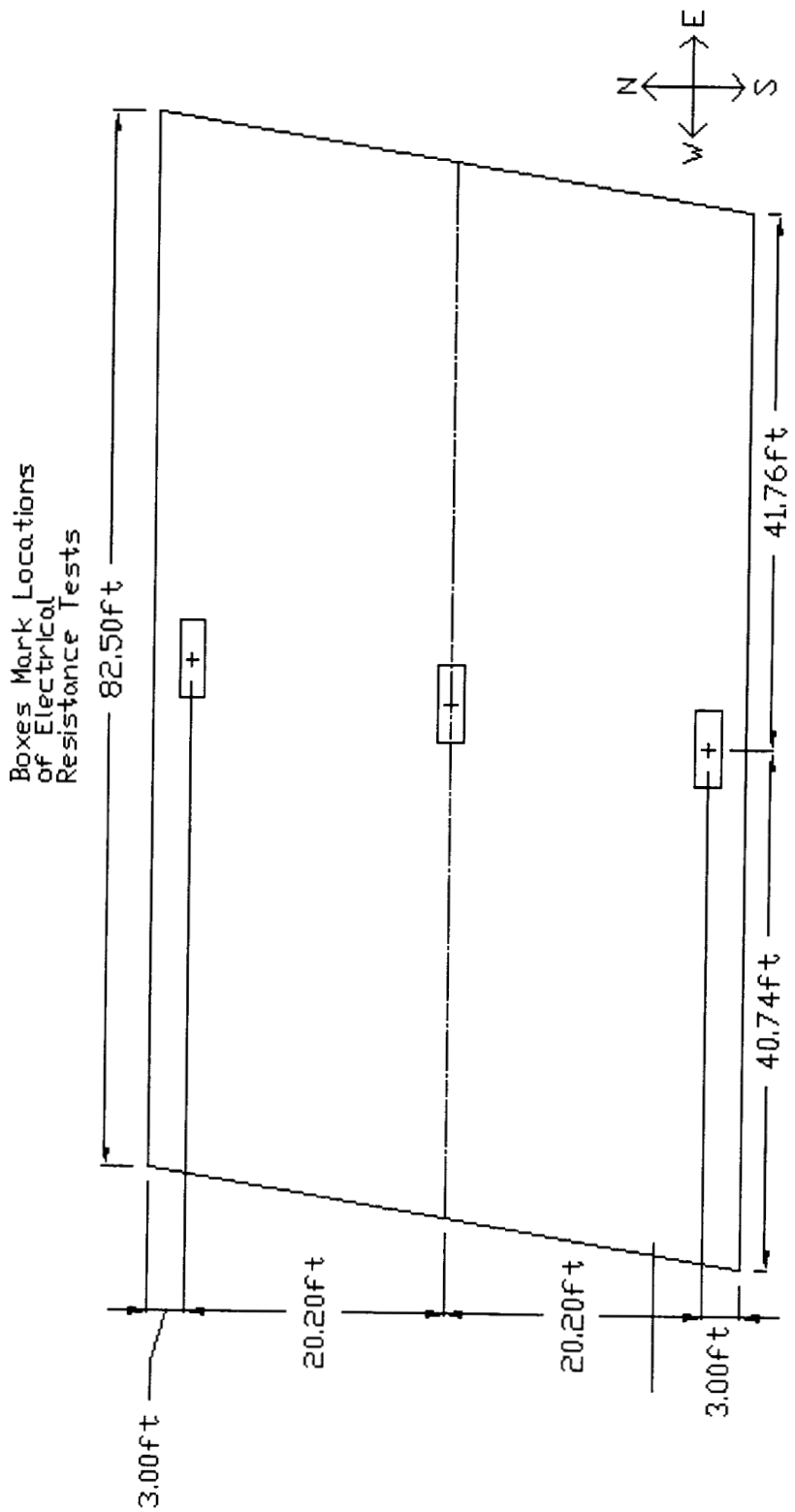


Fig. 3.43: Locations of Electrical Resistance Tests
Wyckoff Road Westbound

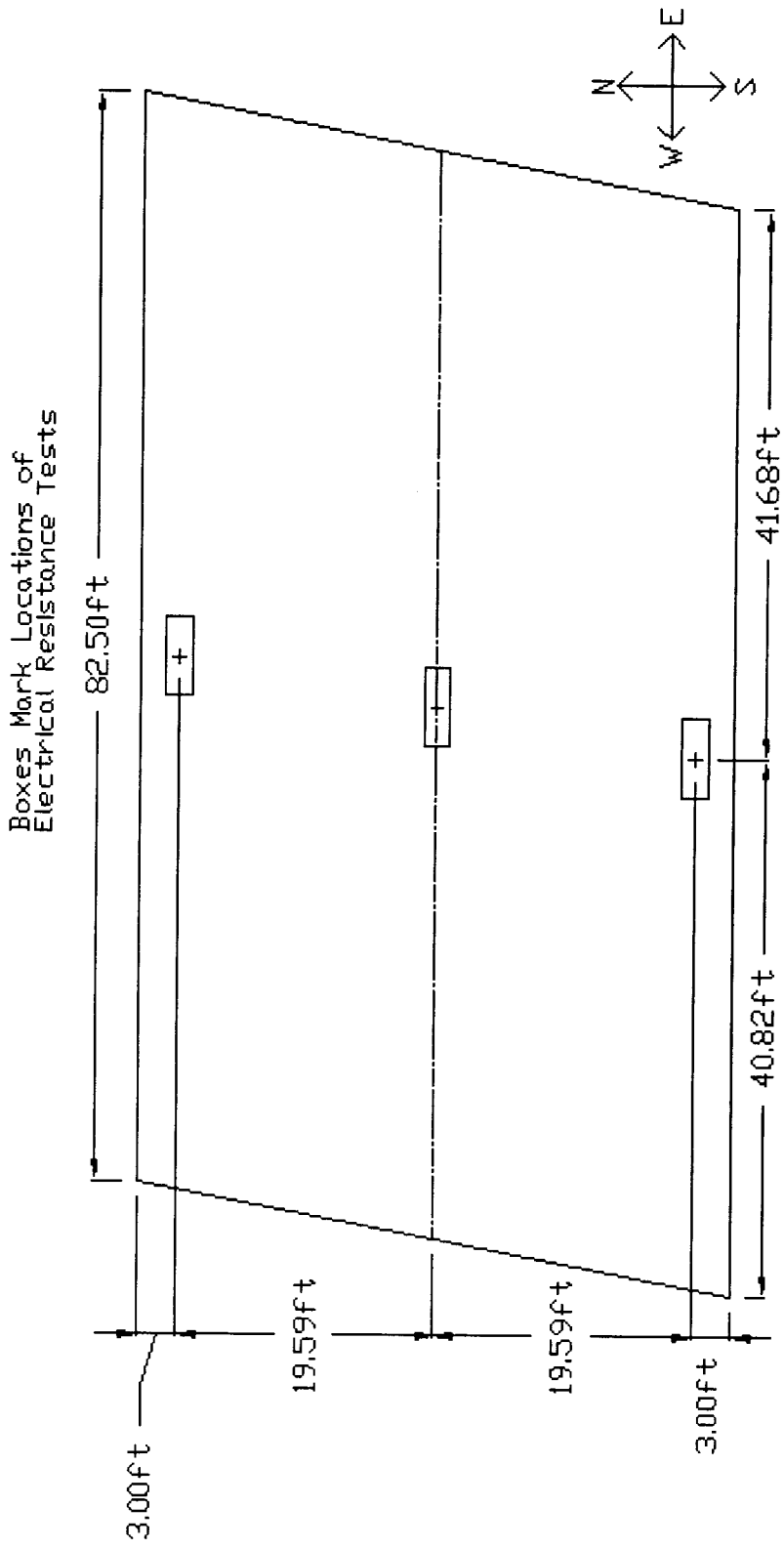


Fig. 3.44: Locations of Electrical Resistance Tests
Wyckoff Road Eastbound

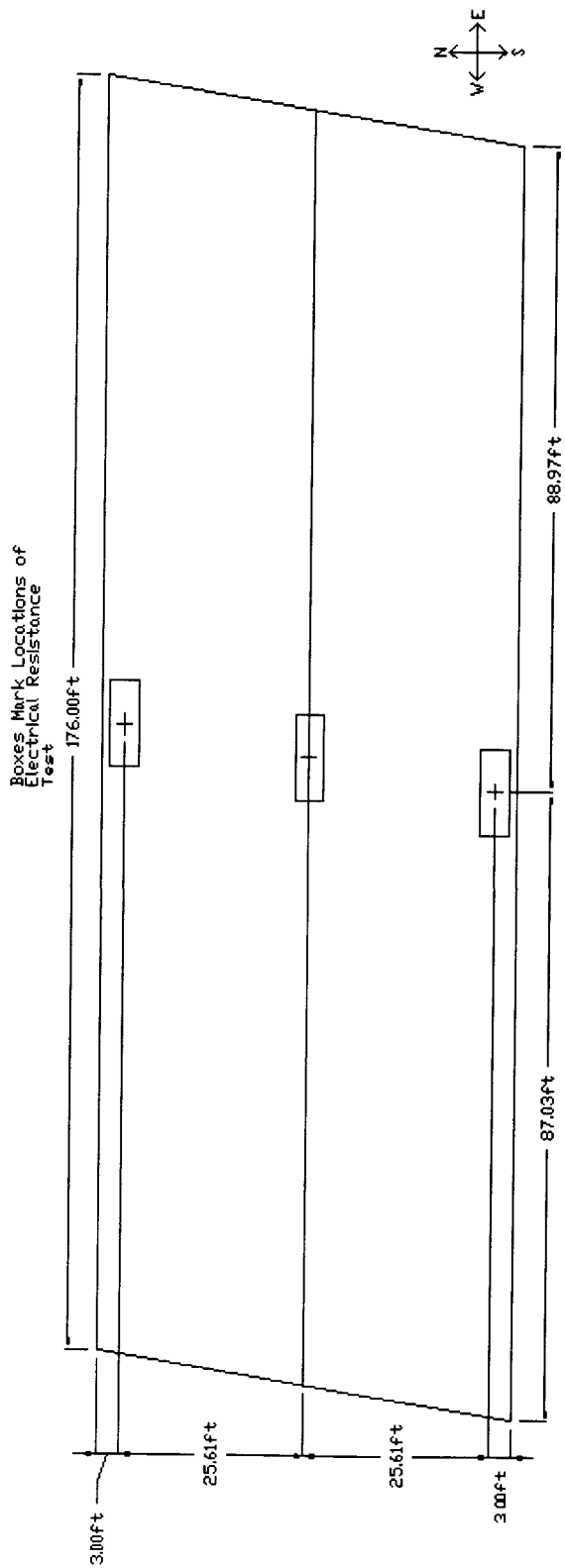


Fig. 3.45: Locations of Electrical Resistance Tests
Route 130 Westbound

3.4 Specimen Preparation for Laboratory Tests

Molds for the ASTM G 109 Test were fabricated from ½ in. Plexiglas because of its impermeability and durability. No. 5 reinforcing bars were used for the test instead of the No. 4 bars specified in the ASTM to better correlate the laboratory test results with data gathered from the field. The connections made to the five bridge decks on Route 133 Hightstown Bypass for the GECOR 6 Corrosion Rate Test were specifically placed on the No. 5 bars that make up the top mat of the reinforcement. Holes were drilled and tapped in one end of each of the pieces of reinforcing bar that were to be placed in the molds to receive stainless threaded rods and nuts. This provided a better connection for the corrosion rate and corrosion potential tests. The wire brushed and wrapped bars were placed into the molds and caulked into place as shown in Fig 3.46.

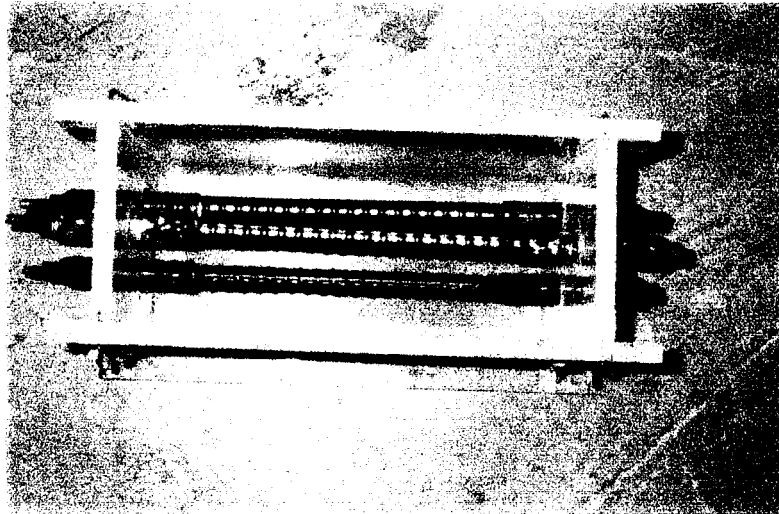


Fig. 3.46: Prepared Minideck Mold

A total of thirty minidecks were cast for the ASTM G 109 Test. All the concrete samples used for the research program were taken from the mixing trucks as the concrete for the individual decks were placed. Six minidecks were cast for each of the five bridges. The concrete taken were from two separate trucks per bridge deck to better correlate the minideck samples to the actual concrete being placed in the new bridge deck. Fresh and hardened concrete properties were taken by the NJDOT Quality Control Team and are provided on Table 4.1 and 4.2 in the Results and Discussion Chapter. The samples were consolidated through rodding and placed under plastic sheets to cure for the first 24 hours. The samples were removed from the molds after the 24 hours and placed in a 100% humidity room to cure for 90 days. Fig. 3.47 shows a minideck after removal from mold.

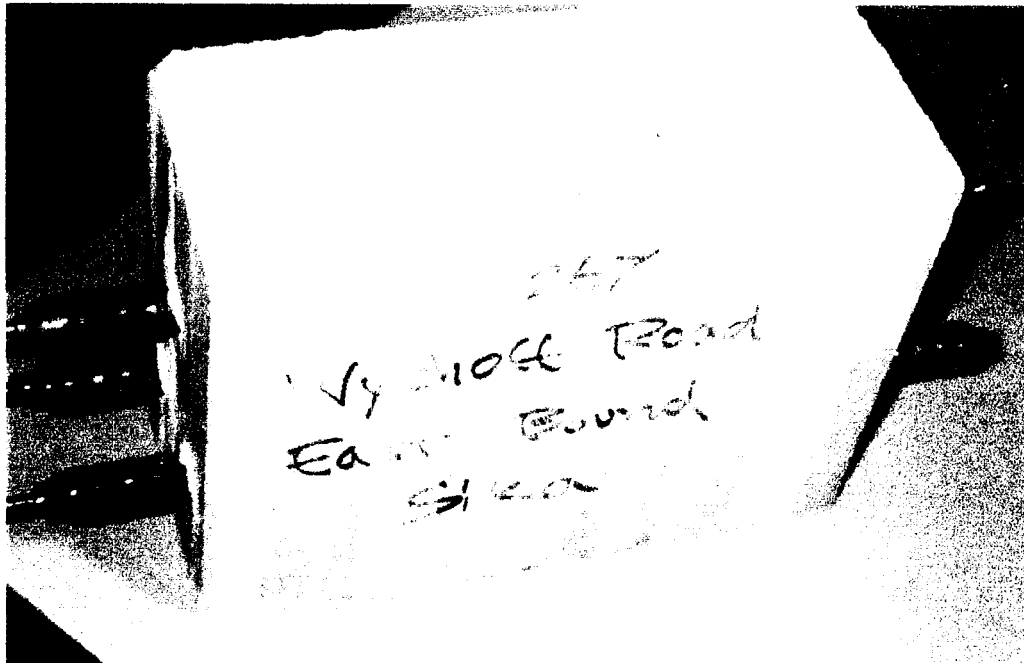


Fig. 3.47: Minideck after Removal from Mold

The minidecks were prepared for accelerated corrosion tests after 90 days. Silicon caulk was then used to fix $\frac{1}{4}$ in. thick Plexiglas dams to the top of each sample in the center. The Plexiglas dam can be seen in Fig. 3.48. Concrete sealing epoxy was used to seal all four sides and the top of the sample except for the area enclosed by the dam. The samples were placed on sturdy racks supported on $\frac{1}{2}$ in. strips of wood. The minideck designations are listed on Table 3.11.

The samples were ponded with 3% NaCl solution and tested for corrosion rate and corrosion potential as per ASTM G 109 and ASTM C 876, respectively. The ponded specimens can be seen in Fig. 3.49. The corrosion data is provided in the Results and Discussion Chapter.



Fig. 3.48: View of Plexiglas Dam

Fig. 3.49: Ponded Minideck Samples

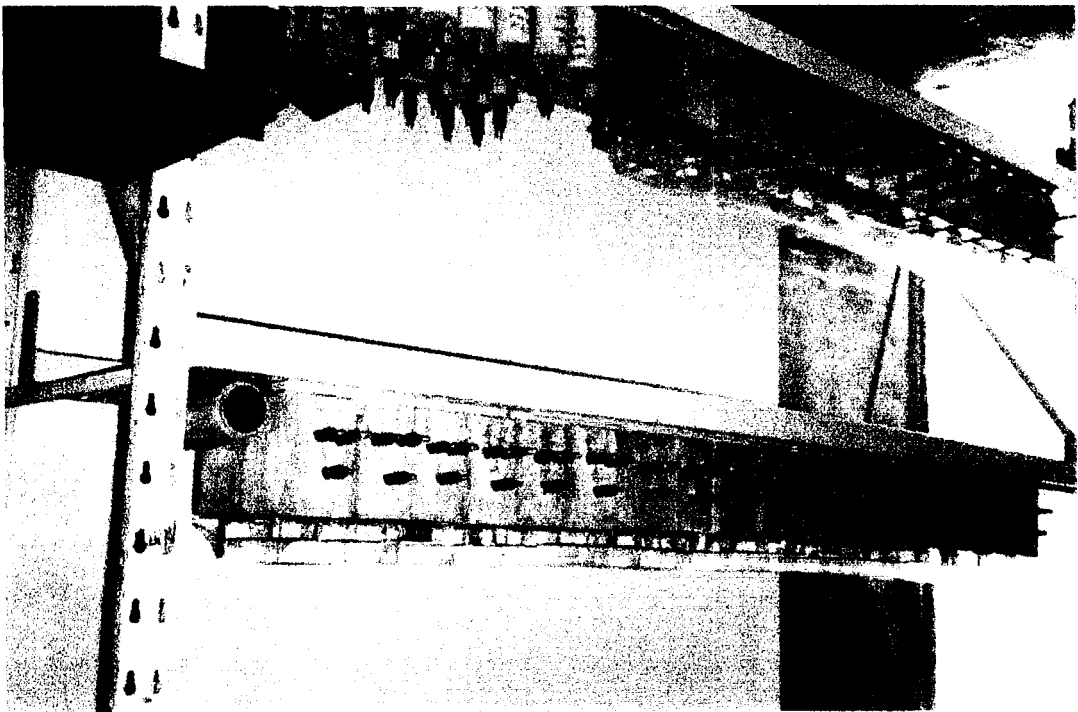
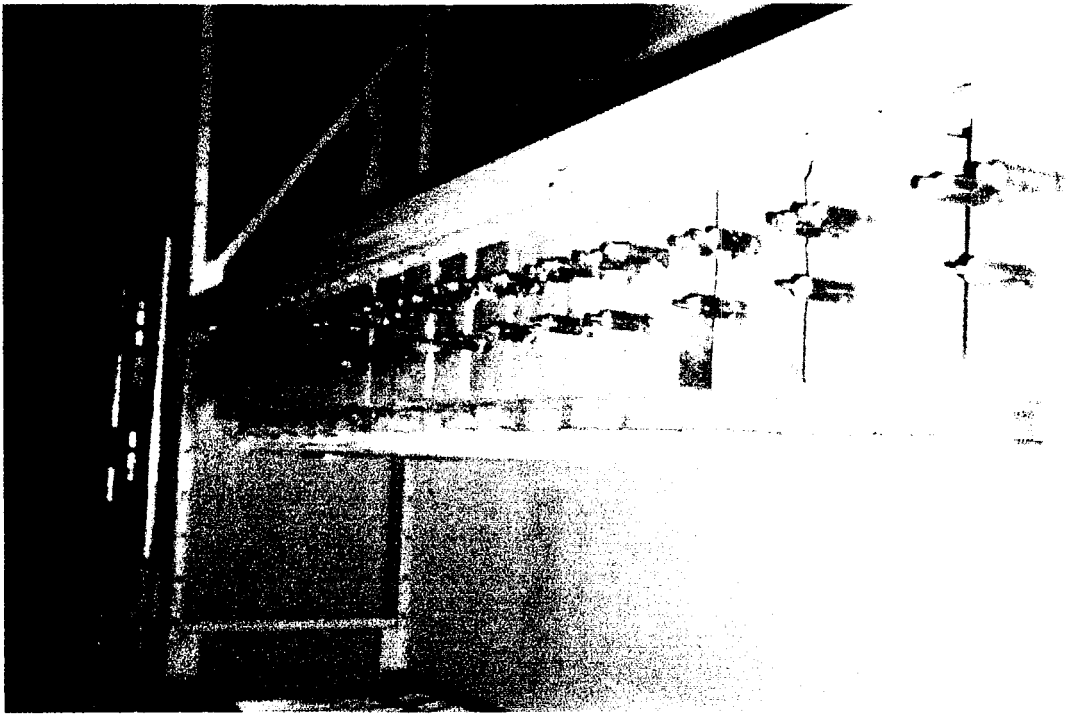


Table 3.11: Minideck Sample Location, Admixture Type, and Designation.

Bridge Location	Corrosion Inhibiting Admixture	ASTM G 109 Minideck Designations
North Main Street - West Bound	W.R. Grace: DCI - S	A
North Main Street - East Bound	Quick Wright Associates, Inc.: XYPEX C-2000	B
Wyckoff Road - West Bound	Master Builders, Inc.: Rheocrete 222+	C
Wyckoff Road - East Bound	Sika Corporation: Ferrogard 901	D
Route 130 - West Bound	Control: none	E

4. Results and Discussion

The results presented consist of fresh and hardened concrete properties, accelerated laboratory tests, and field measurement. Fresh concrete properties are presented in Table 4.1. Hardened concrete properties are presented in Table 4.2

Table 4.1: Fresh Concrete Properties

Minideck	Concrete Temp. (°F)	Slump (inches)	Entrained Air Content (%)
A	65	3.38	6.00
B	64	3.00	5.85
C	82	3.38	5.70
D	78	3.88	5.05
E	84	4.00	5.28

Table 4.2: Hardened Concrete Properties

Minideck	28Day Average Compressive Strength (PSI)
A	5825
B	5305
C	4425
D	6123
E	4935

Form Tables 4.1 and 4.2, it can be seen that the slump and air contents are not significantly different for the various admixtures. The slump varied from 3 to 4 in., where as the air content varied from 5 to 6%.

Compressive strength varied from 4425 to 6125 psi. The variation could be considered a little high.

4.1.1 North Main Street Westbound: Laboratory Tests

The data collected for the ASTM G 109 tests on the concrete samples obtained from North Main Street Westbound are presented on the following Tables 4.3 and 4.4, and Fig. 4.1 and 4.2. The concrete samples contained the corrosion inhibiting admixture W.R. Grace: DCI – S. Corrosion rate and corrosion potential are tabulated on Table 4.3 and 4.4, respectively, and the corresponding graphical variations are presented in Fig. 4.1 and 4.2.

Table 4.3: Minideck A - ASTM G 109 Corrosion Rate ($\mu\text{A}/\text{cm}^2$)

Specimen	Cycle 1	Cycle 2	Cycle 3	Cycle 4	Cycle 5	Cycle 6	Cycle 7	Cycle 8
A1	0.60	0.90	0.60	0.90	1.00	0.90	0.90	1.00
A2	0.30	0.60	0.70	0.80	1.00	0.80	1.00	0.90
A3	0.20	1.00	0.60	1.10	1.00	1.10	1.50	1.50
A4	1.00	0.50	0.30	0.70	0.80	0.70	0.80	0.80
A5	0.30	0.10	0.10	0.00	0.40	0.10	0.10	0.20
A6	0.10	0.30	0.30	0.50	0.40	0.30	0.40	0.40
A Average	0.42	0.57	0.43	0.67	0.77	0.65	0.78	0.80

Table 4.4: Minideck A - ASTM G 109 Corrosion Potential (mV)

Specimen	Cycle 1	Cycle 2	Cycle 3	Cycle 4	Cycle 5	Cycle 6	Cycle 7	Cycle 8
A1	N/A	N/A	-11.67	-12.12	-15.29	-13.88	-23.07	-12.54
A2	N/A	N/A	-2.19	-1.48	-4.97	-3.06	-11.80	-1.09
A3	N/A	N/A	-0.75	-6.80	-5.39	-3.27	-10.46	-0.86
A4	N/A	N/A	-2.07	-2.68	-7.36	-6.44	-16.03	-6.16
A5	N/A	N/A	-5.60	-5.92	-10.28	-9.53	-18.69	-8.99
A6	N/A	N/A	-13.58	-13.91	-18.46	-17.71	-27.64	-20.50
A Average	N/A	N/A	-5.98	-7.15	-10.29	-8.98	-17.95	-8.36

As mentioned earlier, each cycle consists of two weeks of ponding with salt water and two weeks of drying.

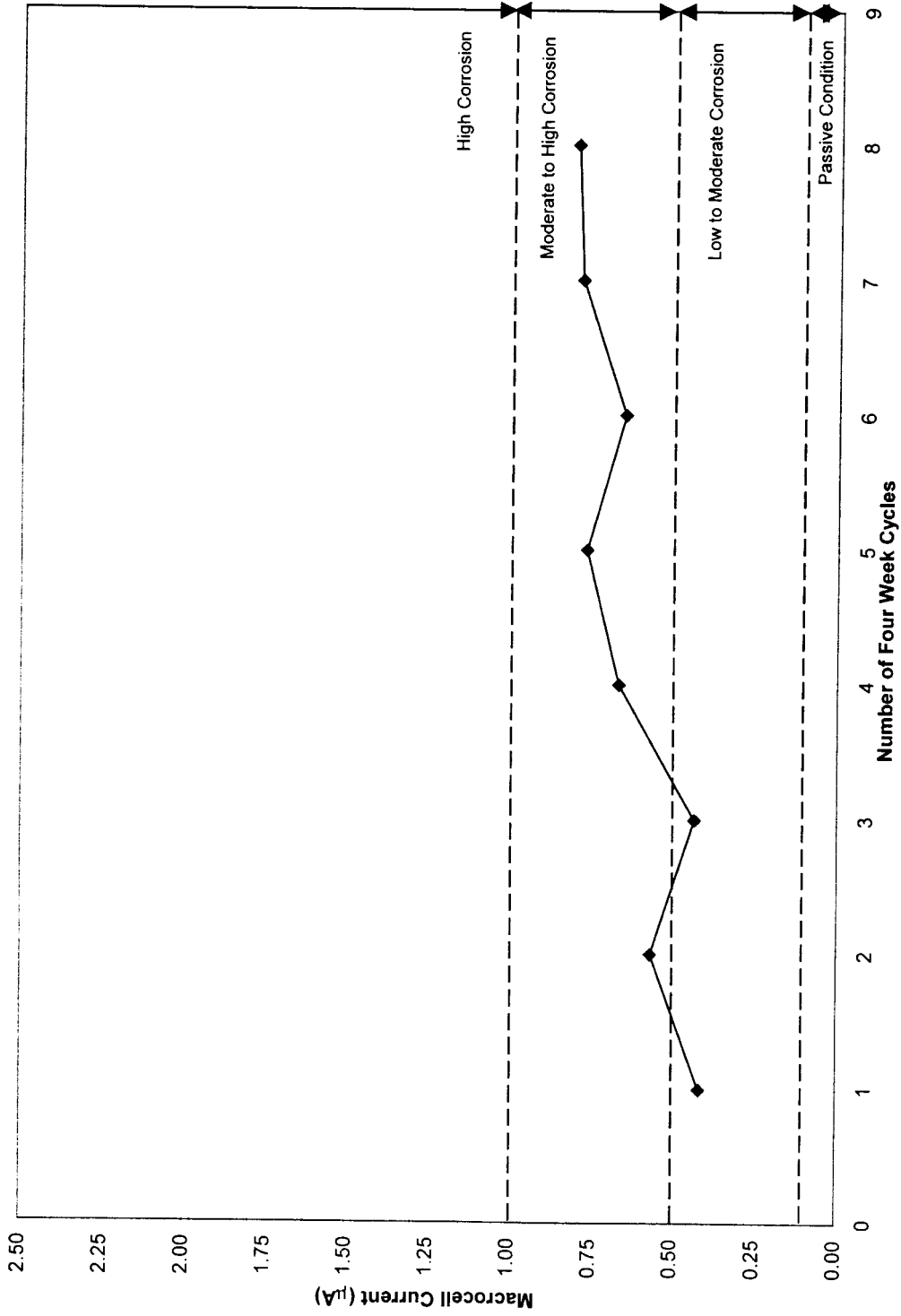


Fig. 4.1: Minideck A - Average Corrosion Rate Macrocell Current (µA)

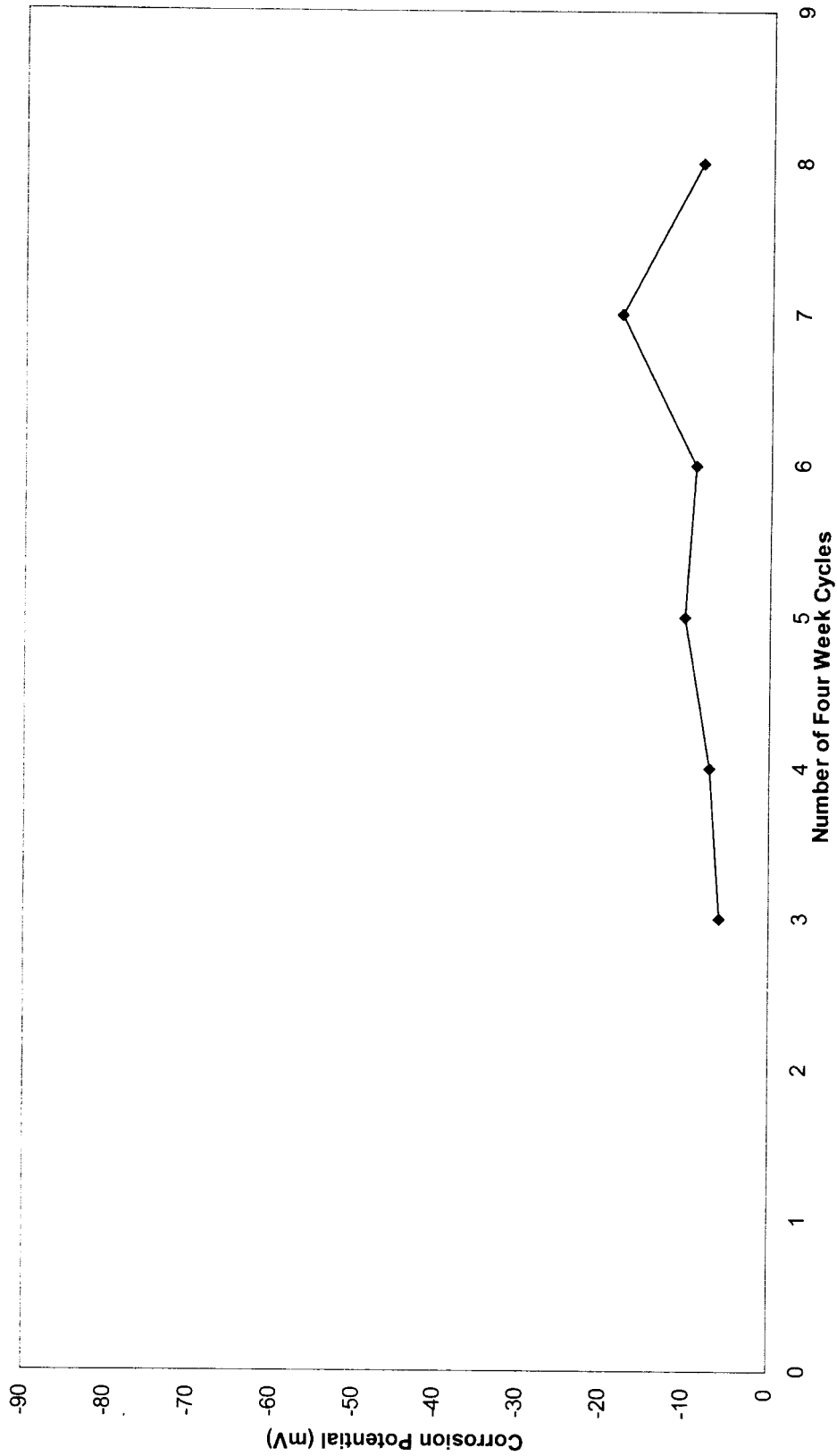


Fig. 4.2: Minideck A - Average Corrosion Potential (mV)

4.1.2 North Main Street Westbound: Field Tests

The data collected for the GECOR 6 Corrosion Rate, Surface Air Flow Permeability, and Electrical Resistance Test for Penetrating Sealers on the bridge deck over North Main Street Westbound are presented in Tables 4.5 to 4.9 and Fig. 4.3 to 4.7. The concrete used in the bridge deck contained the corrosion inhibiting admixture W.R. Grace: DCI – S. GECOR 6: corrosion rate, corrosion potential, and electrical resistance are tabulated on Tables 4.5, 4.6, 4.7, and displayed on Fig. 4.3, 4.4, 4.5, respectively. Air permeability readings are presented on Table 4.8 and Fig. 4.6. Electrical resistance readings are presented in Table 4.9 and Fig. 4.7.

Table 4.5: North Main Street Westbound GECOR 6 Corrosion Rate ($\mu\text{A}/\text{cm}^2$)

Connection #	Reading No.	1st Quarter	2nd Quarter	3rd Quarter	4th Quarter
B1	1	0.181	0.145	0.063	0.197
	2	0.280	0.157	0.096	0.135
	3	0.265	0.084	0.121	0.201
	4	0.216	0.127	0.171	0.181
	5	0.250	0.110	0.129	0.001
B2	1	0.295	0.231	0.109	0.119
	2	0.264	0.140	0.089	0.094
	3	0.244	0.203	0.136	0.137
	4	0.262	0.116	0.154	0.136
	5	0.211	0.145	0.131	0.131
B3	1	0.222	0.162	0.156	0.208
	2	0.205	0.175	0.147	0.127
	3	0.259	0.178	0.138	0.119
	4	0.206	0.136	0.155	0.139
	5	0.263	0.211	0.159	0.156
B4	1	0.191	0.196	0.155	0.362
	2	0.216	0.169	0.151	0.130
	3	0.274	0.413	0.132	0.162
	4	0.183	0.227	0.128	0.150
	5	0.196	0.154	0.133	0.156
Average		0.234	0.174	0.133	0.152

Table 4.6: North Main Street Westbound GECOR 6 Corrosion Potential (mV)

Connection #	Reading No.	1st Quarter	2nd Quarter	3rd Quarter	4th Quarter
B1	1	-88.8	-127.4	-220.7	-234.9
	2	-56.2	-128.1	-168.6	-154.2
	3	-63.5	-124.5	-190.3	-202.5
	4	-75.9	-140.9	-183.2	-194.3
	5	-83.0	-133.4	-187.8	-192.7
B2	1	-78.2	-126.4	-214.7	-219.7
	2	-84.1	-87.8	-211.8	-218.7
	3	-73.5	-123.6	-218.8	-227.1
	4	-76.4	-120.8	-227.5	-233.2
	5	-73.6	-126.3	-221.1	-235.8
B3	1	-86.4	-108.6	-233.3	-253.5
	2	-95.5	-116.7	-240.4	-249.7
	3	-99.8	-116.1	-266.2	-267.4
	4	-89.9	-126.5	-213.3	-220.5
	5	-95.7	-142.3	-216.6	-226.3
B4	1	-91.2	-142.9	-203.3	-239.2
	2	-98.5	-131.5	-222.4	-245.3
	3	-83.1	-153.3	-203.8	-227.6
	4	-83.2	-141.5	-169.7	-181.7
	5	-91.7	-142.3	-191.1	-201.9
Average		-83.410	-128.045	-210.230	-221.308

Table 4.7: North Main Street Westbound GECOR 6 Electrical Resistance (K Ω)

Connection #	Reading No.	1st Quarter	2nd Quarter	3rd Quarter	4th Quarter
B1	1	1.57	1.42	2.86	1.04
	2	1.22	1.60	1.46	1.05
	3	1.17	1.48	1.53	1.20
	4	1.20	1.44	1.39	0.97
	5	1.06	1.46	1.12	0.83
B2	1	1.18	1.11	1.60	1.30
	2	1.23	1.20	1.27	1.11
	3	1.20	1.24	1.29	1.08
	4	1.16	1.24	1.37	1.06
	5	1.24	1.23	1.28	0.97
B3	1	1.21	1.24	1.45	1.14
	2	1.28	1.55	1.60	1.14
	3	1.26	1.30	1.16	0.97
	4	1.32	1.38	1.14	0.93
	5	1.26	1.34	1.17	1.04
B4	1	1.51	1.52	1.12	1.02
	2	1.20	1.40	1.52	1.12
	3	1.75	1.46	1.82	1.61
	4	1.33	1.44	1.26	1.14
	5	1.27	1.38	1.54	1.14
Average		1.28	1.37	1.45	1.09

Table 4.8: North Main Street Westbound Air Permeability
Vacuum (mm Hg), SCCM (ml/min)

Reading No.	1st Quarter		2nd Quarter		3rd Quarter		4th Quarter	
	Vacuum	SCCM	Vacuum	SCCM	Vacuum	SCCM	Vacuum	SCCM
1	783.70	34.75	776.90	53.10	774.80	58.43	776.70	29.02
2	782.20	52.22	796.90	48.09	770.00	57.30	771.80	46.28
3	785.60	24.45	791.60	54.32	708.50	31.27	683.50	32.76
4	786.10	16.66	787.20	55.93	779.10	57.09	678.20	50.49
5	783.70	30.75	795.40	43.18	774.40	57.39	676.90	32.57
6	784.90	24.42	792.30	54.87	780.20	50.07	770.00	32.60
7	779.10	56.79	748.80	45.19	776.30	44.59	679.00	32.55
8	786.30	15.63	790.50	33.31	781.10	39.03	680.40	32.66
9	784.20	34.34	783.90	55.72	779.30	53.01	775.60	23.42
Average	783.98	32.22	784.83	49.30	769.30	49.80	721.34	34.71

Table 4.9: North Main Street Westbound Electrical Resistance Sealer Test (K Ω)

Quarter	Reading No.	DC End to End (Ω) Strip 1	DC End to End (Ω) Strip 2	DC Side to Side (M Ω)	AC (K Ω)	Avg. AC (K Ω)
1	1	9.2	14.5	6.0	150.0	74.0
	2	17.8	8.1	5.0	22.0	
	3	6.0	5.2	10.0	50.0	
2	1	4.7	8.8	27.3	210.0	118.3
	2	4.8	6.4	26.5	57.0	
	3	2.8	2.4	6.7	88.0	
3	1	6.2	2.4	22.0	200.0	124.7
	2	8.6	6.4	36.0	54.0	
	3	2.9	2.2	7.8	120.0	
4	1	4.6	9.1	32.6	36.0	87.3
	2	6.5	6.8	8.5	120.0	
	3	2.6	2.5	23.5	106.0	

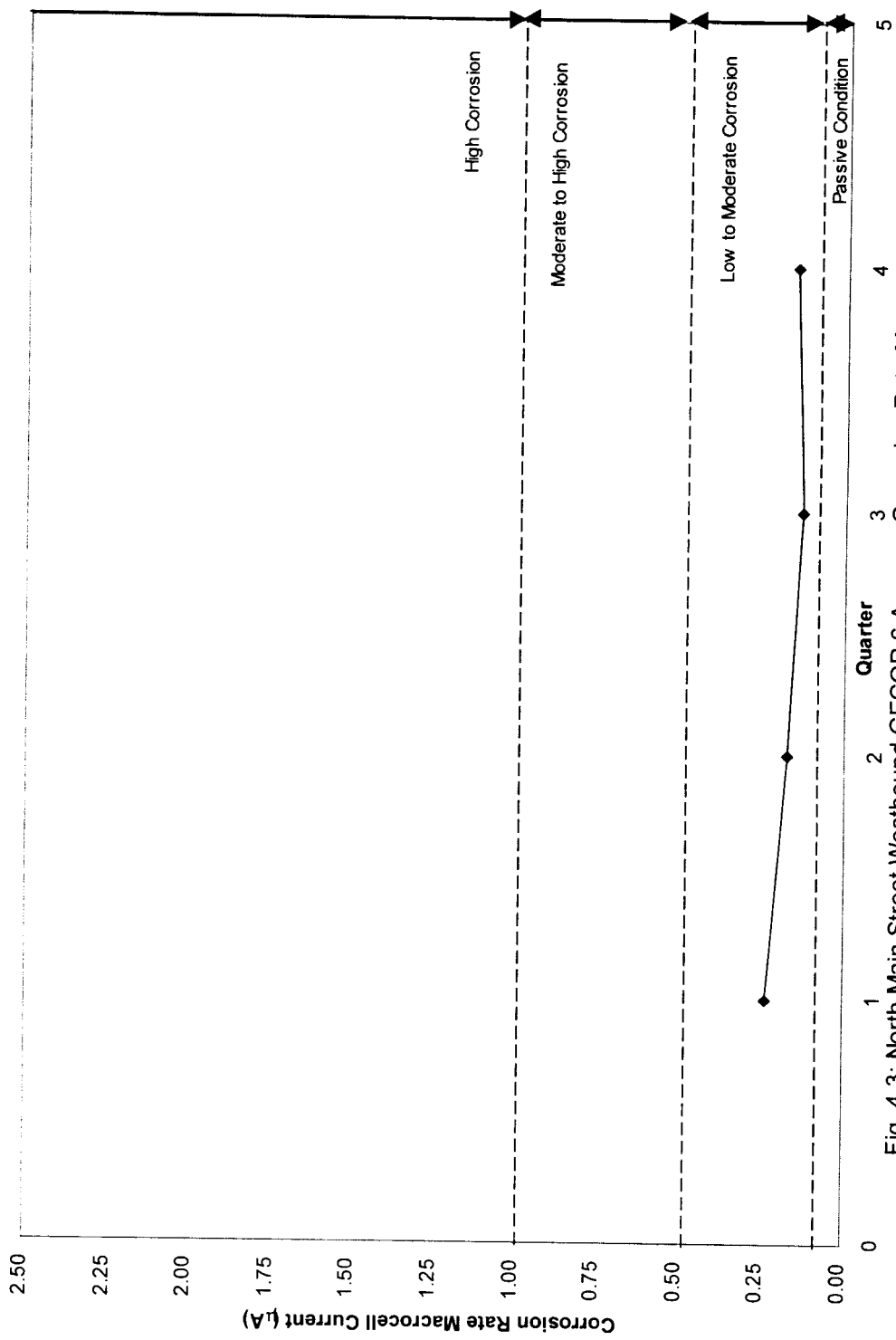


Fig. 4.3: North Main Street Westbound GECOR 6 Average Corrosion Rate Macrocell Current (µA)

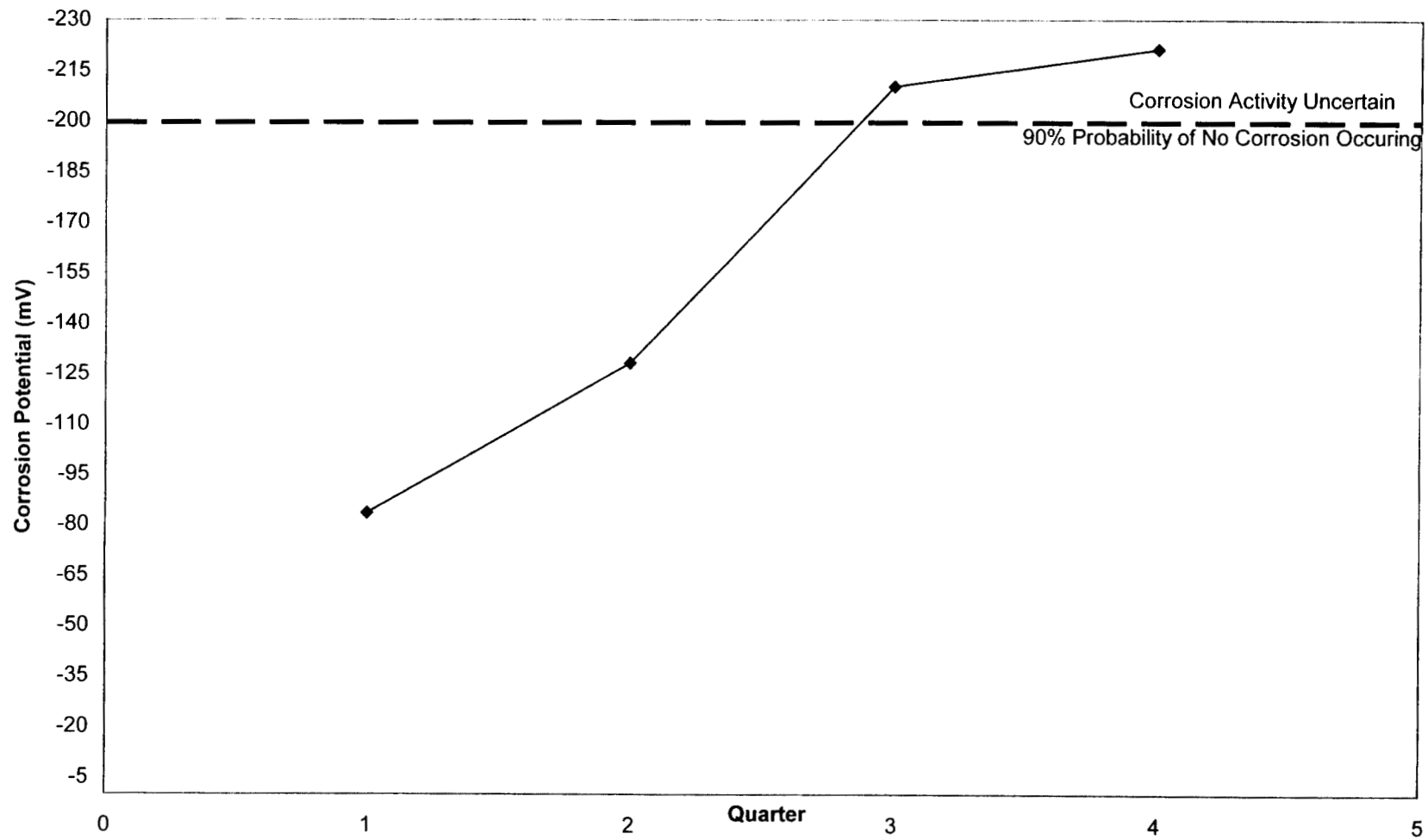


Fig. 4.4: North Main Street Westbound GECOR 6 Average Corrosion Potential (mV)

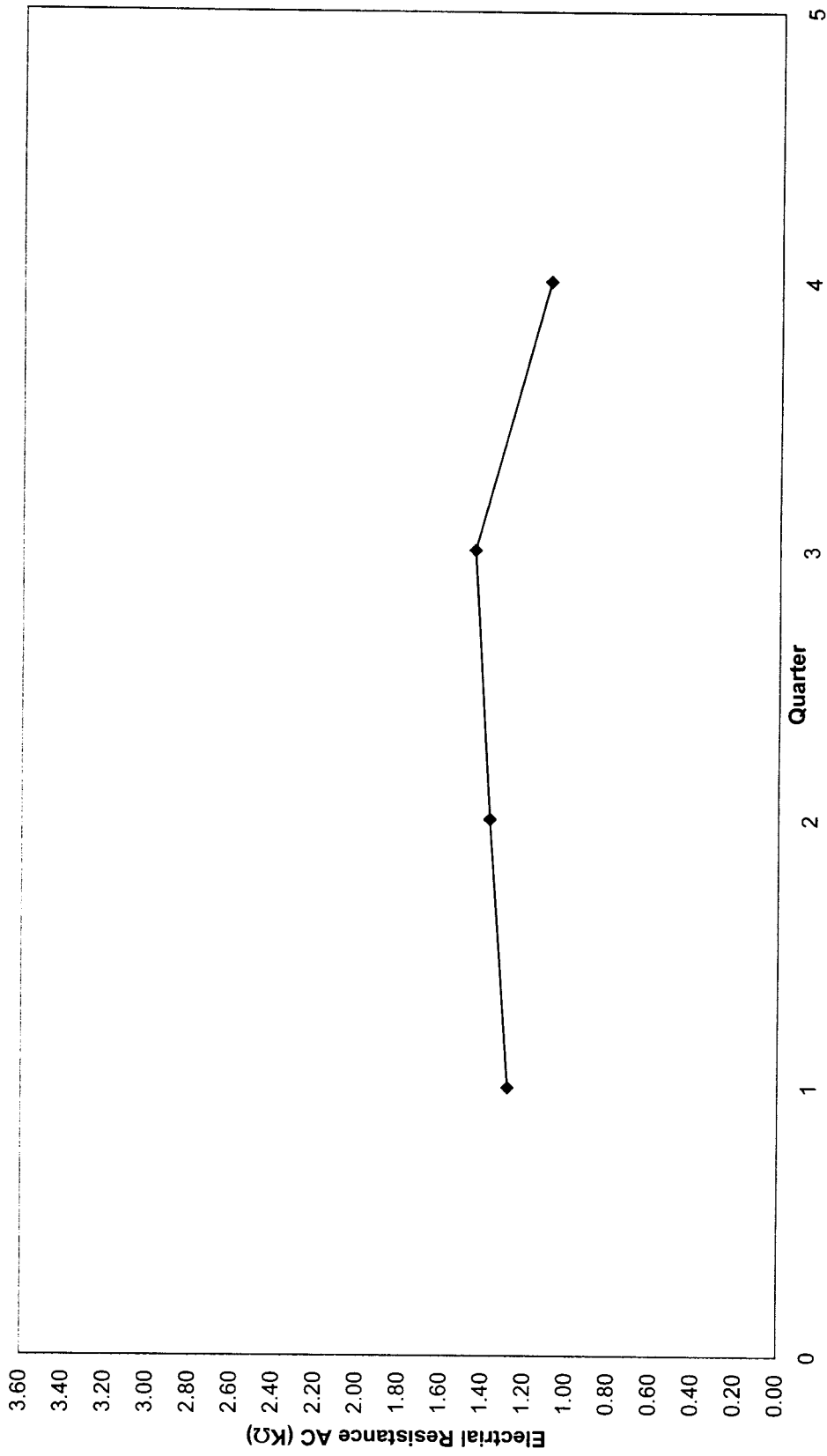


Fig. 4.5: North Main Street Westbound GECOR 6 Average Electrical Resistance AC (KΩ)

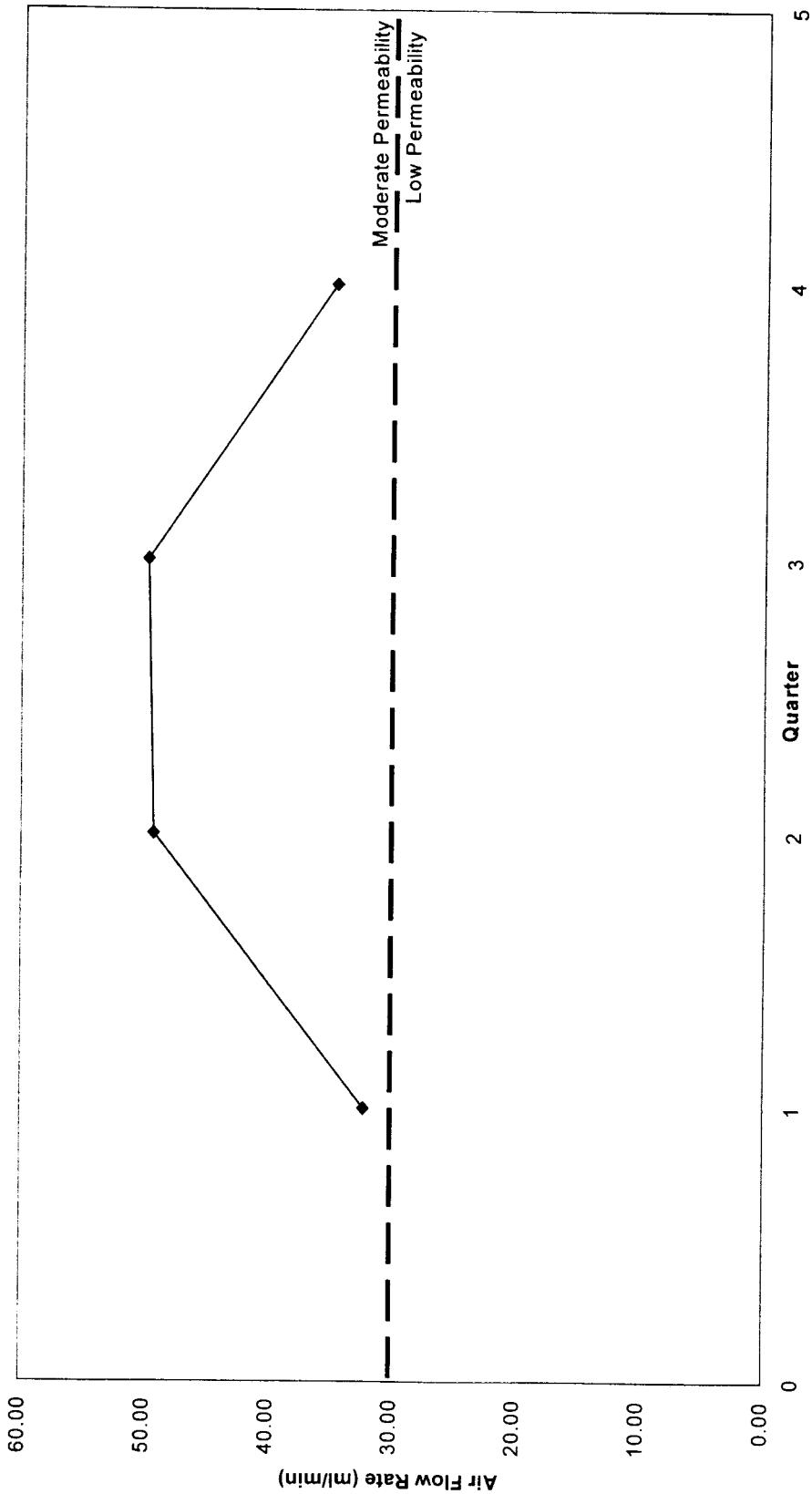


Fig. 4.6: North Main Street Westbound Average Air Flow Rate (ml/min)

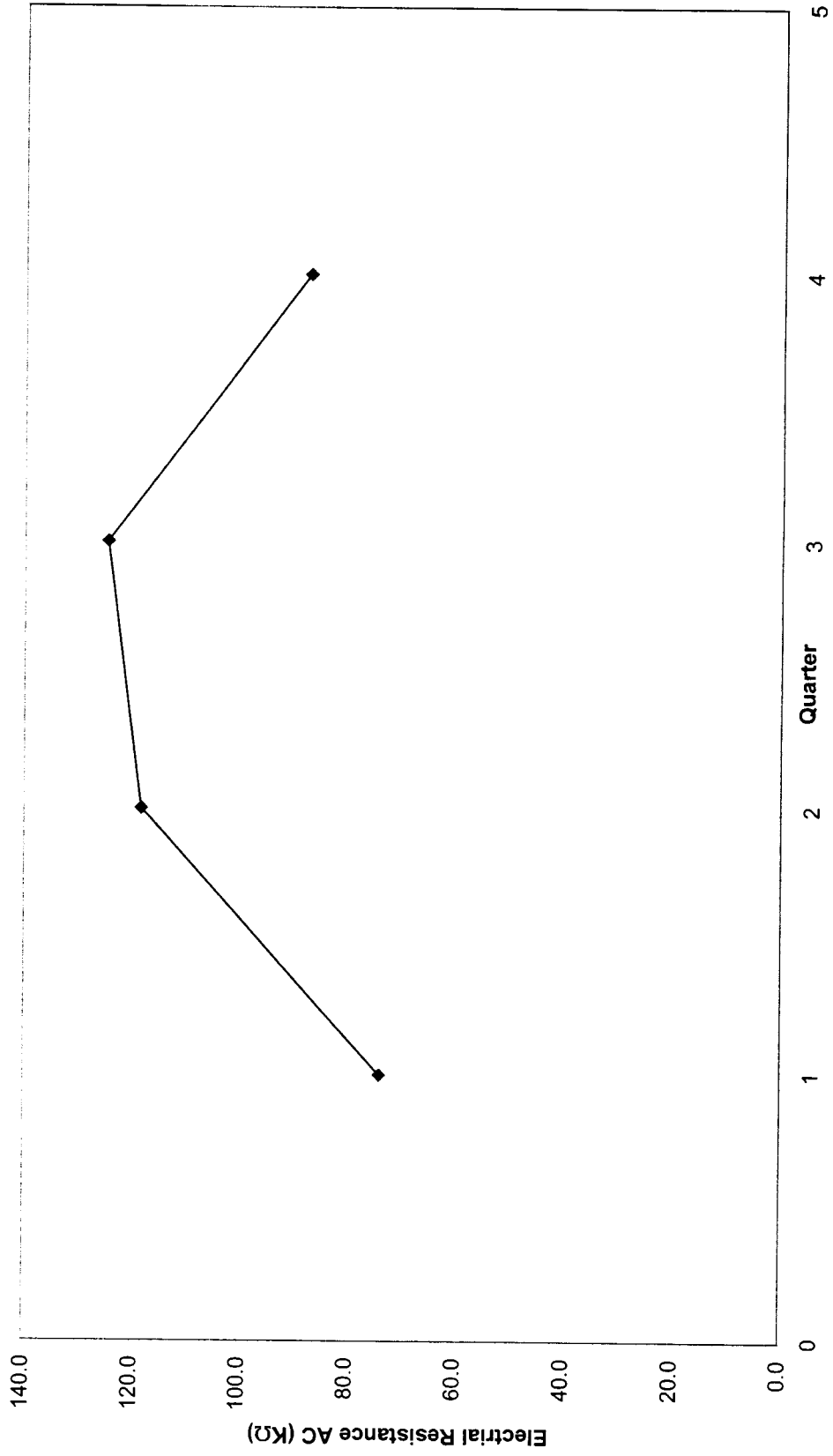


Fig. 4.7: North Main Street Westbound Average Electrical Resistance AC (KΩ)

4.2.1 North Main Street Eastbound Laboratory Tests

The data collected for the ASTM G 109 tests on the concrete samples obtained from North Main Street Eastbound are presented on the following Tables 4.10 and 4.11, and Fig. 4.8 and 4.9. The concrete samples contained the corrosion inhibiting admixture Quick Wright Associates, Inc.: XYPEX C-1000. Corrosion rate and corrosion potential are tabulated on Table 4.10 and 4.11, respectively, and the corresponding graphical variations are presented in Fig. 4.8 and 4.9.

Table 4.10: Minideck B - ASTM G 109 Corrosion Rate ($\mu\text{A}/\text{cm}^2$)

Specimen	Cycle 1	Cycle 2	Cycle 3	Cycle 4	Cycle 5	Cycle 6	Cycle 7	Cycle 8
B1	0.00	0.20	0.20	0.30	0.30	0.30	0.50	0.40
B2	0.10	0.00	0.00	0.10	0.20	0.10	0.30	0.20
B3	0.00	0.10	0.10	0.10	0.30	0.20	0.20	0.20
B4	0.10	0.20	0.10	0.00	0.00	0.10	0.10	0.10
B5	0.10	0.30	0.40	0.20	0.40	0.50	0.50	0.50
B6	0.30	0.30	0.50	0.30	0.50	0.20	0.40	0.40
B Average	0.10	0.18	0.22	0.17	0.28	0.23	0.33	0.30

Table 4.11: Minideck B - ASTM G 109 Corrosion Potential (mV)

Specimen	Cycle 1	Cycle 2	Cycle 3	Cycle 4	Cycle 5	Cycle 6	Cycle 7	Cycle 8
B1	N/A	N/A	-21.52	-21.55	-24.51	-21.98	-31.16	-20.19
B2	N/A	N/A	-18.61	-17.65	-20.35	-18.32	-27.87	-15.69
B3	N/A	N/A	-20.51	-23.42	-30.03	-31.47	-45.88	-37.66
B4	N/A	N/A	-19.45	-19.27	-21.94	-19.32	-28.53	-17.60
B5	N/A	N/A	-17.75	-17.26	-20.33	-17.48	-25.77	-14.35
B6	N/A	N/A	-16.33	-18.64	-22.87	-23.64	-35.04	-27.19
B Average	N/A	N/A	-19.03	-19.63	-23.34	-22.04	-32.38	-22.11

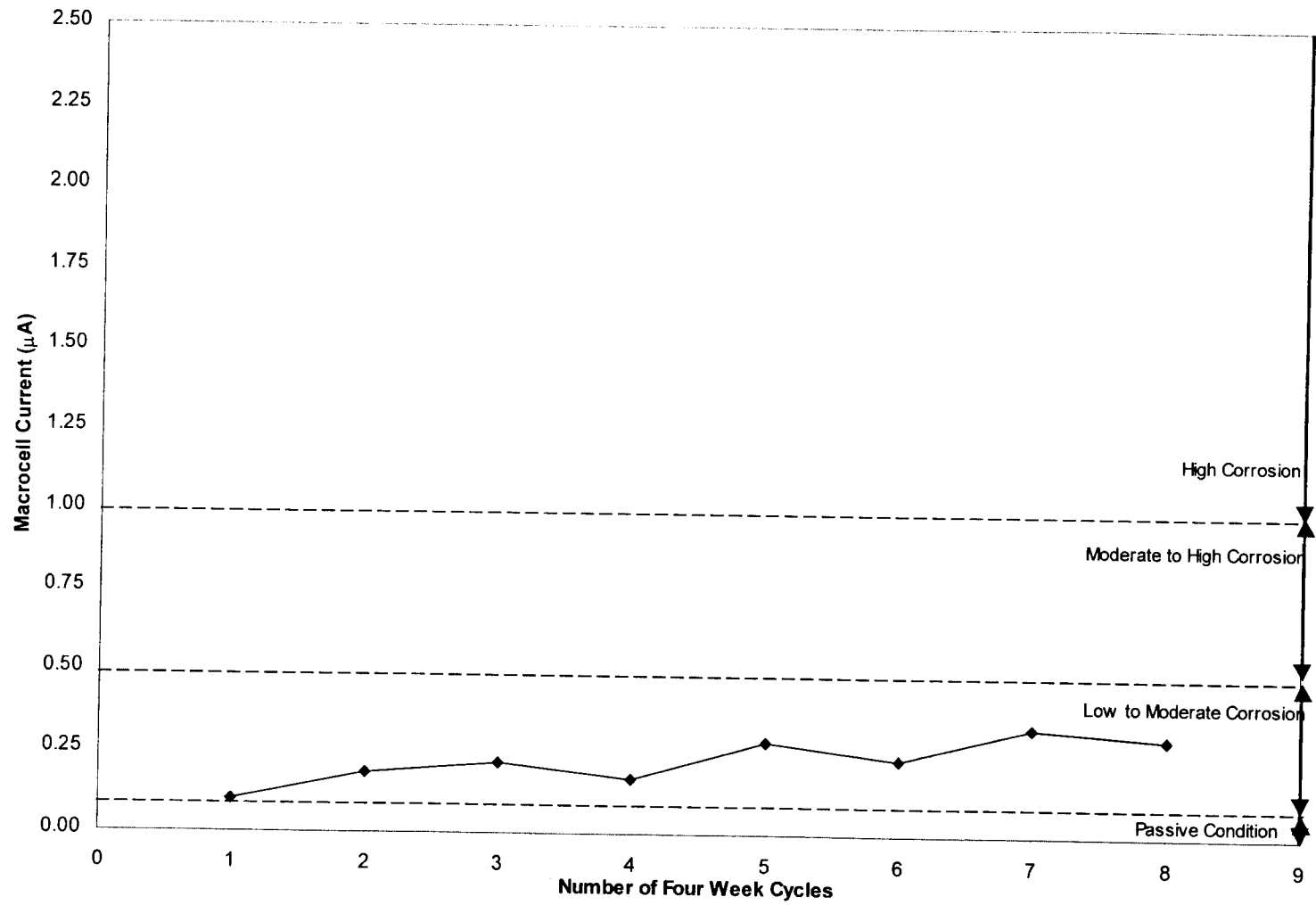


Fig. 4.8: Minideck B - Average Corrosion Rate Macrocell Current (µA)

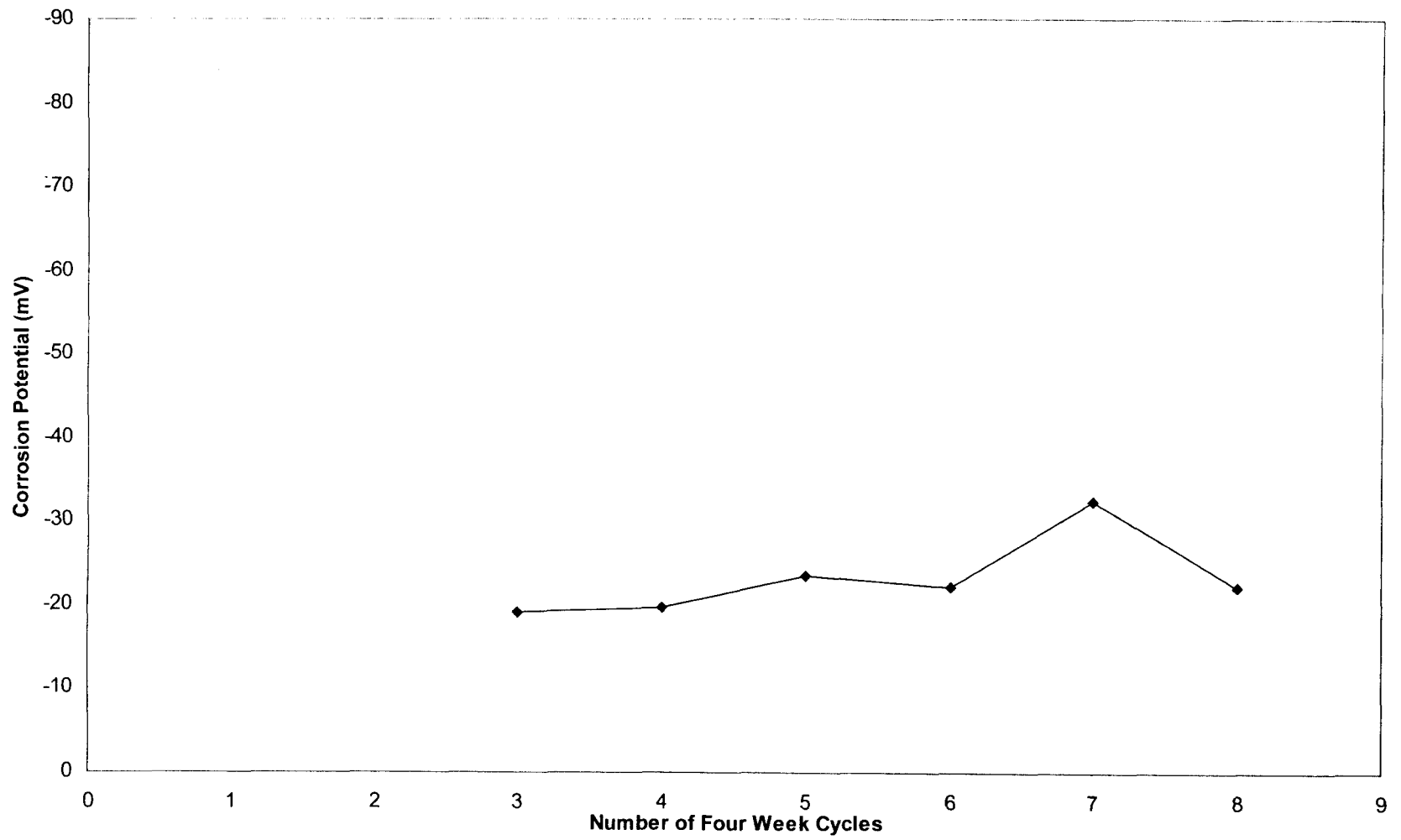


Fig. 4.9: Minideck B - Average Corrosion Potential (mV)

4.2.2 North Main Street Eastbound: Field Tests

The data collected for the GECOR 6 Corrosion Rate, Surface Air Flow Permeability, and Electrical Resistance Test for Penetrating Sealers on the bridge deck over North Main Street Eastbound are presented in Tables 4.12 to 4.16 and Fig. 4.10 to 4.14. The concrete used in the bridge deck contained the corrosion inhibiting admixture Quick Wright Associates, Inc.: XYPEX C-1000. GECOR 6: corrosion rate, corrosion potential, and electrical resistance are tabulated on Tables 4.12, 4.13, 4.14, and displayed on Fig. 4.10, 4.11, 4.12, respectively. Air permeability readings are presented on Table 4.15 and Fig. 4.13. Electrical resistance readings are presented in Table 4.16 and Fig. 4.14.

Table 4.12: North Main Street Eastbound GECOR 6 Corrosion Rate ($\mu\text{A}/\text{cm}^2$)

Connection #	Reading No.	1st Quarter	2nd Quarter	3rd Quarter	4th Quarter
B1	1	0.050	0.156	0.294	0.259
	2	0.093	0.231	0.382	0.209
	3	0.090	0.068	0.138	0.455
	4	0.091	0.179	0.276	0.200
	5	0.050	0.120	0.264	0.398
B2	1	0.098	0.115	0.215	0.743
	2	0.140	0.139	0.409	0.654
	3	0.080	0.909	0.242	0.252
	4	0.081	0.084	0.307	0.328
	5	0.077	0.140	0.269	0.253
B3	1	0.087	0.134	0.478	0.884
	2	0.100	0.287	0.432	0.296
	3	0.069	0.083	0.323	0.539
	4	0.056	0.130	0.354	0.342
	5	0.097	0.101	0.288	0.666
B4	1	0.088	0.067	0.110	0.088
	2	0.152	0.087	0.507	0.438
	3	0.091	0.105	0.241	0.361
	4	0.089	0.085	0.324	0.539
	5	0.100	0.069	0.424	0.593
	Average	0.089	0.164	0.314	0.425

Table 4.13: North Main Street Eastbound GECOR 6 Corrosion Potential (mV)

Connection #	Reading No.	1st Quarter	2nd Quarter	3rd Quarter	4th Quarter
B1	1	-54.9	-98.0	-143.5	-139.6
	2	-16.8	-67.8	-87.3	-89.6
	3	-16.7	-24.8	-92.2	-125.8
	4	-19.8	-35.5	-88.6	-103.4
	5	-5.8	-57.1	-66.6	-91.2
B2	1	-63.1	-82.2	-130.2	-177.9
	2	-57.4	-51.3	-118.6	-135.6
	3	-20.3	-106.9	-154.6	-155.4
	4	-8.1	-15.2	-107.7	-129.1
	5	-33.1	-34.5	-100.3	-118.0
B3	1	-71.5	-148.9	-162.1	-176.6
	2	-5.6	-69.0	-109.6	-104.6
	3	-6.9	-26.7	-100.9	-123.5
	4	-66.9	-92.0	-137.0	-151.6
	5	-32.9	-32.0	-117.0	-139.2
B4	1	-73.6	-68.4	-112.5	-125.5
	2	-51.3	-17.6	-123.4	-114.1
	3	-24.2	-39.5	-96.4	-113.3
	4	-3.6	-36.8	-108.4	-126.7
	5	-3.1	-15.0	-104.7	-131.3
Average		-31.780	-55.960	-113.080	-128.600

Table 4.14: North Main Street Eastbound GECOR 6 Electrical Resistance (K Ω)

Connection #	Reading No.	1st Quarter	2nd Quarter	3rd Quarter	4th Quarter
B1	1	2.75	2.69	1.23	1.36
	2	1.70	1.71	1.55	1.40
	3	1.51	1.29	1.20	1.27
	4	1.61	1.15	2.77	1.34
	5	1.69	1.34	1.31	1.22
B2	1	1.47	0.99	1.53	1.00
	2	1.70	1.01	1.48	1.02
	3	1.52	0.73	1.02	1.02
	4	1.47	1.20	1.46	1.28
	5	1.53	1.08	1.60	1.26
B3	1	1.43	0.87	1.30	1.14
	2	1.56	0.82	1.18	1.18
	3	1.45	1.01	1.47	1.21
	4	1.55	1.30	1.31	1.27
	5	1.41	0.99	1.12	1.02
B4	1	1.27	0.99	3.21	3.73
	2	1.69	0.89	0.78	1.20
	3	1.54	1.05	1.16	1.10
	4	1.71	1.05	1.42	1.16
	5	1.36	1.12	0.90	0.94
Average		1.60	1.16	1.45	1.31

Table 4.15: North Main Street Eastbound Air Permeability
Vacuum (mm Hg), SCCM (ml/min)

Reading No.	1st Quarter		2nd Quarter		3rd Quarter		4th Quarter	
	Vacuum	SCCM	Vacuum	SCCM	Vacuum	SCCM	Vacuum	SCCM
1	784.00	33.50	713.70	27.18	778.40	58.19	690.60	32.39
2	785.50	19.80	792.50	51.18	781.50	32.72	688.00	32.21
3	783.70	26.79	744.20	39.60	781.30	54.76	685.90	32.32
4	784.80	21.72	736.30	35.25	780.00	43.27	684.00	32.42
5	785.50	15.55	785.30	55.75	780.70	46.36	681.90	32.31
6	783.50	20.72	759.60	48.72	777.10	55.34	773.60	45.85
7	780.20	35.04	748.20	40.64	770.90	58.03	681.60	32.48
8	782.20	26.70	797.20	35.74	781.80	21.95	769.90	56.67
9	774.80	55.23	761.80	50.72	777.90	44.31	682.30	32.84
Average	782.69	28.34	759.87	42.75	778.84	46.10	704.20	37.15

Table 4.16: North Main Street Eastbound Electrical Resistance Sealer Test (K Ω)

Quarter	Reading No.	DC End to End (Ω) Strip 1	DC End to End (Ω) Strip 2	DC Side to Side (M Ω)	AC (K Ω)	Avg. AC (K Ω)
1	1	6.8	9.4	5.3	15.0	19.7
	2	1.7	2.2	4.6	32.0	
	3	2.4	3.2	8.3	12.0	
2	1	4.5	6.3	16.3	37.0	34.0
	2	2.5	2.2	22.3	39.0	
	3	1.8	2.3	19.8	26.0	
3	1	5.0	6.5	8.0	25.0	21.0
	2	7.6	5.2	2.3	22.0	
	3	1.7	2.4	5.8	16.0	
4	1	27.1	14.2	20.9	24.0	28.3
	2	25.3	24.4	19.5	34.0	
	3	24.5	7.7	20.8	27.0	

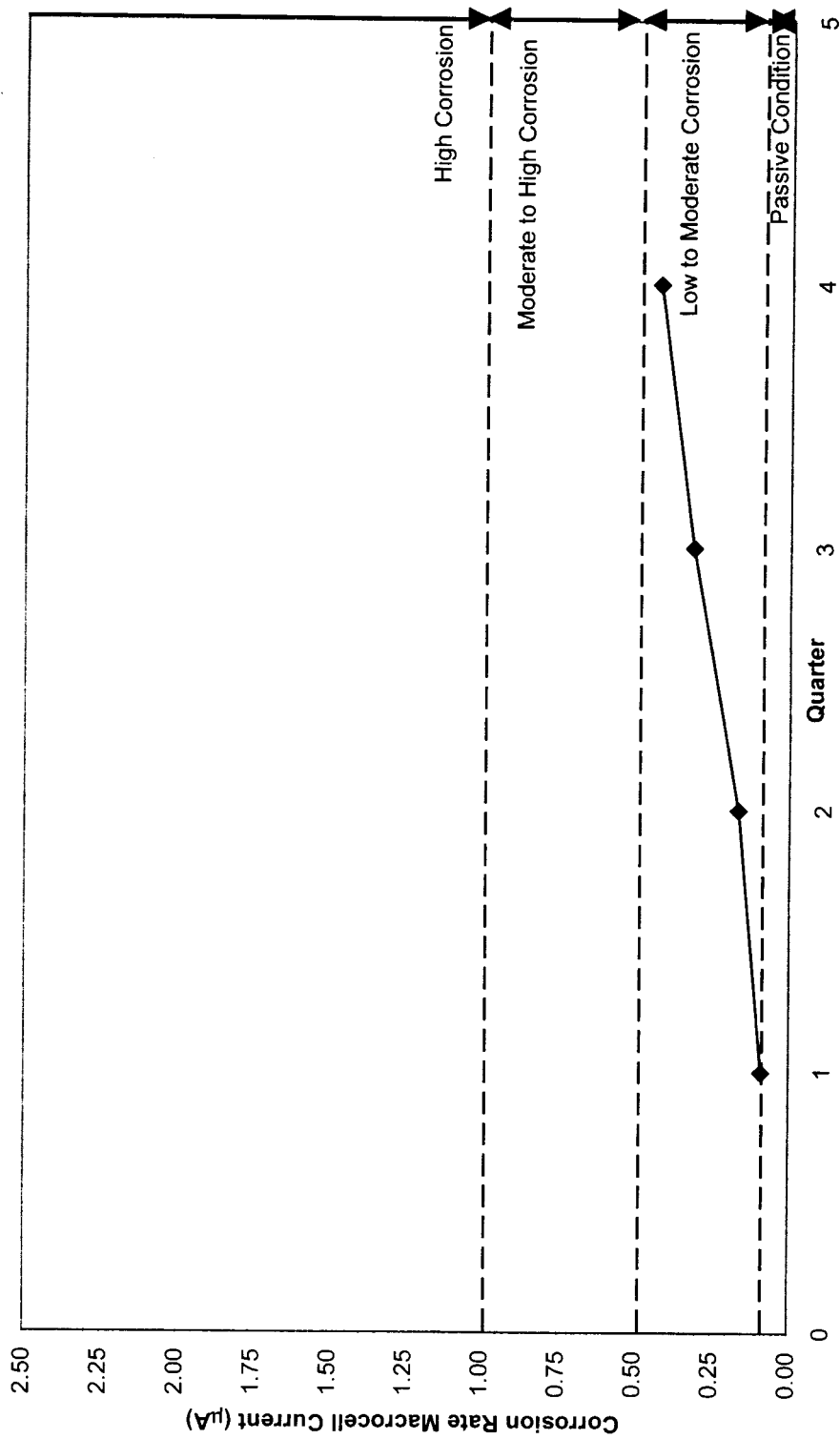


Fig. 4.10: North Main Street Eastbound Average Corrosion Rate Macrocell Current (µA)

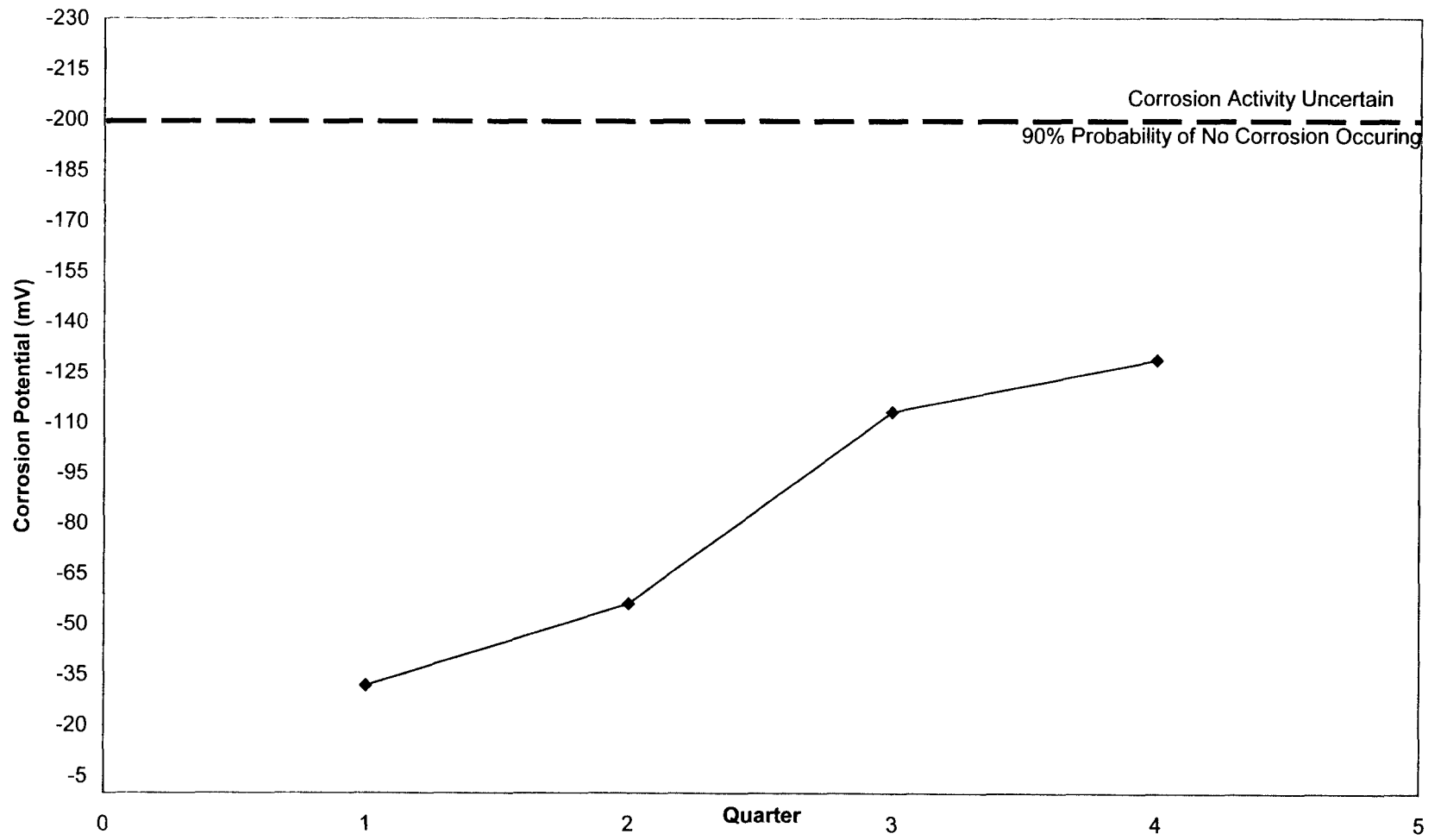


Fig. 4.11: North Main Street Eastbound GECOR 6 Average Corrosion Potential (mV)

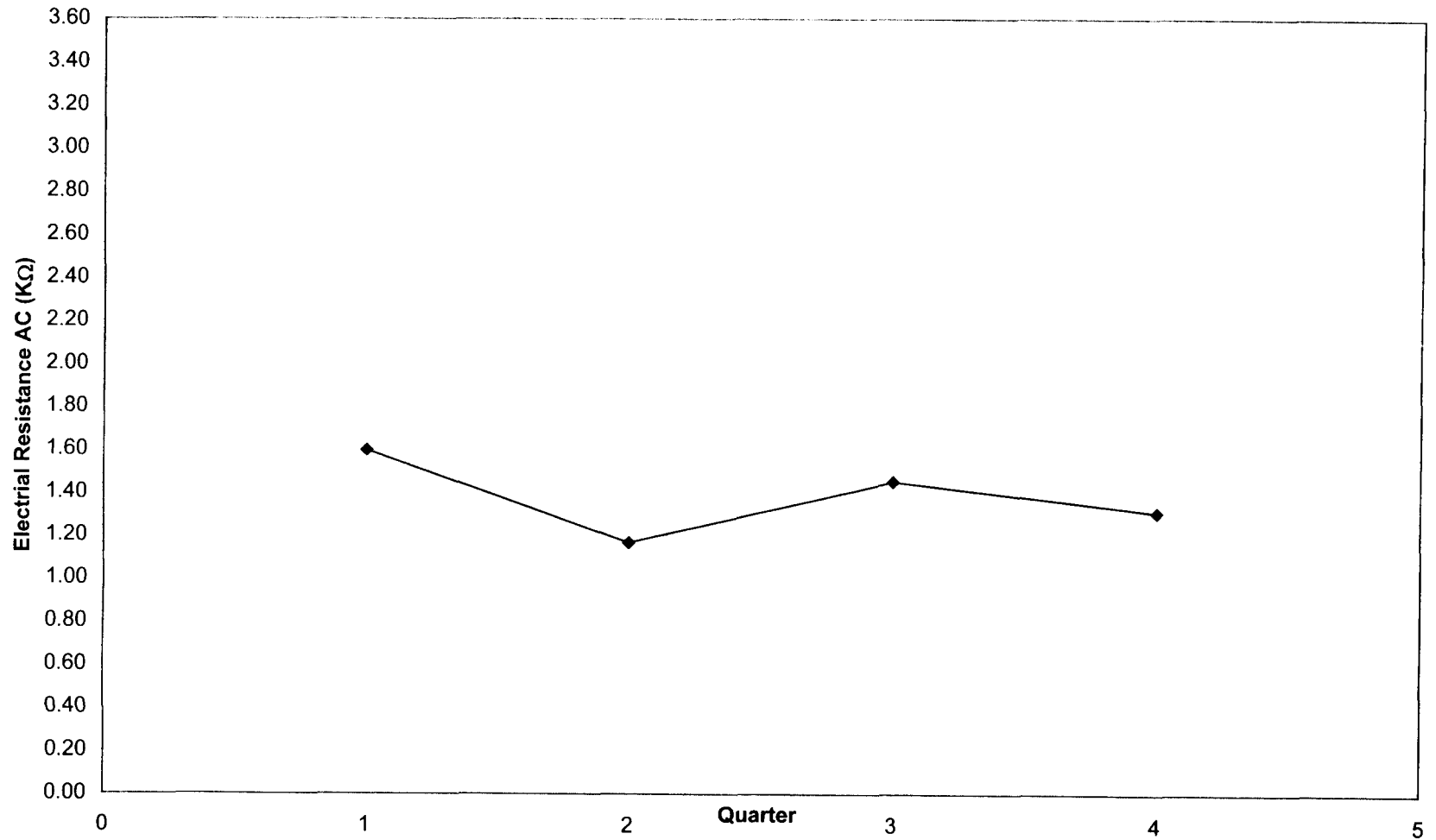


Fig. 4.12: North Main Street Eastbound GECOR 6 Average Electrical Resistance AC (KΩ)

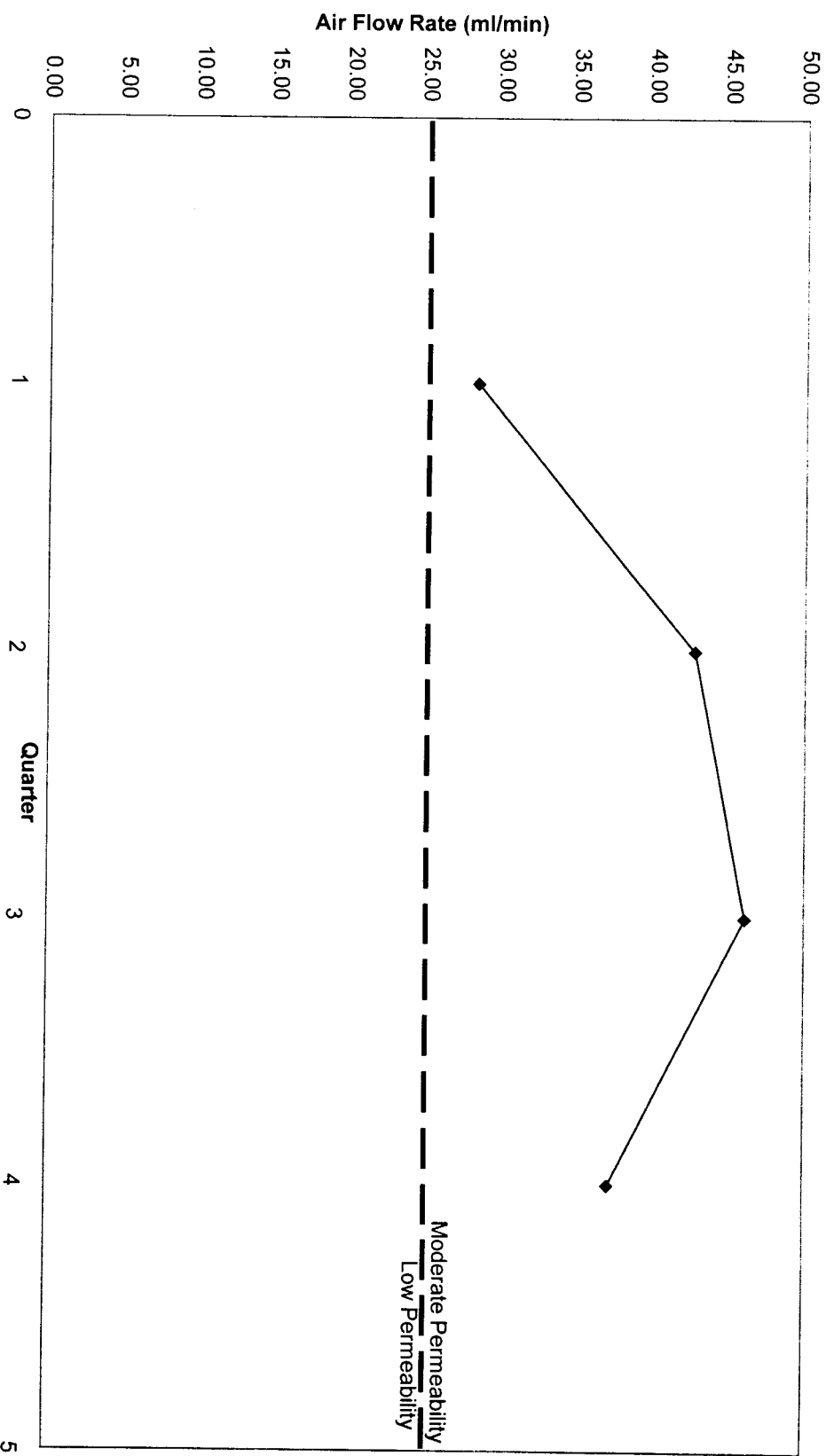


Fig. 4.13: North Main Street Eastbound Average Air Flow Rate (ml/min)

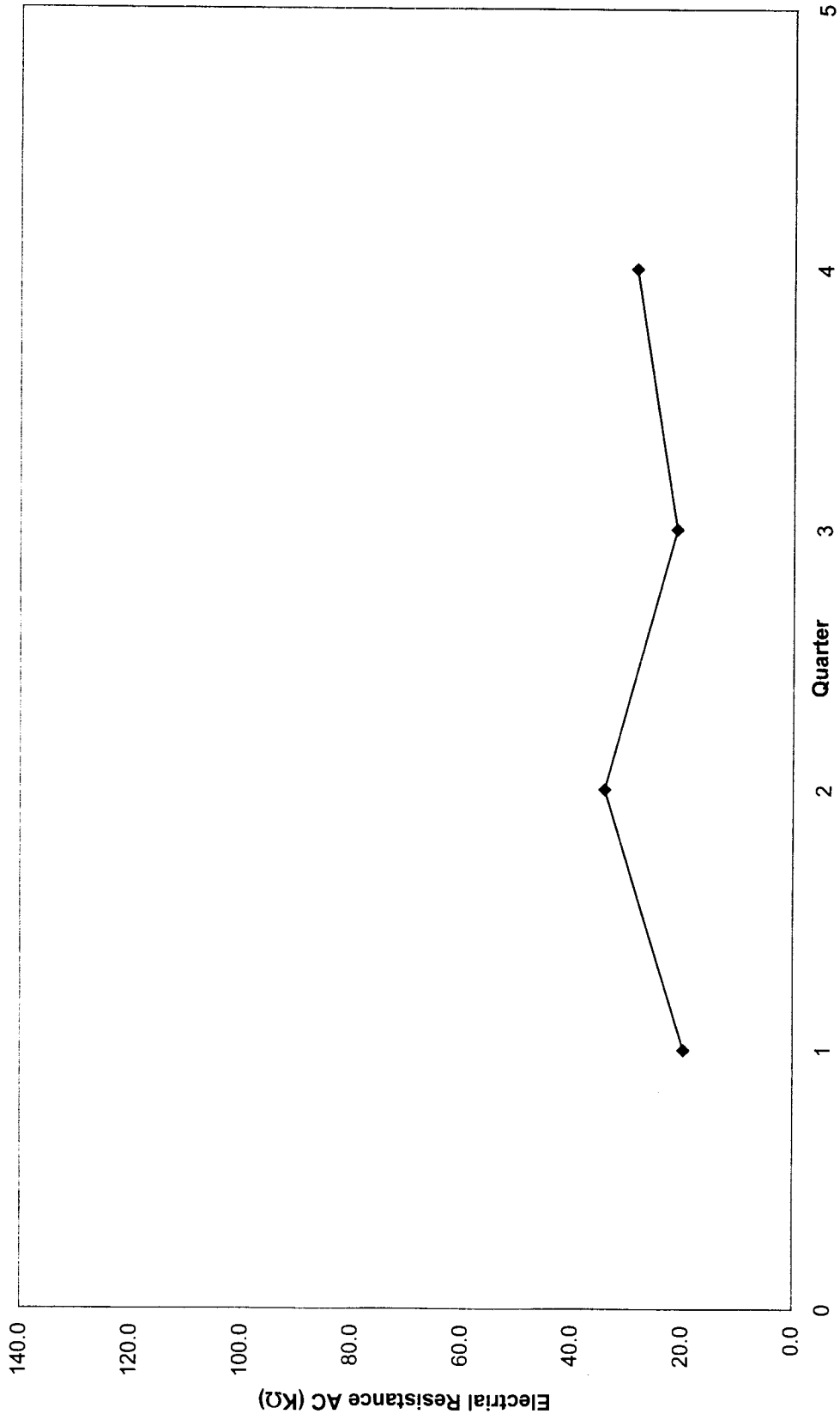


Fig. 4.14: North Main Street Eastbound Average Electrical Resistance AC (KΩ)

4.3.1 Wyckoff Road Westbound: Laboratory Tests

The data collected for the ASTM G 109 tests on the concrete samples obtained from Wyckoff Road Westbound are presented on the following Tables 4.17 and 4.18, and Fig. 4.15 and 4.16. The concrete samples contained the corrosion inhibiting admixture Master Builders, Inc.: Rheocrete 222+. Corrosion rate and corrosion potential are tabulated on Table 4.17 and 4.18, respectively, and the corresponding graphical variations are presented on Fig. 4.15 and 4.16.

Table 4.17: Minideck C - ASTM G 109 Corrosion Rate ($\mu\text{A}/\text{cm}^2$)

Specimen	Cycle 1	Cycle 2	Cycle 3	Cycle 4	Cycle 5	Cycle 6	Cycle 7	Cycle 8
C1	0.10	0.00	0.00	0.00	0.00	0.00	0.10	0.10
C2	0.10	0.20	0.40	0.40	0.40	0.30	0.40	0.40
C3	0.60	0.60	1.20	1.00	1.30	1.20	1.30	1.40
C4	0.40	0.70	0.60	0.70	0.60	0.40	0.80	0.60
C5	0.20	0.30	0.50	0.40	0.50	0.40	0.60	0.50
C6	0.00	0.10	0.20	0.20	0.10	0.20	0.30	0.30
C Average	0.23	0.32	0.48	0.45	0.48	0.42	0.58	0.55

Table 4.18: Minideck C - ASTM G 109 Corrosion Potential (mV)

Specimen	Cycle 1	Cycle 2	Cycle 3	Cycle 4	Cycle 5	Cycle 6	Cycle 7	Cycle 8
C1	N/A	N/A	-14.31	-13.82	-17.82	-14.80	-25.45	-12.50
C2	N/A	N/A	-6.39	-6.22	-10.01	-6.85	-17.94	-7.23
C3	N/A	N/A	-32.81	-31.44	-36.36	-33.52	-44.23	-30.50
C4	N/A	N/A	-35.54	-34.81	-38.87	-35.27	-46.52	-33.90
C5	N/A	N/A	-14.24	-13.47	-18.28	-16.65	-27.81	-16.43
C6	N/A	N/A	-21.82	-21.75	-25.78	-23.66	-35.38	-23.36
C Average	N/A	N/A	-20.85	-20.25	-24.52	-21.79	-32.89	-20.65

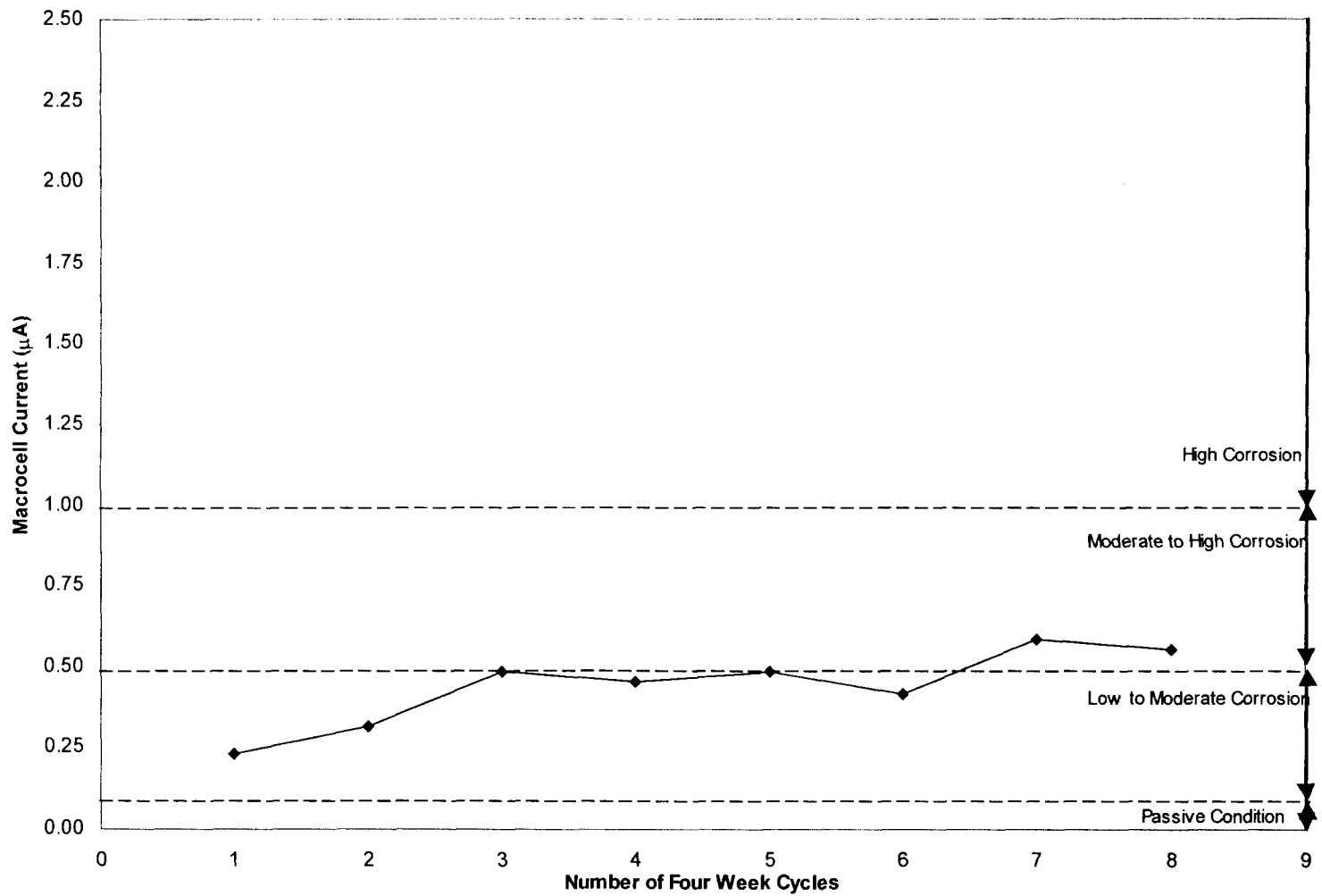


Fig. 4.15: Minideck C - Average Corrosion Rate Macrocell Current (µA)

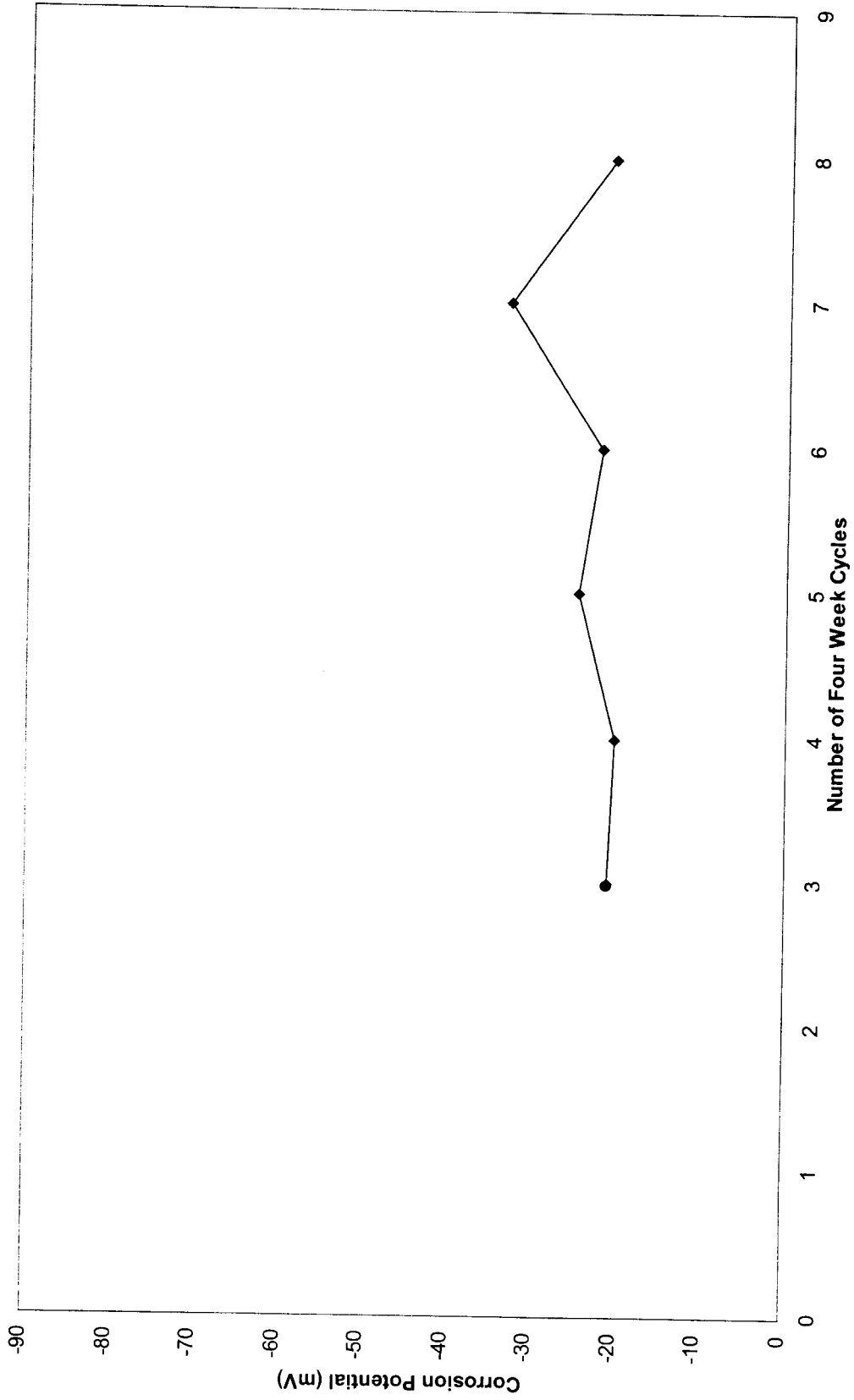


Fig. 4.16: Minideck C - Average Corrosion Potential (mV)

4.3.2 Wyckoff Road Westbound: Field Tests

The data collected for the GECOR 6 Corrosion Rate, Surface Air Flow Permeability, and Electrical Resistance Test for Penetrating Sealers on the bridge deck over Wyckoff Road Westbound are presented in Tables 4.19 to 4.23 and Fig. 4.17 to 4.21. The concrete used in the bridge deck contained the corrosion inhibiting admixture Master Builders, Inc.: Rheocrete 222+. GECOR 6: corrosion rate, corrosion potential, and electrical resistance are tabulated on Tables 4.19, 4.20, 4.21 and displayed on Fig. 4.17, 4.18, 4.19, respectively. Air permeability readings are presented on Table 4.22 and Fig. 4.20. Electrical resistance readings are presented in Table 4.23 and Fig. 4.21.

Table 4.19: Wyckoff Road Westbound GECOR 6 Corrosion Rate ($\mu\text{A}/\text{cm}^2$)

Connection #	Reading No.	1st Quarter	2nd Quarter	3rd Quarter	4th Quarter
B1	1	0.061	0.150	0.069	0.381
	2	0.040	0.095	0.057	0.315
	3	0.063	0.098	0.066	0.434
	4	0.082	0.155	0.065	0.119
	5	0.064	0.110	0.031	0.567
B2	1	0.069	0.188	0.037	0.233
	2	0.059	0.114	0.049	0.233
	3	0.083	0.104	0.044	0.336
	4	0.067	0.144	0.046	0.312
	5	0.089	0.176	0.059	0.558
B3	1	0.100	0.121	0.276	0.223
	2	0.116	0.248	0.051	0.303
	3	0.059	0.204	0.096	0.324
	4	0.064	0.117	0.048	0.263
	5	0.072	0.150	0.030	0.468
B4	1	0.075	0.181	0.021	0.492
	2	0.126	0.209	0.032	0.441
	3	0.068	0.079	0.043	0.277
	4	0.107	0.191	0.044	0.309
	5	0.066	0.136	0.042	0.347
Average		0.077	0.149	0.060	0.347

Table 4.20: Wyckoff Road Westbound GECOR 6 Corrosion Potential (mV)

Connection #	Reading No.	1st Quarter	2nd Quarter	3rd Quarter	4th Quarter
B1	1	-23.6	-111.2	-52.4	-118.2
	2	-30.4	-82.3	-49.4	-110.2
	3	-14.6	-72.2	-91.5	-118.8
	4	9.6	-92.9	-58.7	-118.8
	5	-15.1	-98.1	-77.5	-145.1
B2	1	-40.2	-127.8	-67.4	-202.1
	2	-51.2	-95.8	-57.8	-127.9
	3	-20.9	-104.5	-66.9	-117.2
	4	7.9	-97.6	-76.9	-115.0
	5	-7.8	-83.8	-98.6	-134.9
B3	1	-216.7	-139.0	-109.4	-163.6
	2	-30.9	-120.8	-65.9	-140.6
	3	-4.7	-118.6	-90.3	-109.5
	4	29.4	-77.0	-69.7	-108.7
	5	9.1	-94.6	-131.2	-137.5
B4	1	-20.5	-111.2	-153.7	-162.3
	2	-23.3	-101.7	-60.3	-141.1
	3	-24.0	-117.4	-101.8	-143.5
	4	-65.8	-134.8	-66.4	-142.9
	5	-4.3	-84.1	-129.4	-155.8
Average		-26.900	-103.270	-83.760	-135.685

Table 4.21: Wyckoff Road Westbound GECOR 6 Electrical Resistance (KΩ)

Connection #	Reading No.	1st Quarter	2nd Quarter	3rd Quarter	4th Quarter
B1	1	4.47	1.96	3.43	2.05
	2	4.83	1.57	3.02	2.46
	3	3.43	1.11	2.98	1.44
	4	2.47	2.21	2.87	1.63
	5	3.00	1.58	3.07	1.19
B2	1	3.77	1.45	3.22	1.34
	2	3.67	1.32	2.53	1.37
	3	2.90	1.24	2.91	1.06
	4	2.80	1.15	2.22	1.22
	5	2.54	1.30	3.30	1.13
B3	1	2.67	1.36	1.54	1.37
	2	2.72	1.49	2.64	1.34
	3	3.25	1.40	1.93	1.25
	4	2.28	1.09	2.51	1.20
	5	2.72	1.46	3.23	0.89
B4	1	3.20	1.86	4.14	0.98
	2	2.99	1.56	2.92	0.96
	3	3.33	1.86	2.52	0.97
	4	3.05	1.75	2.42	0.99
	5	2.89	1.87	2.66	0.87
Average		3.15	1.53	2.80	1.29

Table 4.22: Wyckoff Road Westbound Air Permeability
Vacuum (mm Hg), SCCM (ml/min)

Reading No.	1st Quarter		2nd Quarter		3rd Quarter		4th Quarter	
	Vacuum	SCCM	Vacuum	SCCM	Vacuum	SCCM	Vacuum	SCCM
1	774.30	18.15	796.40	52.19	779.70	45.51	761.10	51.47
2	775.10	13.63	794.80	39.29	781.20	27.93	772.20	53.36
3	772.40	39.17	783.20	50.18	780.90	25.63	770.90	47.67
4	773.90	31.85	786.60	55.28	738.40	50.95	771.80	51.99
5	772.70	39.21	788.80	55.33	780.60	30.06	684.50	31.79
6	772.30	39.56	790.10	54.22	780.70	30.64	776.50	31.11
7	774.10	30.45	781.10	35.36	778.10	44.68	776.90	37.25
8	775.70	16.88	788.60	34.38	780.20	23.03	770.10	59.19
9	774.20	32.28	788.50	53.01	778.80	22.67	775.00	43.25
Average	773.86	29.02	788.68	47.69	775.40	33.46	762.11	45.23

Table 4.23: Wyckoff Road Westbound Electrical Resistance Sealer Test (K Ω)

Quarter	Reading No.	DC End to End (Ω) Strip 1	DC End to End (Ω) Strip 2	DC Side to Side (M Ω)	AC (K Ω)	Avg. AC (K Ω)
1	1	2.2	2.6	5.3	150.0	75.3
	2	2.3	2.5	14.6	44.0	
	3	1.8	1.7	10.5	32.0	
2	1	1.7	2.2	36.8	120.0	92.3
	2	2.2	2.5	40.0	80.0	
	3	1.8	1.9	38.0	77.0	
3	1	1.9	2.3	7.8	110.0	92.3
	2	2.3	4.3	14.7	120.0	
	3	1.9	1.8	28.7	47.0	
4	1	3.5	2.9	20.5	39.0	104.7
	2	4.1	2.7	16.5	85.0	
	3	2.6	4.0	19.8	190.0	

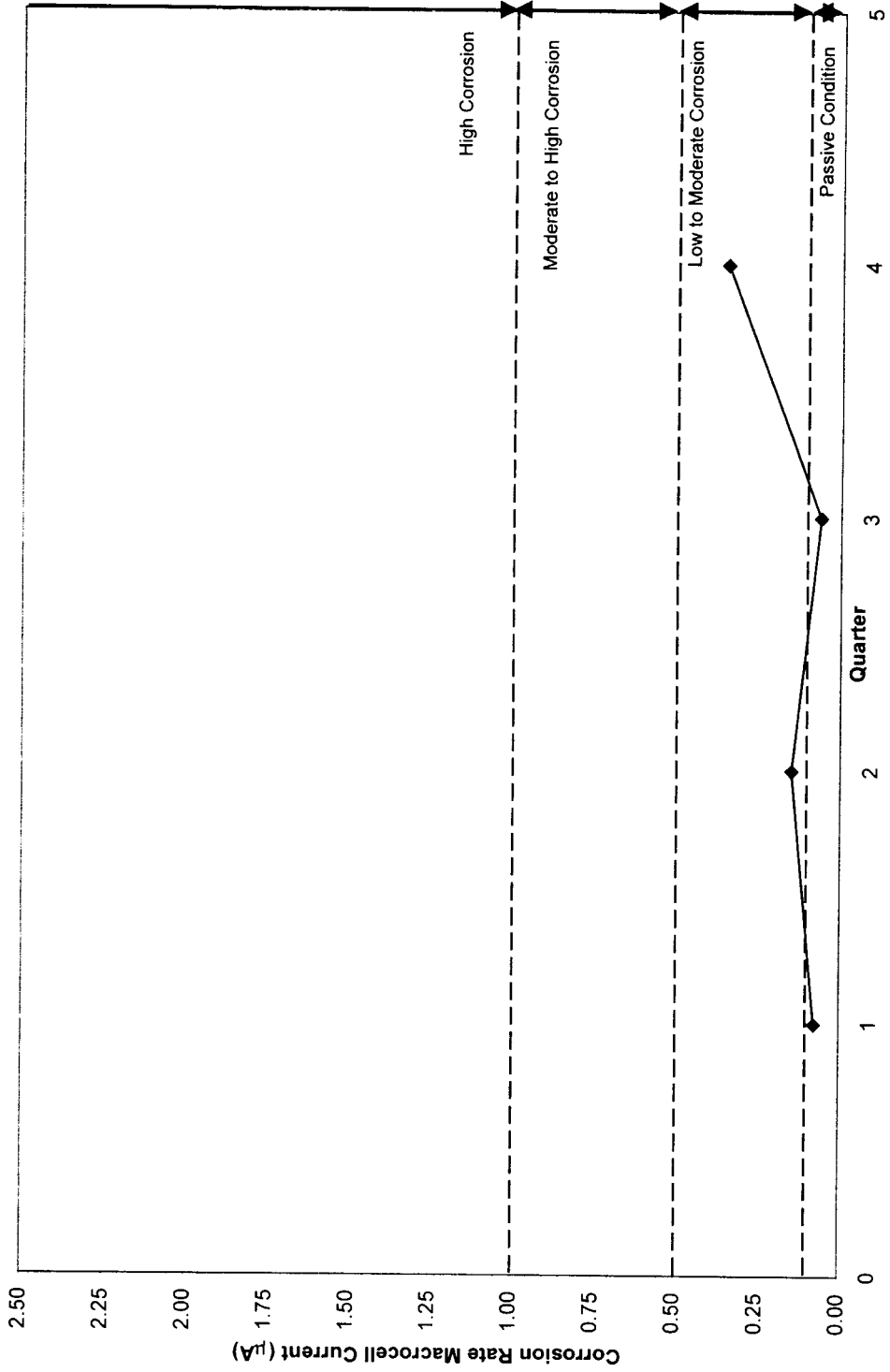


Fig. 4.17: Wyckoff Road Westbound GECOR 6 Average Corrosion Rate Macrocell Current (µA)

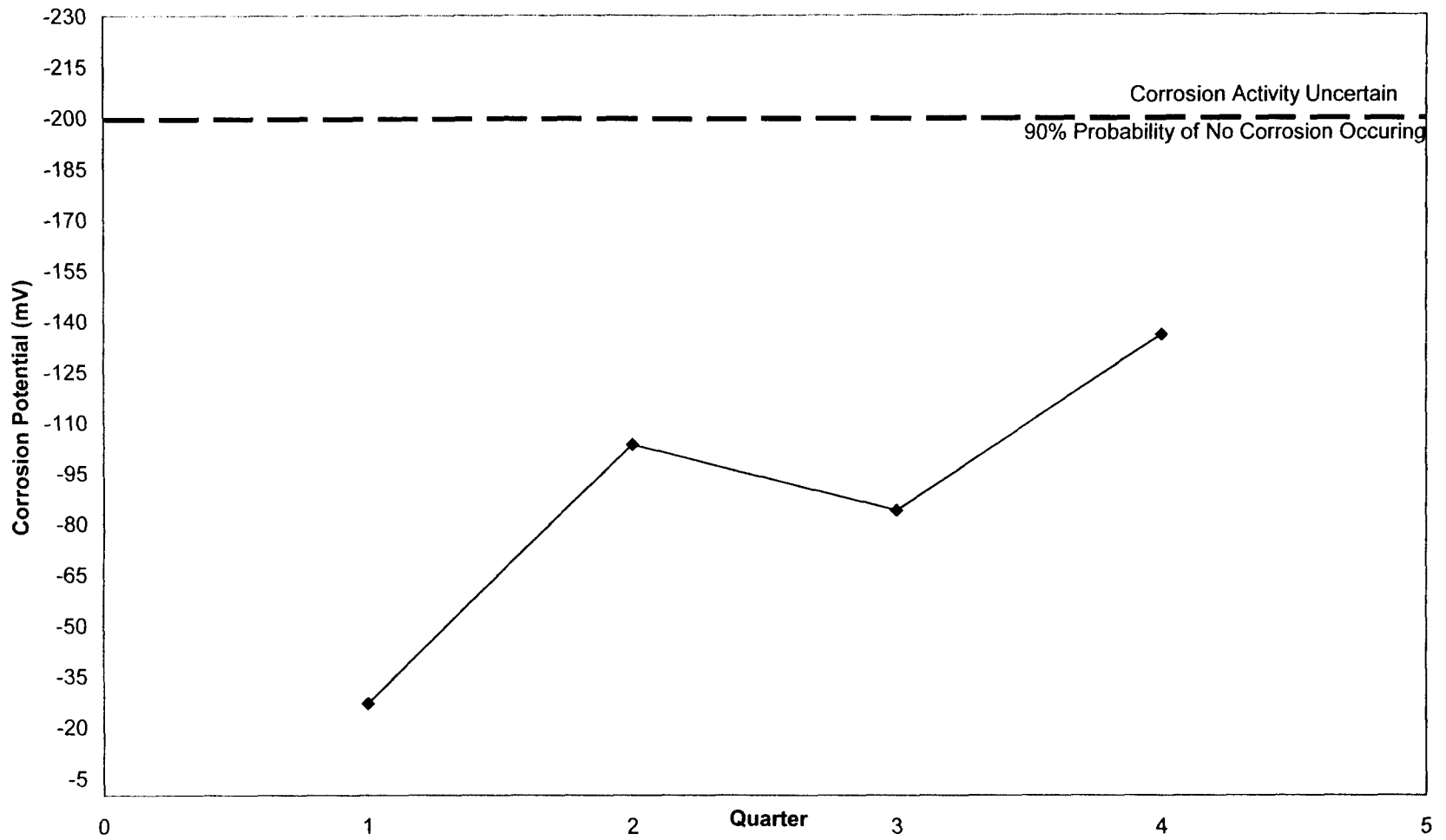


Fig. 4.18: Wyckoff Raod Westbound GECOR 6 Average Corrosion Potential (mV)

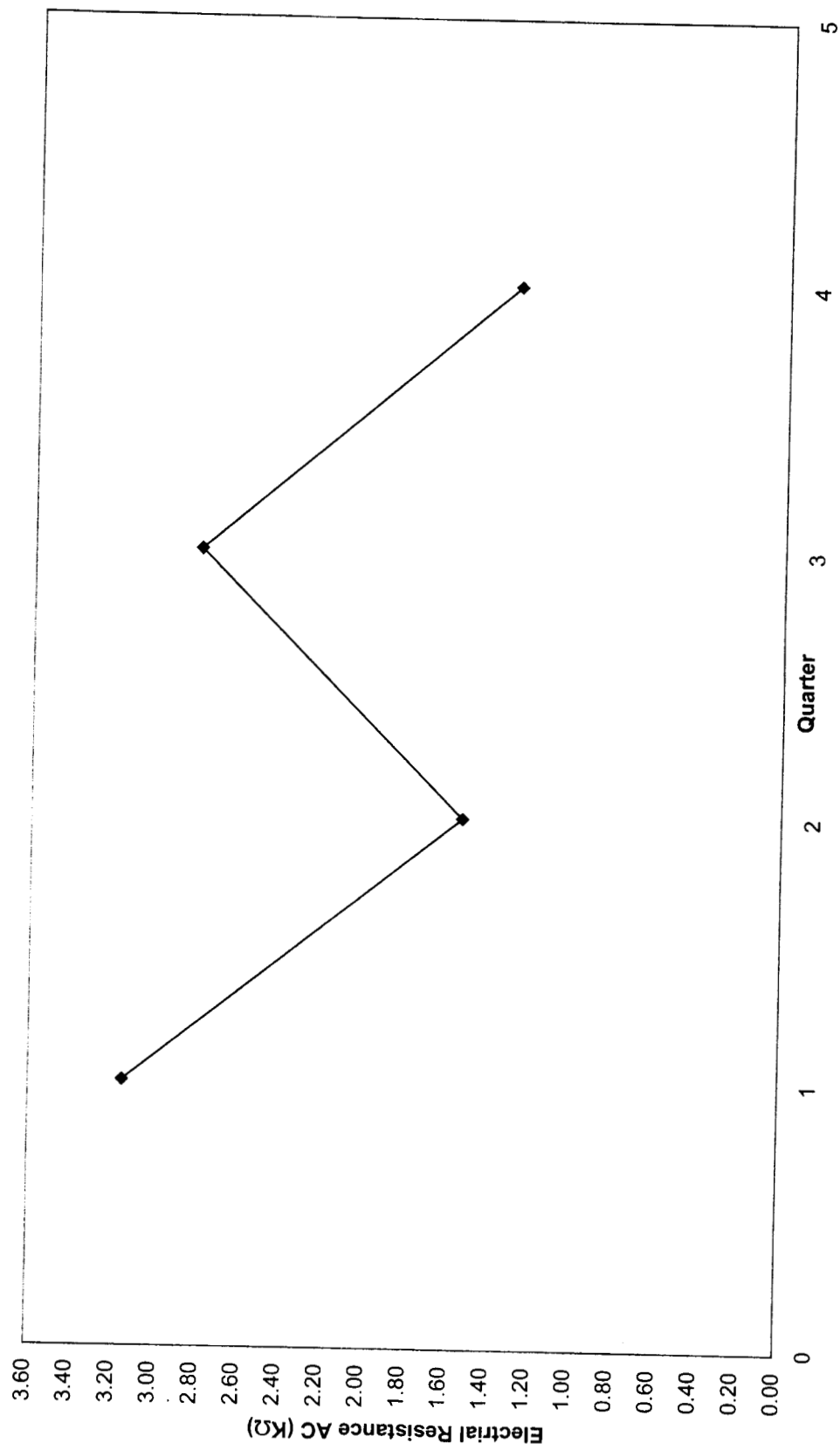


Fig. 4.19: Wyckoff Road Westbound GECOR 6 Average Electrical Resistance AC (KΩ)

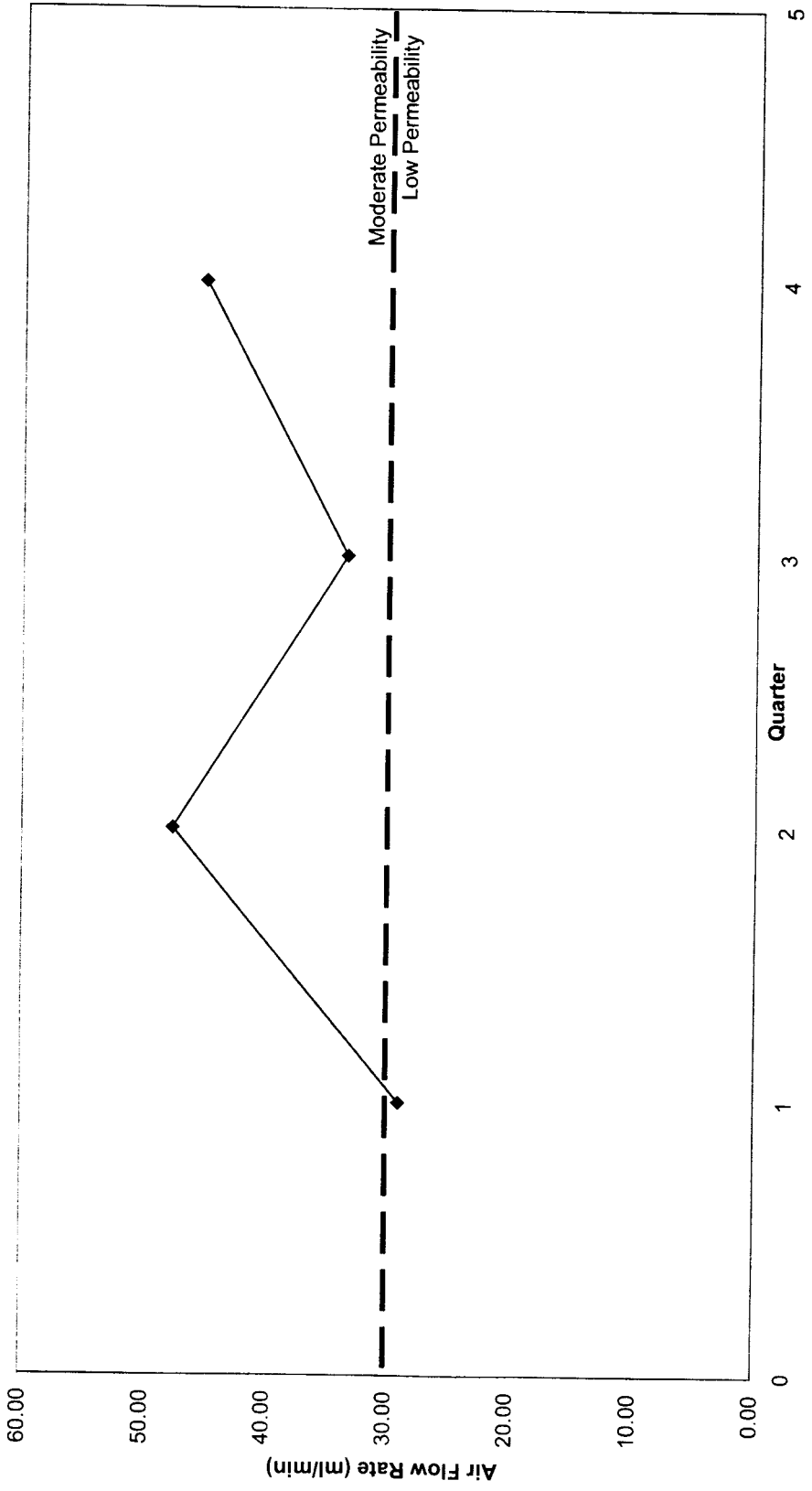


Fig. 4.20: Wyckoff Road Westbound Average Air Flow Rate (ml/min)

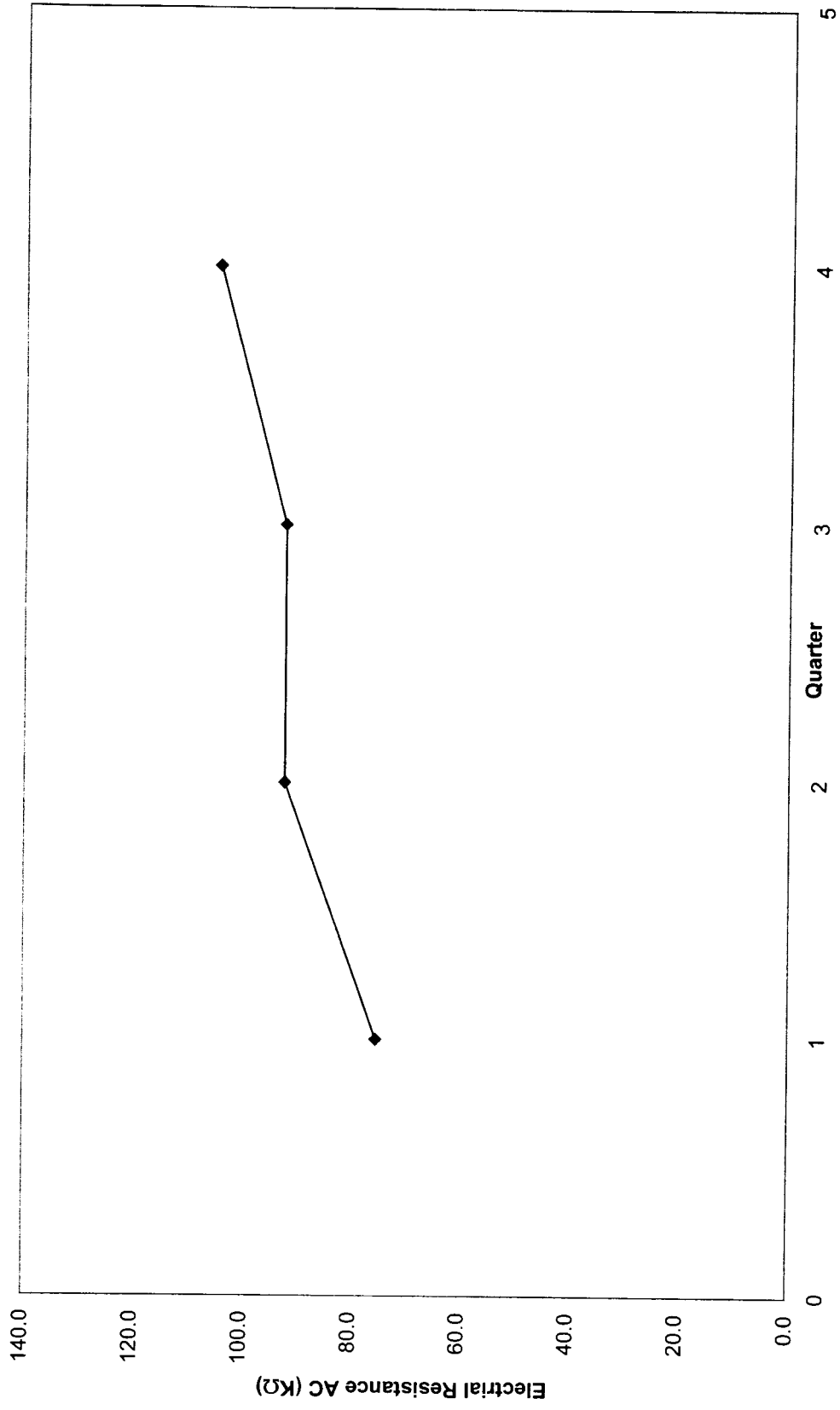


Fig. 4.21: Wyckoff Road Westbound Average Electrical Resistance AC (KΩ)

4.4.1 Wyckoff Road Eastbound: Laboratory Tests

The data collected for the ASTM G 109 tests on the concrete samples obtained from Wyckoff Road Eastbound are presented on the following Tables 4.24 and 4.25, and Fig. 4.22 and 4.23. The concrete samples contained the corrosion inhibiting admixture Sika Corporation: Ferrogard 901. Corrosion rate and corrosion potential are tabulated on Table 4.24 and 4.25, respectively, and the corresponding graphical variations are presented in Fig. 4.22 and 4.23.

Table 4.24: Minideck D - ASTM G 109 Corrosion Rate ($\mu\text{A}/\text{cm}^2$)

Specimen	Cycle 1	Cycle 2	Cycle 3	Cycle 4	Cycle 5	Cycle 6	Cycle 7	Cycle 8
D1	0.70	1.00	1.40	0.80	1.10	0.70	1.00	1.00
D2	0.80	0.80	0.90	1.10	1.20	1.20	1.30	1.20
D3	0.40	0.80	0.80	0.80	0.80	0.80	0.80	0.90
D4	0.20	0.50	0.40	1.10	0.40	0.30	0.40	0.40
D5	0.70	0.80	1.20	1.30	1.30	0.80	1.20	1.10
D6	0.70	0.80	1.20	1.30	1.40	1.20	1.40	1.40
D Average	0.58	0.78	0.98	1.07	1.03	0.83	1.02	1.00

Table 4.25: Minideck D - ASTM G 109 Corrosion Potential (mV)

Specimen	Cycle 1	Cycle 2	Cycle 3	Cycle 4	Cycle 5	Cycle 6	Cycle 7	Cycle 8
D1	N/A	N/A	-20.97	-16.84	-20.13	-15.07	-22.00	-8.25
D2	N/A	N/A	-17.64	-14.79	-17.93	-13.59	-19.78	-5.63
D3	N/A	N/A	-20.80	-18.51	-21.74	-17.93	-23.80	-13.50
D4	N/A	N/A	-6.80	-5.35	-8.82	-3.96	-8.14	-4.73
D5	N/A	N/A	-18.30	-16.55	-20.00	-15.17	-22.06	-9.65
D6	N/A	N/A	-18.38	-16.55	-19.83	-15.23	-20.22	-6.77
D Average	N/A	N/A	-17.15	-14.77	-18.08	-13.49	-19.33	-8.09

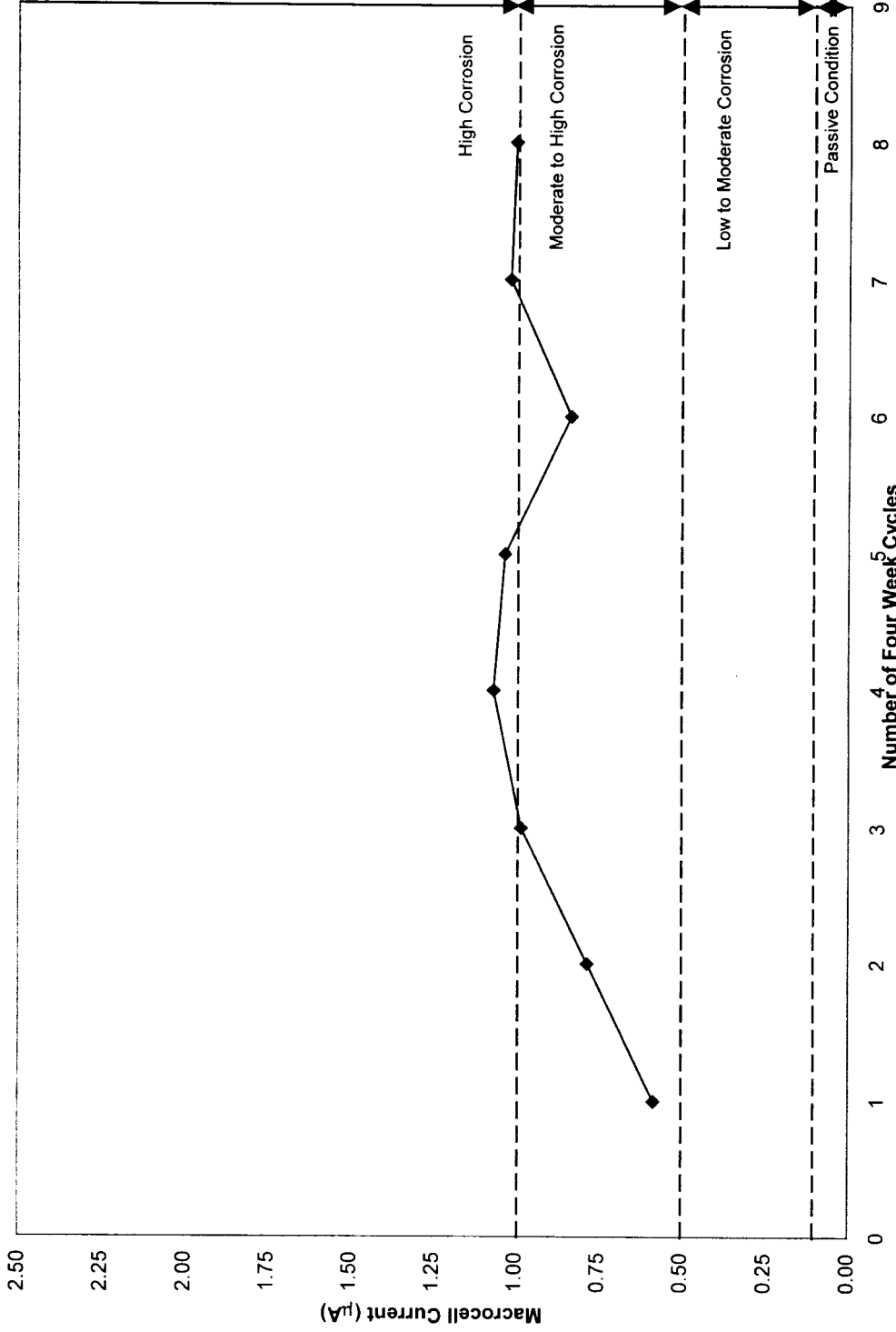


Fig. 4.22: Minideck D - Average Corrosion Rate Macrocell Current (µA)

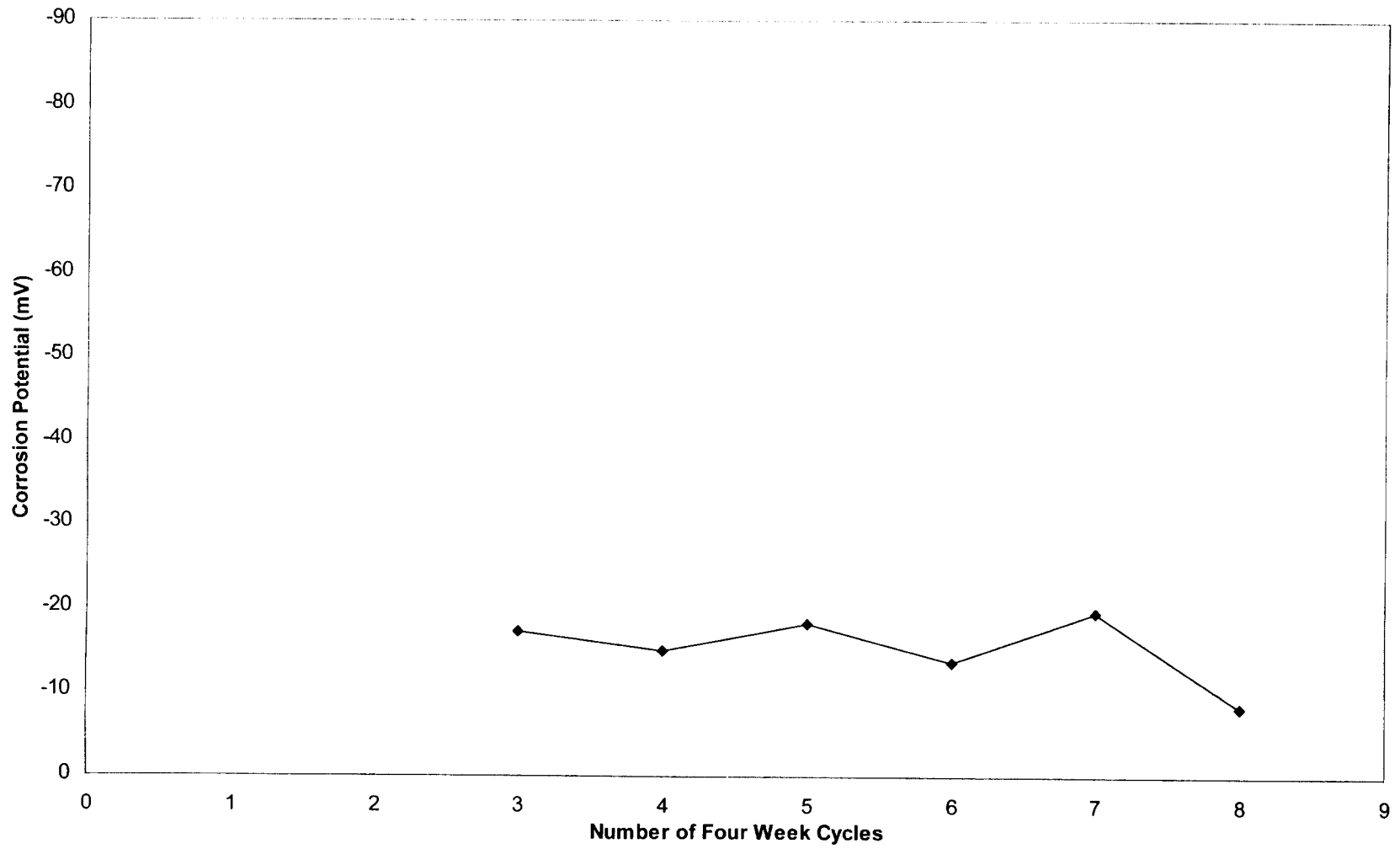


Fig. 4.23: Minideck D - Average Corrosion Potential (mV)

4.4.2 Wyckoff Road Eastbound: Field Tests

The data collected for the GECOR 6 Corrosion Rate, Surface Air Flow Permeability, and Electrical Resistance Test for Penetrating Sealers on the bridge deck over Wyckoff Road Eastbound are presented in Tables 4.26 to 4.30 and Fig. 4.24 to 4.28. The concrete used in the bridge deck contained the corrosion inhibiting admixture Sika Corporation: Ferrogard 901. GECOR 6: corrosion rate, corrosion potential, and electrical resistance are tabulated on Tables 4.26, 4.27, 4.28 and displayed on Fig. 4.24, 4.25, 4.26, respectively. Air permeability readings are presented on Table 4.29 and Fig. 4.27. Electrical resistance readings are presented in Table 4.30 and Fig. 4.28.

Table 4.26: Wyckoff Road Eastbound GECOR 6 Corrosion Rate ($\mu\text{A}/\text{cm}^2$)

Connection #	Reading No.	1st Quarter	2nd Quarter	3rd Quarter	4th Quarter
B1	1	0.038	0.146	0.257	0.071
	2	0.048	0.118	0.249	0.092
	3	0.033	0.089	0.214	0.210
	4	0.168	0.125	0.168	0.150
	5	0.153	0.198	0.283	0.092
B2	1	0.190	0.578	0.229	0.078
	2	0.134	0.593	0.379	0.078
	3	0.094	0.105	0.285	0.112
	4	0.176	0.142	0.274	0.105
	5	0.162	0.146	0.320	0.130
B3	1	0.135	0.106	0.314	0.142
	2	0.096	0.120	0.356	0.066
	3	0.110	0.083	0.198	0.134
	4	0.126	0.132	0.234	0.062
	5	0.200	0.179	0.195	0.043
B4	1	0.036	0.223	0.210	0.153
	2	0.028	0.180	0.321	0.112
	3	0.084	0.140	0.708	0.085
	4	0.169	0.210	0.369	0.088
	5	0.108	0.138	0.623	0.115
Average		0.114	0.188	0.309	0.106

Table 4.27: Wyckoff Road Eastbound GECOR 6 Corrosion Potential (mV)

Connection #	Reading No.	1st Quarter	2nd Quarter	3rd Quarter	4th Quarter
B1	1	-29.0	-85.3	-101.1	-89.2
	2	10.5	-25.0	-97.7	-98.4
	3	9.7	-38.3	-94.0	-151.5
	4	-1.3	-56.7	-99.6	-124.1
	5	-13.3	-82.9	-110.4	-125.9
B2	1	-59.2	-162.3	-172.0	-89.2
	2	-27.3	-78.2	-107.3	-77.6
	3	17.1	-1.0	-82.8	-93.4
	4	-1.3	-17.7	-81.9	-117.6
	5	-4.2	-18.5	-100.3	-136.6
B3	1	-81.0	-82.7	-143.2	-104.6
	2	-27.5	-33.2	-110.2	-82.0
	3	-1.2	-14.9	-77.4	-131.4
	4	-0.7	-16.9	-69.8	-94.1
	5	-2.2	-41.7	-86.5	-155.6
B4	1	-28.1	-82.1	-134.2	-146.2
	2	-7.6	-52.7	-114.2	-115.1
	3	-1.7	-60.2	-118.9	-94.8
	4	-3.8	-67.5	-89.0	-99.7
	5	-7.2	-41.9	-114.7	-124.8
	Average	-12.965	-52.985	-105.260	-112.590

Table 4.28: Wyckoff Road Eastbound GECOR 6 Electrical Resistance (K Ω)

Connection #	Reading No.	1st Quarter	2nd Quarter	3rd Quarter	4th Quarter
B1	1	3.54	1.72	2.09	1.89
	2	4.17	1.91	1.55	2.31
	3	3.14	1.72	1.44	2.36
	4	1.20	1.11	1.45	2.05
	5	1.75	0.85	1.37	2.11
B2	1	1.67	0.72	1.42	2.05
	2	2.04	0.73	1.45	2.04
	3	1.59	1.01	1.40	2.18
	4	1.72	1.11	1.38	1.55
	5	1.74	1.07	1.46	2.16
B3	1	1.84	0.87	1.61	1.45
	2	1.48	0.95	1.70	1.83
	3	1.60	0.69	1.62	1.28
	4	1.94	0.71	1.65	1.89
	5	1.83	0.85	1.34	2.47
B4	1	5.16	1.16	1.32	1.81
	2	3.97	0.90	1.48	2.02
	3	2.05	0.73	0.97	2.22
	4	2.02	1.30	1.53	1.85
	5	1.67	0.85	1.46	2.20
	Average	2.31	1.05	1.48	1.99

Table 4.29: Wyckoff Road Eastbound Air Permeability
Vacuum (mm Hg), SCCM (ml/min)

Reading No.	1st Quarter		2nd Quarter		3rd Quarter		4th Quarter	
	Vacuum	SCCM	Vacuum	SCCM	Vacuum	SCCM	Vacuum	SCCM
1	767.80	15.71	784.80	53.20	782.90	29.68	770.70	58.96
2	769.70	16.55	796.20	34.31	784.00	13.77	688.10	31.41
3	766.30	36.41	793.50	40.39	780.90	45.06	689.50	31.25
4	766.50	57.78	707.50	27.18	781.60	47.23	770.00	57.04
5	775.70	17.08	797.90	34.84	776.40	58.21	694.10	31.57
6	774.30	22.94	793.60	53.07	774.70	59.08	690.80	31.19
7	773.80	28.53	791.50	54.90	778.60	34.94	768.50	56.29
8	775.10	19.15	793.10	52.09	780.10	28.33	695.90	32.23
9	775.50	17.00	792.80	52.40	780.50	43.66	766.20	44.83
Average	771.63	25.68	783.43	44.71	779.97	40.00	725.98	41.64

Table 4.30: Wyckoff Road Eastbound Electrical Resistance Sealer Test (K Ω)

Quarter	Reading No.	DC End to End (Ω)		DC Side to Side (M Ω)	AC (K Ω)	Avg. AC (K Ω)
		Strip 1	Strip 2			
1	1	3.0	2.7	36.0	25.0	25.3
	2	2.1	2.4	16.0	35.0	
	3	1.9	2.2	7.8	16.0	
2	1	2.1	3.1	23.0	170.0	88.3
	2	4.7	24.2	31.0	68.0	
	3	1.5	1.8	17.4	27.0	
3	1	1.7	1.4	7.4	32.0	26.3
	2	4.3	5.2	7.8	18.0	
	3	1.0	1.4	12.9	29.0	
4	1	6.5	3.8	7.2	60.0	73.0
	2	1.0	3.2	15.0	84.0	
	3	1.0	1.3	8.1	75.0	

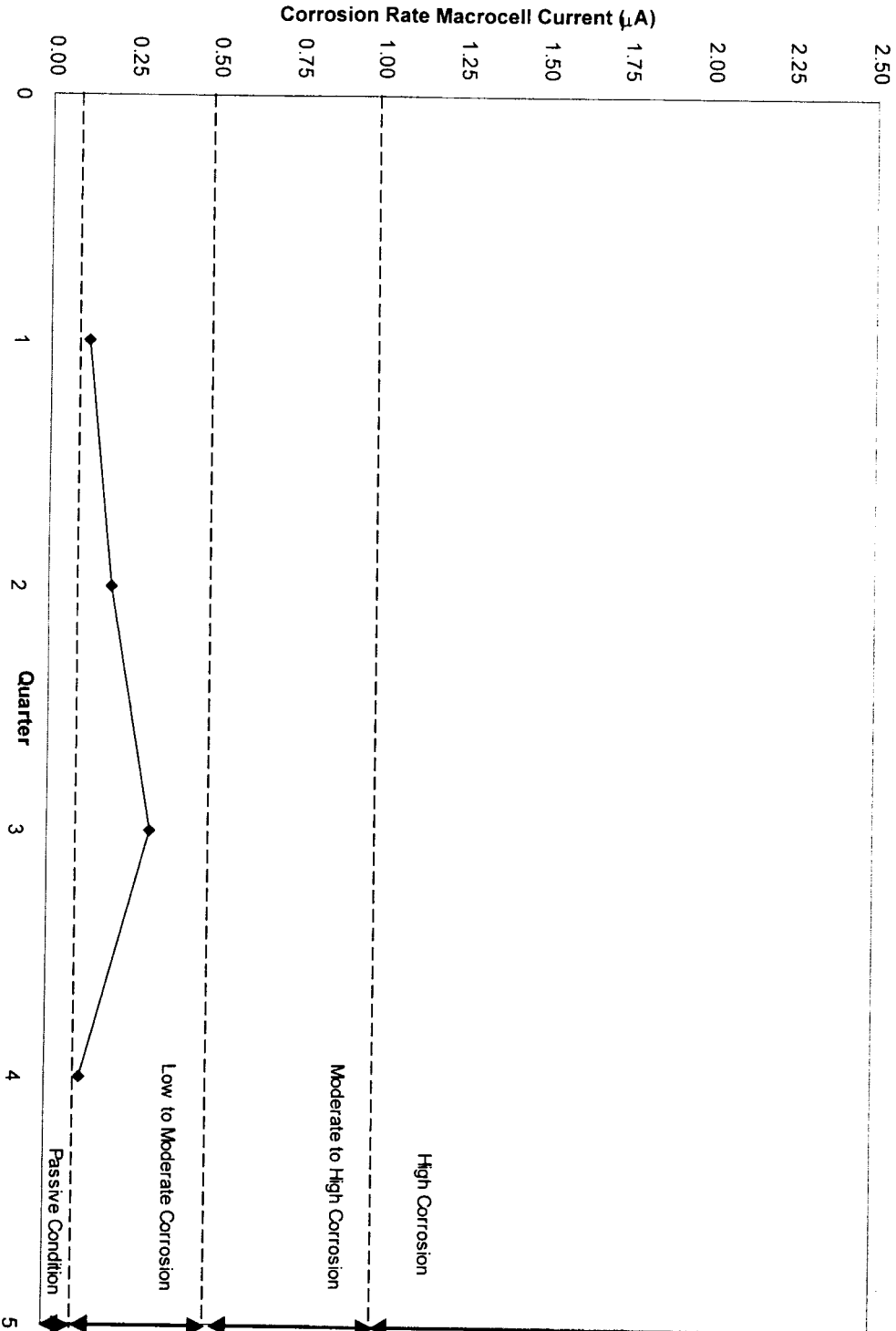


Fig. 4.24: Wyckoff Road Eastbound GECOR 6 Average Corrosion Rate Macrocell Current (µA)

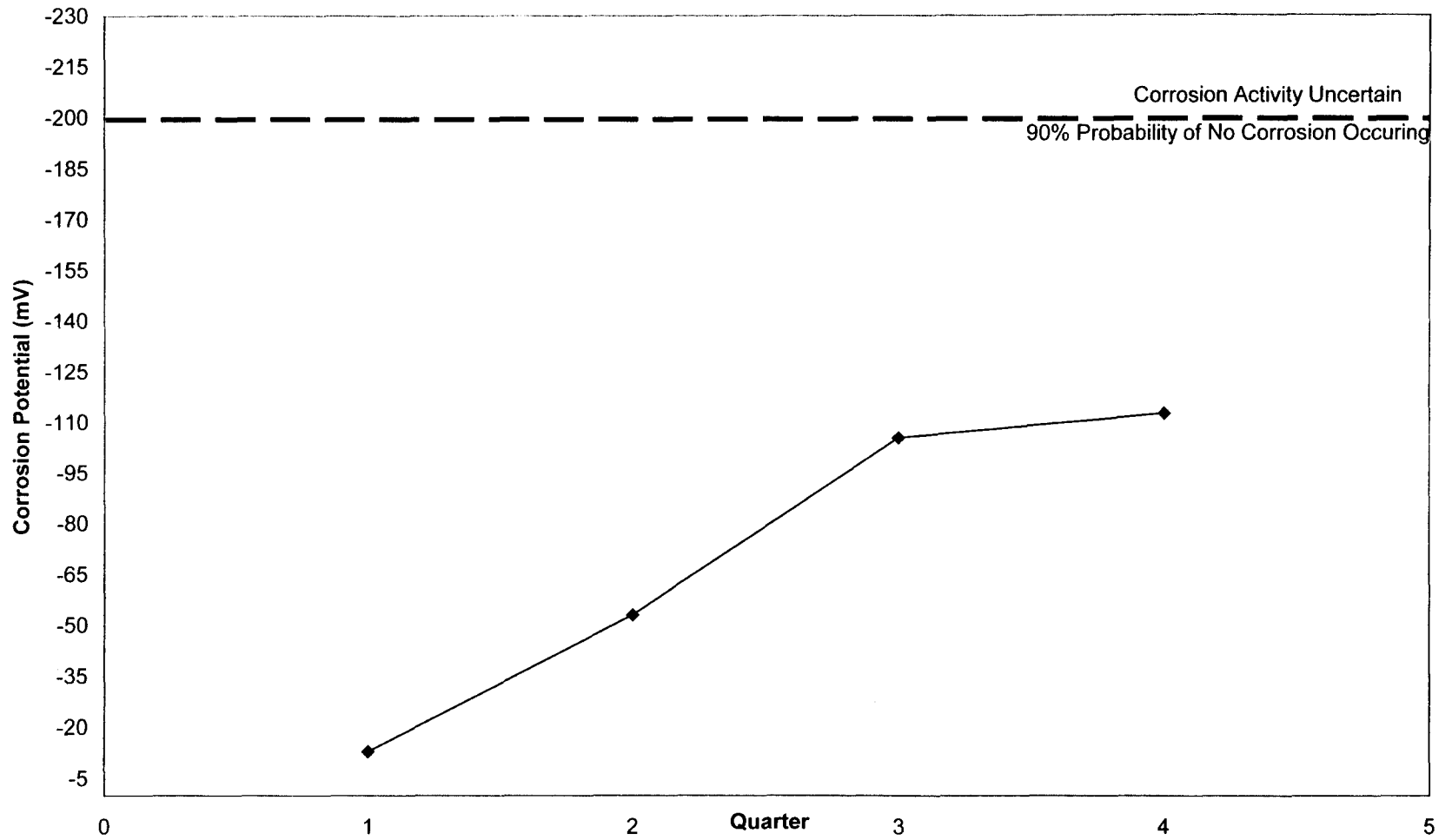


Fig. 4.25: Wyckoff Road Eastbound GECOR 6 Average Corrosion Potential (mV)

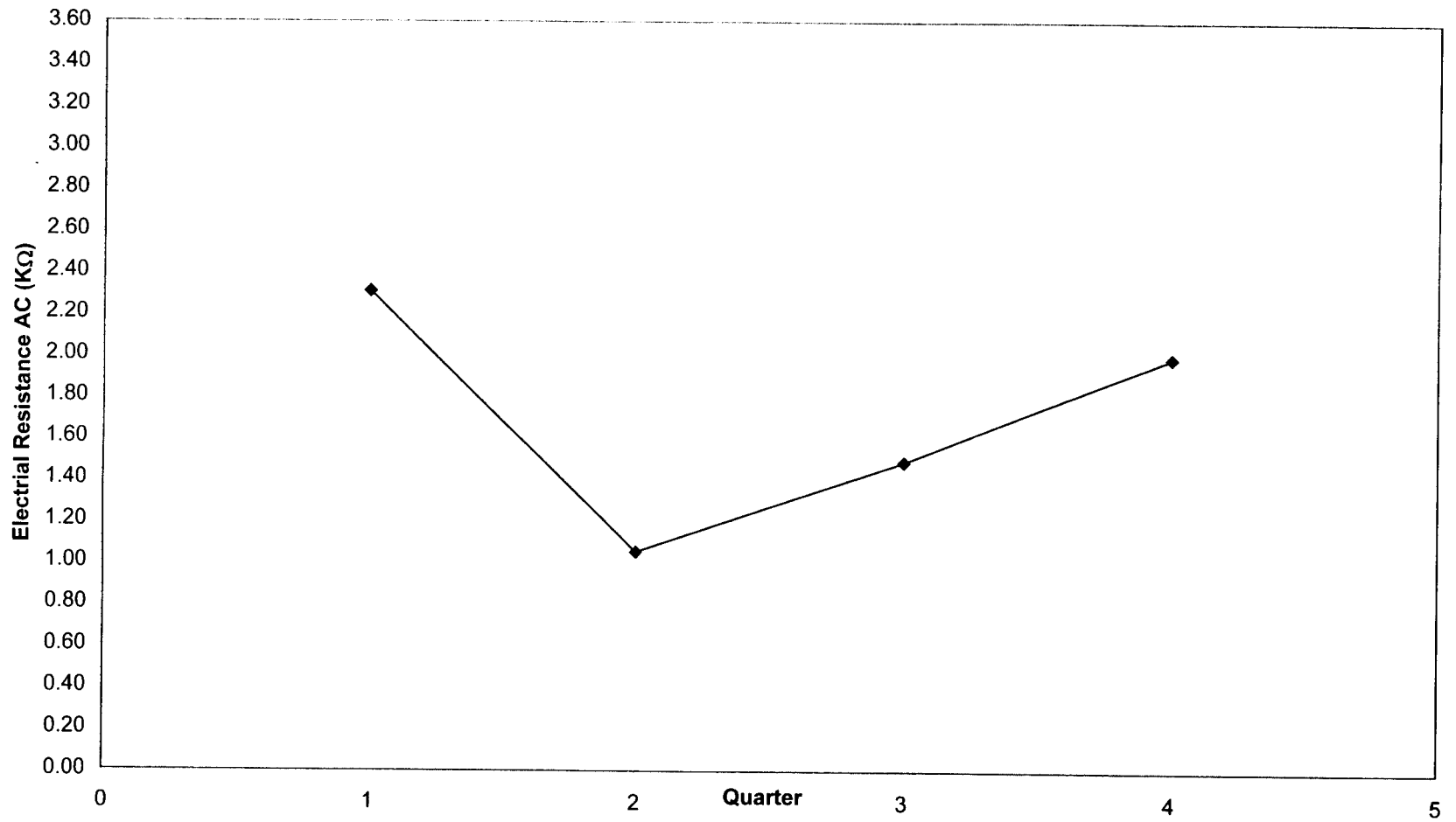


Fig. 4.26: Wyckoff Road Eastbound GECOR 6 Average Electrical Resistance AC (KΩ)

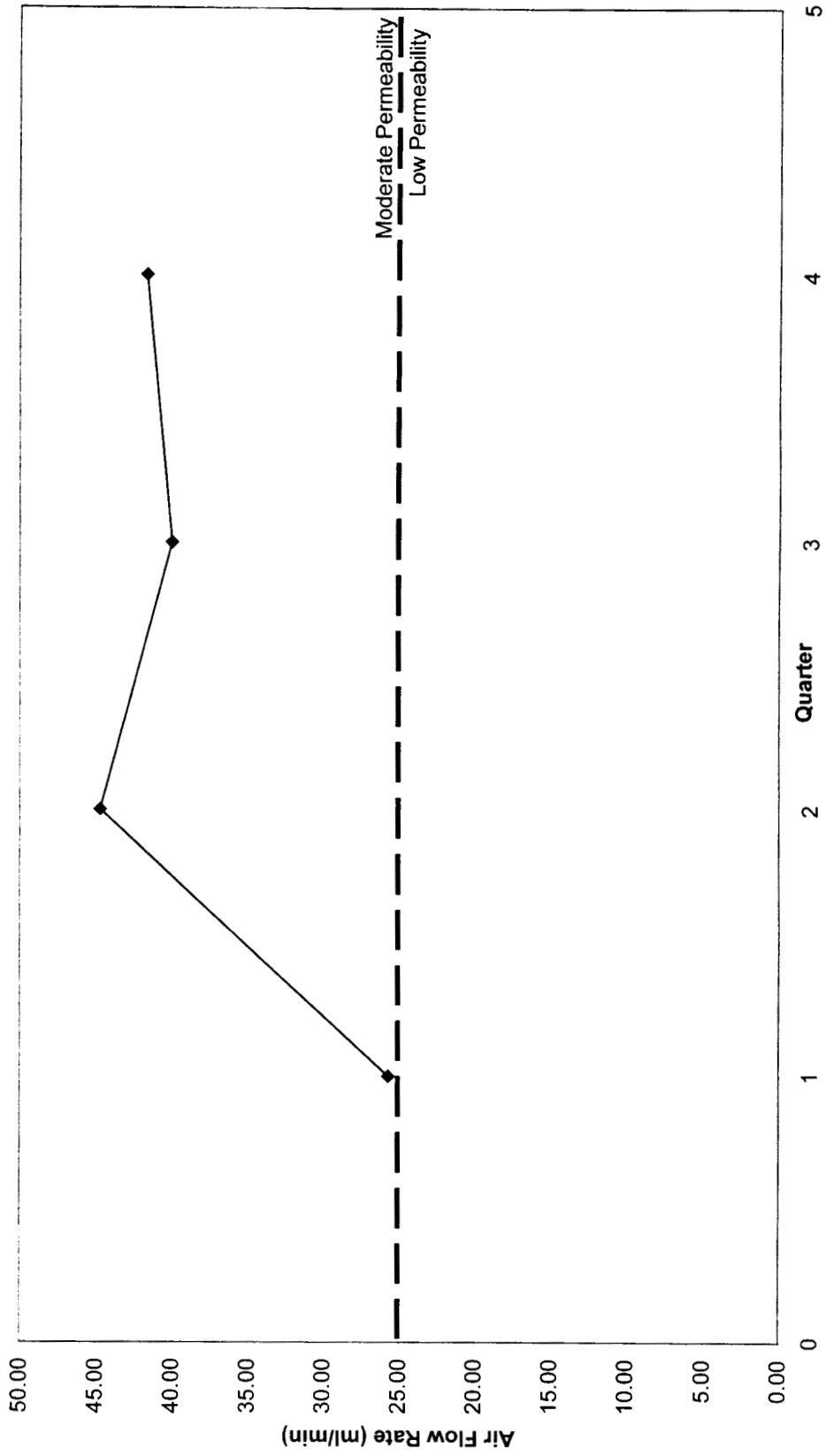


Fig. 4.27: Wyckoff Road Westbound Average Air Flow Rate (m/min)

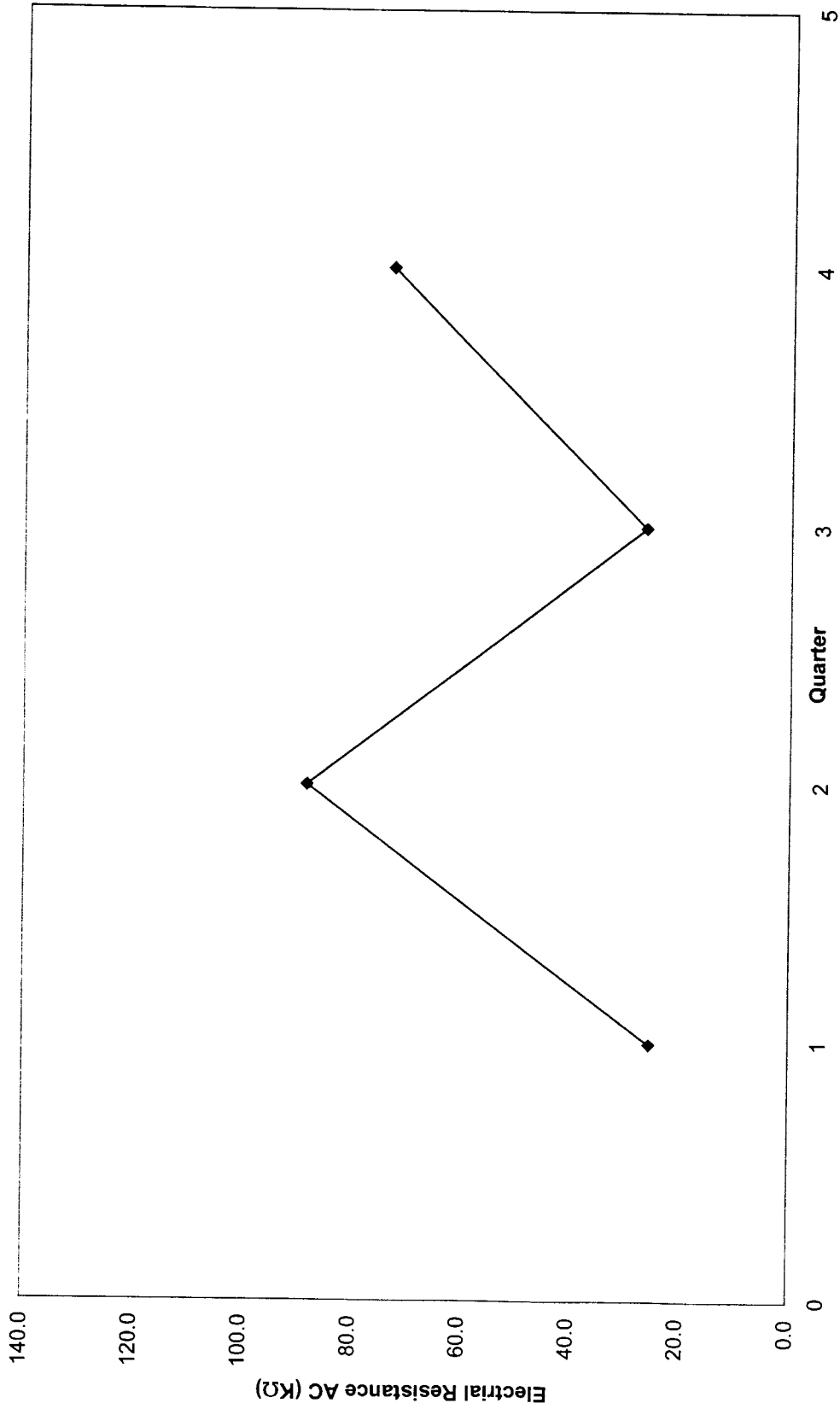


Fig. 4.28: Wyckoff Road Eastbound Average Electrical Resistance AC (KΩ)

4.5.1 Route 130 Westbound: Laboratory Tests

The data collected for the ASTM G 109 tests on the concrete samples obtained from Route 130 Westbound are presented on the following Tables 4.31 and 4.32, and Fig. 4.29 and 4.30. The concrete samples did not contain any corrosion inhibiting admixture. Corrosion rate and corrosion potential are tabulated on Table 4.31 and 4.32, respectively, and the corresponding graphical variations are presented in Fig. 4.29 and 4.30.

Table 4.31: Minideck E - ASTM G 109 Corrosion Rate ($\mu\text{A}/\text{cm}^2$)

Specimen	Cycle 1	Cycle 2	Cycle 3	Cycle 4	Cycle 5	Cycle 6	Cycle 7	Cycle 8
E1	0.80	1.40	1.40	1.20	1.90	1.80	N/A	N/A
E2	3.00	1.80	1.40	0.80	0.50	0.50	N/A	N/A
E3	2.00	1.40	1.30	0.80	0.70	0.00	N/A	N/A
E4	0.90	1.10	0.90	0.40	0.80	0.80	N/A	N/A
E5	0.90	0.90	0.60	0.30	0.70	0.60	N/A	N/A
E6	7.00	3.10	2.00	0.90	0.50	0.40	N/A	N/A
E Average	2.43	1.62	1.27	0.73	0.85	0.68	N/A	N/A

Table 4.32: Minideck E - ASTM G 109 Corrosion Potential (mV)

Specimen	Cycle 1	Cycle 2	Cycle 3	Cycle 4	Cycle 5	Cycle 6	Cycle 7	Cycle 8
E1	-94.32	-73.40	-66.60	-55.86	-62.34	-38.95	N/A	N/A
E2	-87.97	-64.68	-53.10	-39.54	-45.07	-18.83	N/A	N/A
E3	-62.93	-46.52	-42.77	-33.97	-40.54	-22.73	N/A	N/A
E4	-73.88	-53.66	-48.76	-41.68	-50.61	-32.22	N/A	N/A
E5	-79.75	-56.92	-51.90	-43.13	-50.35	-30.42	N/A	N/A
E6	-110.52	-77.53	-70.85	-52.01	-55.15	-33.19	N/A	N/A
E Average	-84.90	-62.12	-55.66	-44.37	-50.68	-29.39	N/A	N/A

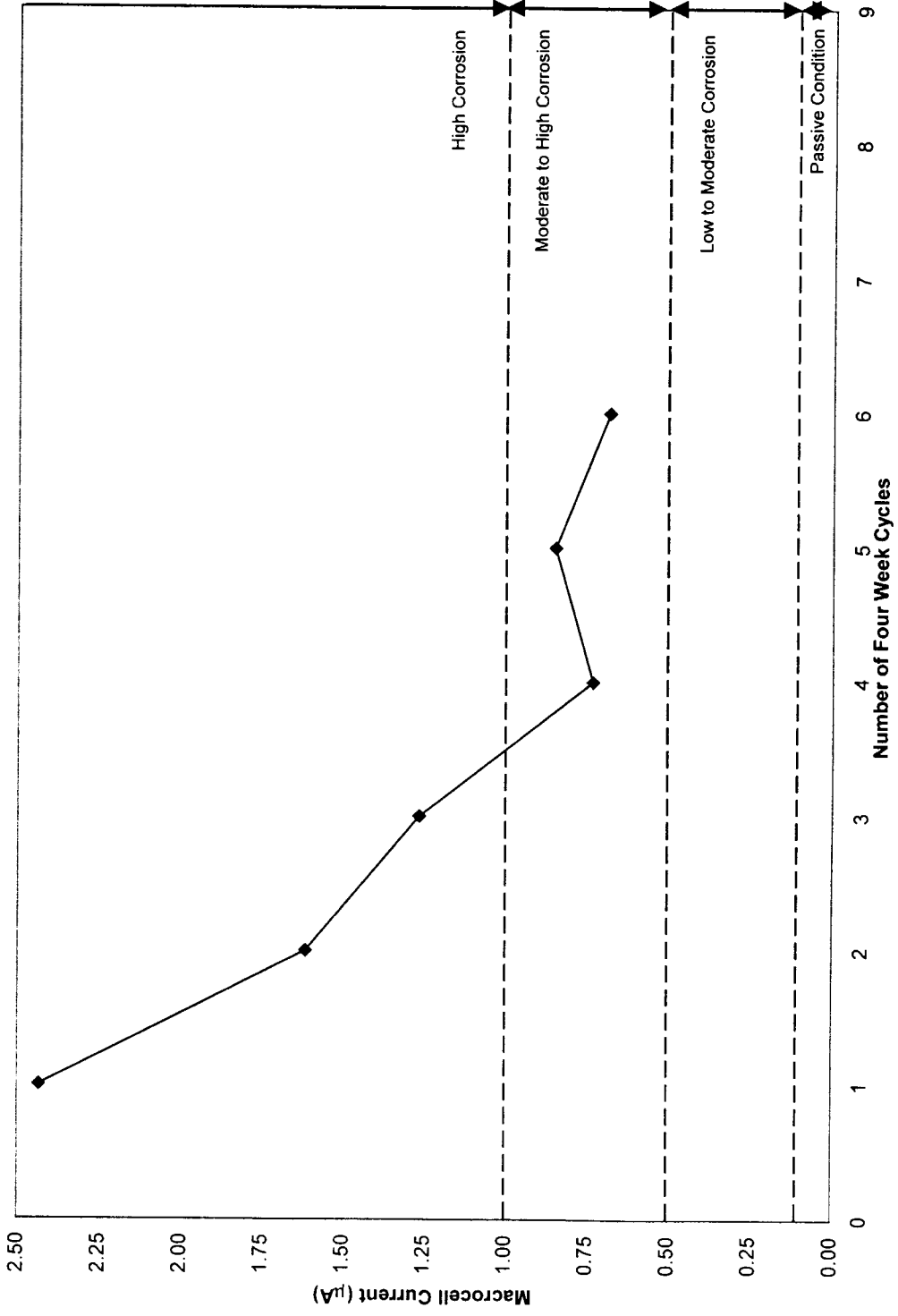


Fig. 4.29: Minideck E - Average Corrosion Rate Macrocell Current (μA)

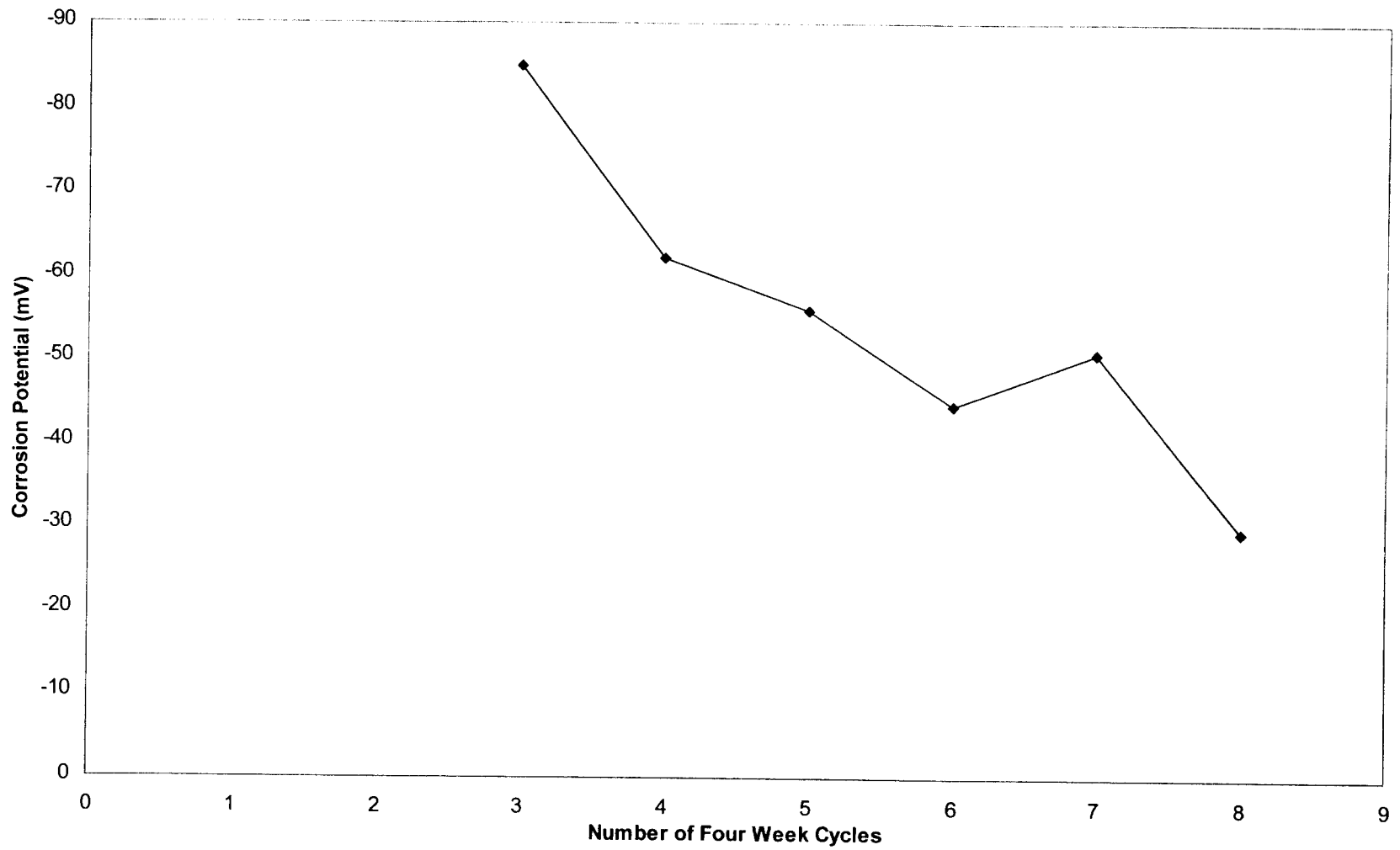


Fig. 4.30: Minideck E - Average Corrosion Potential (mV)

4.5.2 Route 130 Westbound: Field Tests

The data collected for the GECOR 6 Corrosion Rate, Surface Air Flow Permeability, and Electrical Resistance Test for Penetrating Sealers on the bridge deck over Route 130 Westbound are presented in Tables 4.33 to 4.37 and Fig. 4.31 to 4.35. The concrete used in the bridge deck did not contain any corrosion inhibiting admixtures. GECOR 6 corrosion rate, corrosion potential, and electrical resistance are tabulated on Tables 4.33, 4.34, 4.35 and displayed on Fig. 4.31, 4.32, 4.33, respectively. Air permeability readings are presented on Table 4.36 and Fig. 4.34. Electrical resistance readings are presented in Table 4.37 and Fig. 4.35.

Table 4.33: Route 130 Westbound GECOR 6 Corrosion Rate ($\mu\text{A}/\text{cm}^2$)

Connection #	Reading No.	1st Quarter	2nd Quarter	3rd Quarter	4th Quarter
B1	1	0.096	0.276	0.100	0.093
	2	0.185	0.142	0.262	0.050
	3	0.203	0.190	0.129	0.073
	4	0.138	0.109	0.101	0.092
	5	0.132	0.096	0.115	0.103
B2	1	0.235	0.096	0.104	0.077
	2	0.202	0.145	0.054	0.066
	3	0.172	0.169	0.098	0.091
	4	0.174	0.189	0.107	0.414
	5	0.161	0.223	0.130	0.099
B3	1	0.152	0.132	0.258	0.058
	2	0.088	0.223	0.074	0.075
	3	0.210	0.198	0.064	0.078
	4	0.209	0.173	0.080	0.095
	5	0.209	0.261	0.088	0.091
B4	1	0.139	0.267	0.096	0.056
	2	0.222	0.231	0.058	0.075
	3	0.277	0.209	0.073	0.071
	4	0.313	0.317	0.061	0.074
	5	0.271	0.343	0.524	0.073
B5	1	0.266	0.107	0.053	0.055
	2	0.212	0.151	0.087	0.099
	3	0.177	0.119	0.064	0.067
	4	0.220	0.250	0.072	0.079
	5	0.250	0.198	0.788	0.091
Average		0.208	0.200	0.147	0.094

Table 4.34: Route 130 Westbound GECOR 6 Corrosion Potential (mV)

Connection #	Reading No.	1st Quarter	2nd Quarter	3rd Quarter	4th Quarter
B1	1	123.2	26.8	21.5	28.7
	2	86.1	52.5	-23.9	54.0
	3	65.1	107.0	-5.3	-3.2
	4	-6.0	55.4	-13.9	-30.6
	5	-42.4	20.9	-8.2	-22.2
B2	1	76.2	82.8	6.7	15.9
	2	45.1	34.6	52.4	30.7
	3	27.9	34.1	-3.2	-16.0
	4	7.6	53.1	0.4	-66.4
	5	-6.8	57.2	-7.1	-7.7
B3	1	74.1	70.9	-37.5	21.0
	2	1.0	-12.5	33.6	9.6
	3	33.2	70.8	49.1	17.5
	4	33.6	61.7	43.8	10.1
	5	-8.3	45.7	56.1	19.4
B4	1	52.3	16.9	37.1	37.1
	2	18.6	30.4	109.3	31.0
	3	21.8	40.0	53.1	13.5
	4	23.1	76.3	109.2	40.5
	5	13.7	47.7	-8.1	10.6
B5	1	89.3	98.2	68.6	15.7
	2	67.5	78.7	42.1	3.5
	3	23.0	52.8	47.9	11.0
	4	18.7	37.3	46.0	11.3
	5	2.3	22.8	-64.5	18.8
Average		30.695	49.975	31.750	11.355

Table 4.35: Route 130 Westbound GECOR 6 Electrical Resistance (K Ω)

Connection #	Reading No.	1st Quarter	2nd Quarter	3rd Quarter	4th Quarter
B1	1	1.78	1.59	1.41	1.48
	2	1.79	1.80	1.24	1.27
	3	1.51	1.65	1.49	1.33
	4	2.14	2.20	1.54	1.34
	5	2.23	2.15	1.40	1.28
B2	1	1.85	2.07	1.68	1.07
	2	1.50	1.63	1.10	1.11
	3	1.47	1.64	1.01	1.10
	4	1.53	1.69	0.97	0.99
	5	1.71	1.87	1.24	1.22
B3	1	1.81	2.05	1.02	1.19
	2	2.08	1.89	0.97	1.08
	3	1.51	1.48	1.11	1.14
	4	1.37	1.67	1.30	1.32
	5	1.41	1.67	1.33	1.30
B4	1	1.97	1.97	1.37	1.18
	2	1.80	1.75	1.07	1.26
	3	1.70	1.66	1.18	1.42
	4	1.67	1.63	1.28	1.06
	5	1.43	1.56	1.09	1.03
B5	1	2.11	2.52	1.73	1.28
	2	1.73	1.58	1.71	1.24
	3	1.72	2.22	1.28	1.00
	4	1.87	2.39	1.84	1.20
	5	1.76	2.11	0.85	1.22
Average		1.70	1.85	1.26	1.17

Table 4.36: Route 130 Westbound Air Permeability
Vacuum (mm Hg), SCCM (ml/min)

Reading No.	1st Quarter		2nd Quarter		3rd Quarter		4th Quarter	
	Vacuum	SCCM	Vacuum	SCCM	Vacuum	SCCM	Vacuum	SCCM
1	787.10	14.60	793.40	41.32	780.50	22.69	770.00	46.13
2	784.40	30.59	791.90	33.74	780.40	38.76	771.70	50.38
3	784.30	33.99	786.30	36.71	779.40	52.22	773.10	48.80
4	784.00	24.70	754.90	48.30	764.30	57.09	770.00	56.45
5	782.60	52.15	783.20	56.57	779.90	47.57	773.50	46.30
6	780.30	56.52	792.10	46.45	780.80	40.45	774.90	38.78
7	784.50	45.54	787.60	52.38	779.40	52.13	769.90	58.79
8	786.30	37.45	785.00	45.44	776.20	58.48	776.00	43.58
9	786.60	28.42	784.80	54.20	782.50	42.71	774.00	45.66
Average	784.46	36.00	784.36	46.12	778.16	45.79	772.57	48.32

Table 4.37: Route 130 Westbound Electrical Resistance Sealer Test (K Ω)

Quarter	Reading No.	DC End to End (Ω) Strip 1	DC End to End (Ω) Strip 2	DC Side to Side (M Ω)	AC (K Ω)	Avg. AC (K Ω)
1	1	16.3	19.0	7.5	48.0	30.3
	2	11.1	10.1	8.0	11.0	
	3	32.6	17.5	7.0	32.0	
2	1	3.5	11.1	6.0	57.0	88.7
	2	4.9	4.9	11.4	49.0	
	3	7.1	8.9	10.3	160.0	
3	1	2.8	2.5	8.5	51.0	75.7
	2	5.7	4.8	17.5	46.0	
	3	9.2	9.9	12.6	130.0	
4	1	2.3	2.3	23.8	79.0	69.0
	2	8.5	2.5	17.9	30.0	
	3	2.6	6.1	17.6	98.0	

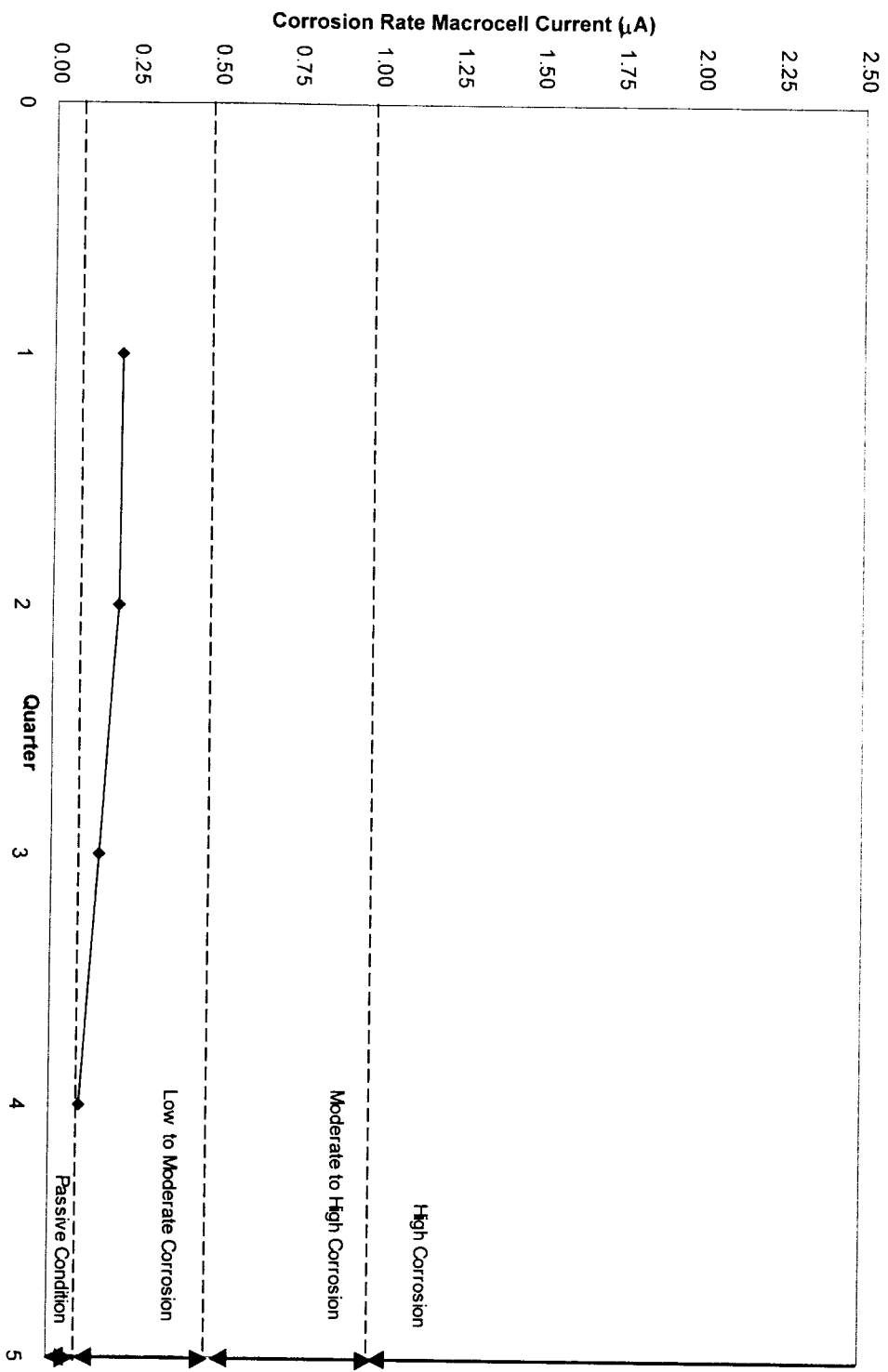


Fig. 4.31 : Route 130 Westbound GECOR 6 Average Corrosion Rate Macrocell Current (μA)

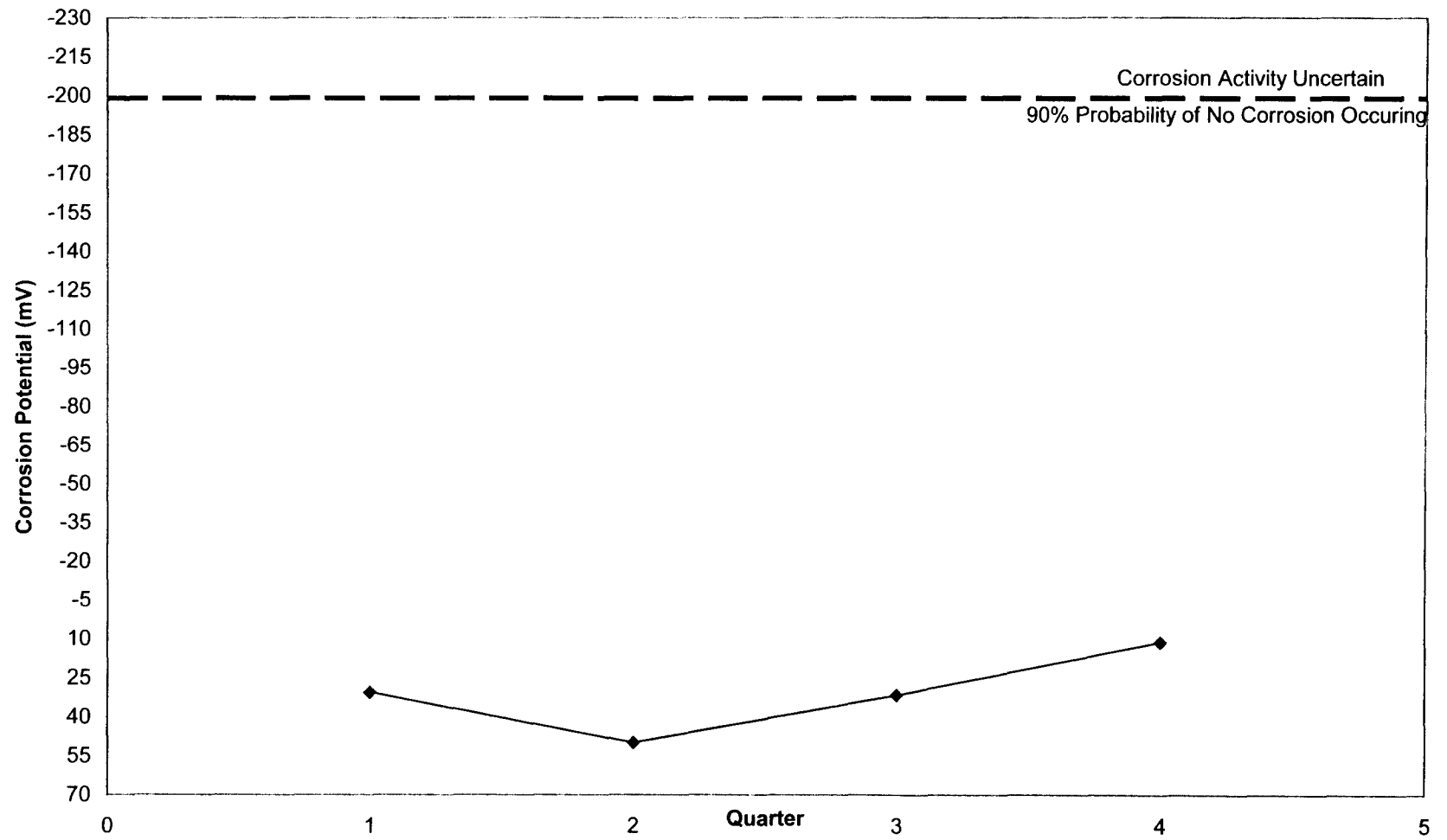


Fig. 4.32: Route 130 Westbound GECOR 6 Average Corrosion Potential (mV)

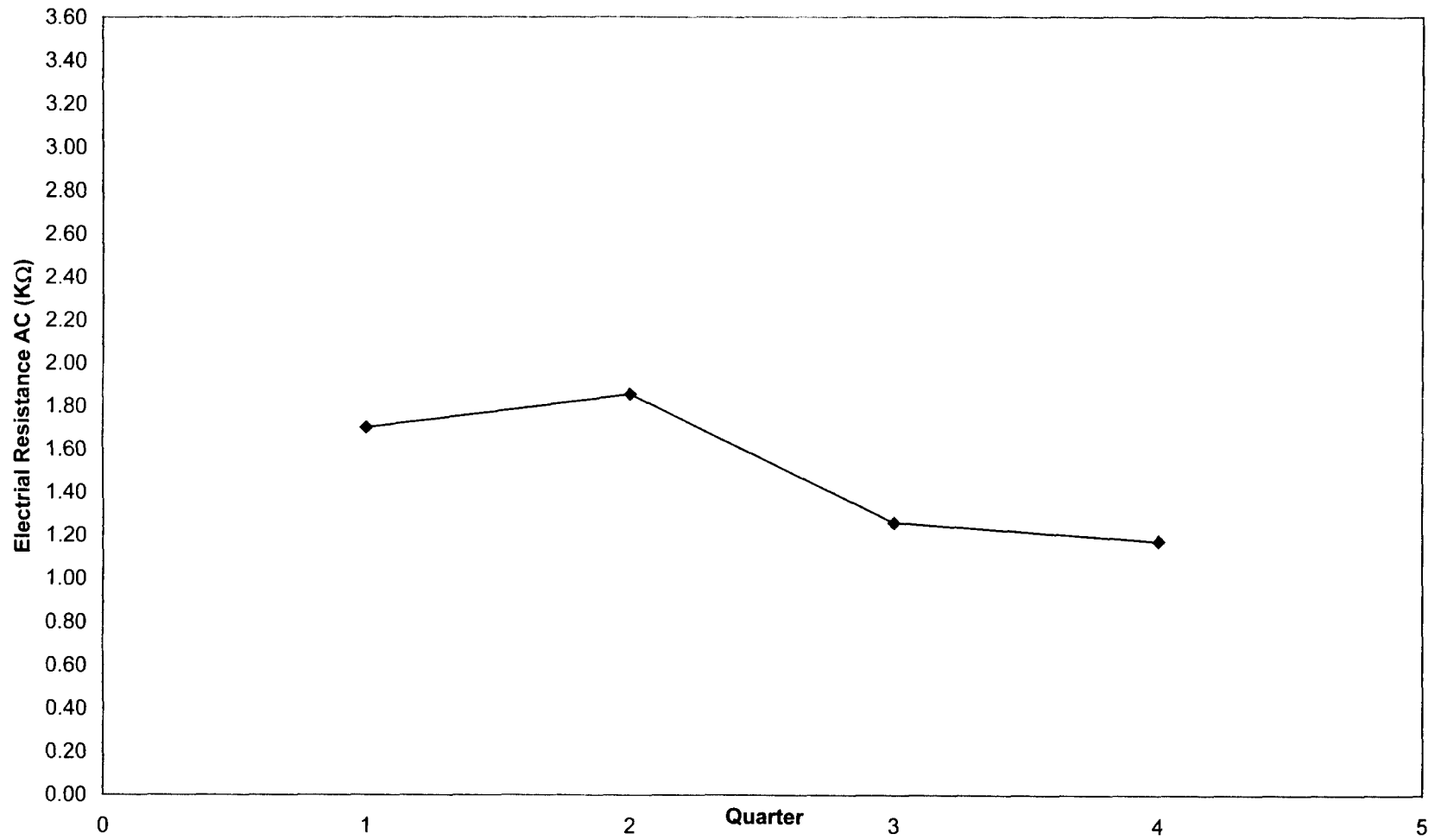


Fig. 4.33: Route 130 Westbound GECOR 6 Average Electrical Resistance AC (KΩ)

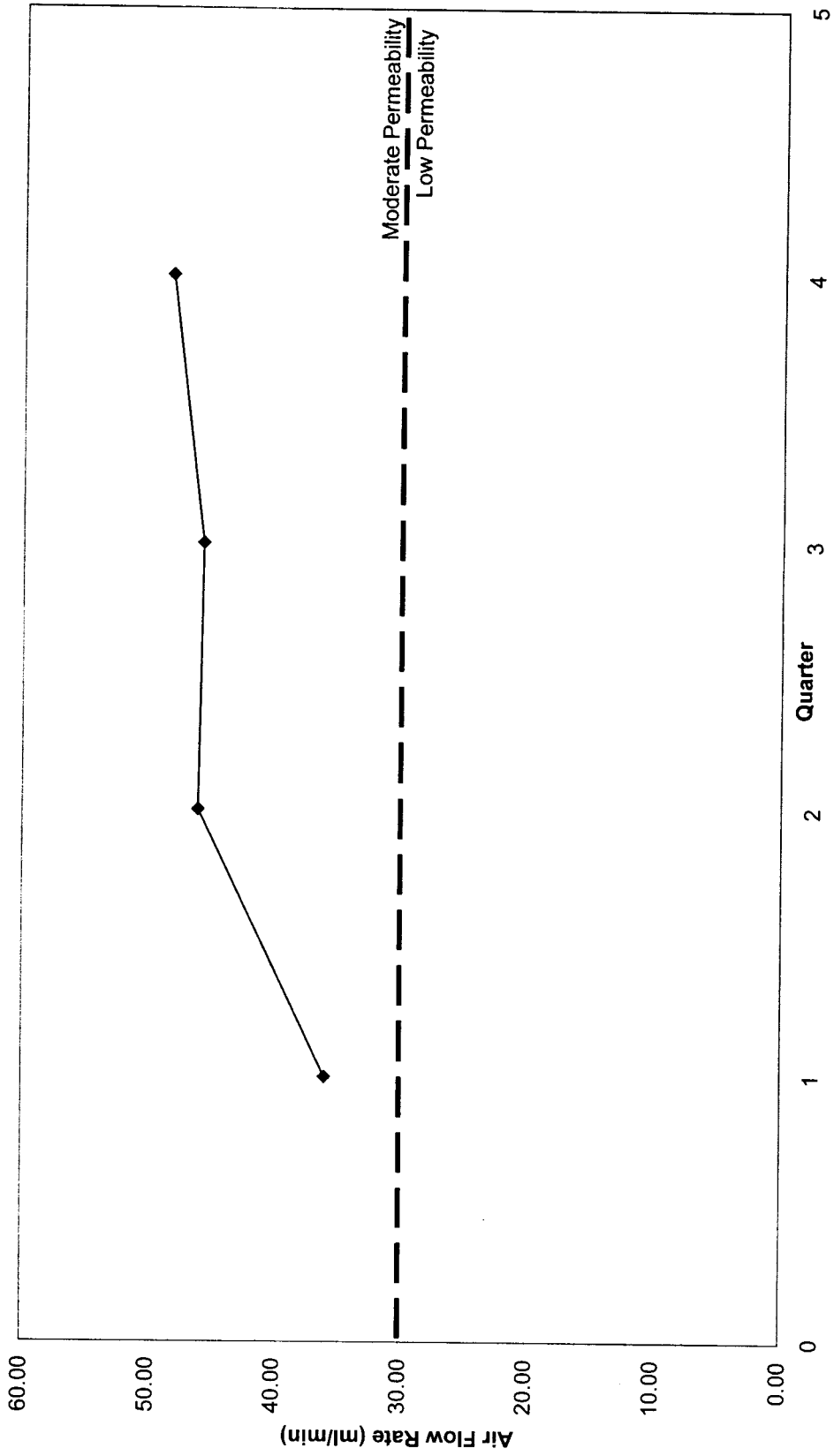


Fig. 4.34: Wyckoff Road Westbound Average Air Flow Rate (ml/min)

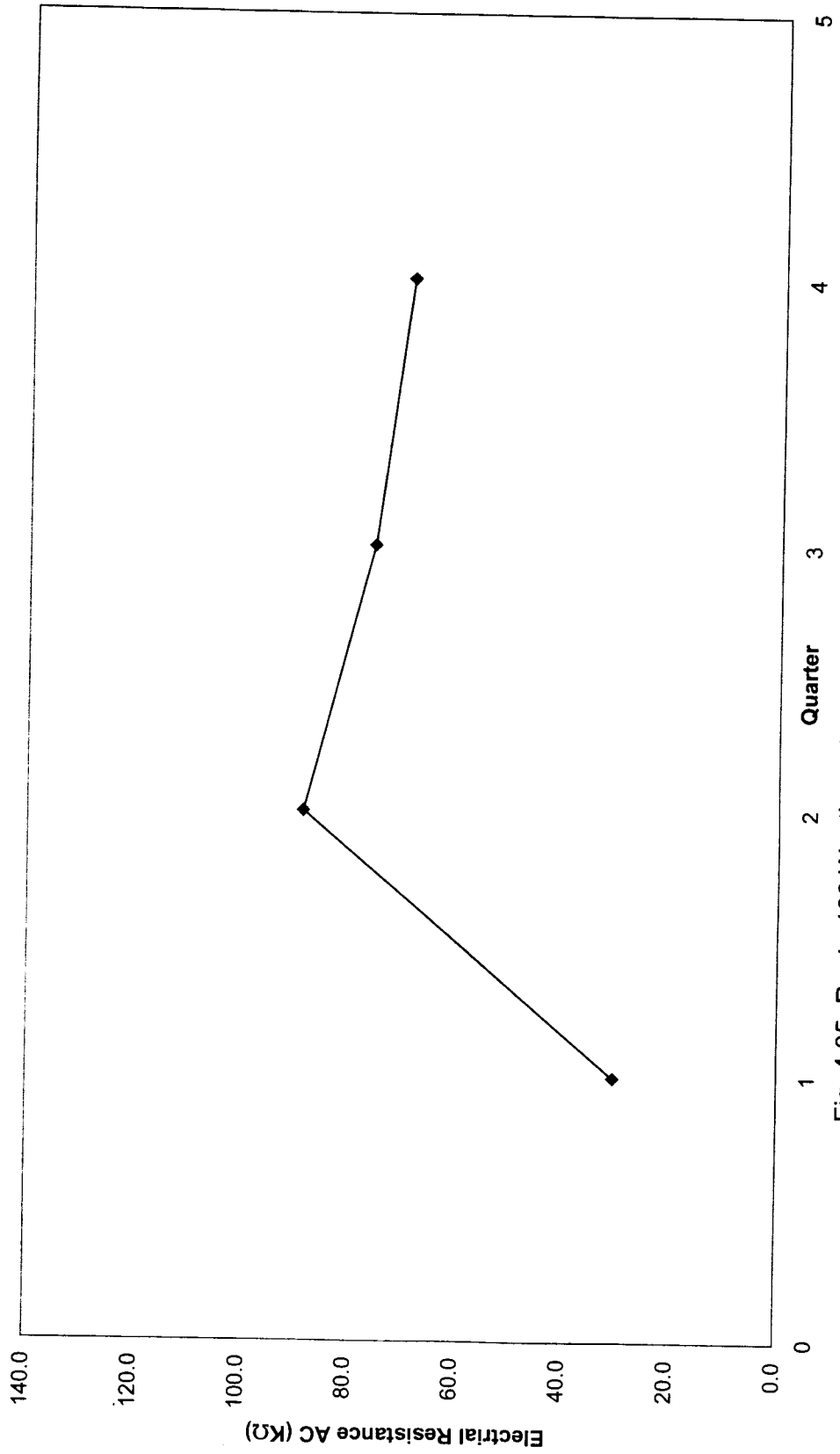


Fig. 4.35: Route 130 Westbound Average Electrical Resistance AC (KΩ)

4.6 Comparison of Corrosion Inhibiting Admixtures

The performance of the individual corrosion inhibiting admixtures are compared in Fig. 4.36 to 4.42. All four of the admixtures including the control are plotted and compared within each test method used in the experimental program. ASTM G 109 Corrosion Rate, ASTM G 109 Corrosion Potential, GECOR 6 Corrosion Rate, GECOR 6 Corrosion Potential, GECOR 6 Electrical Resistance, Surface Air Flow Permeability, and the Electrical Resistance Test for Penetrating Sealers are presented in Fig. 4.36, 4.37, 4.38, 4.39, 4.40, 4.41, and 4.42, respectively.

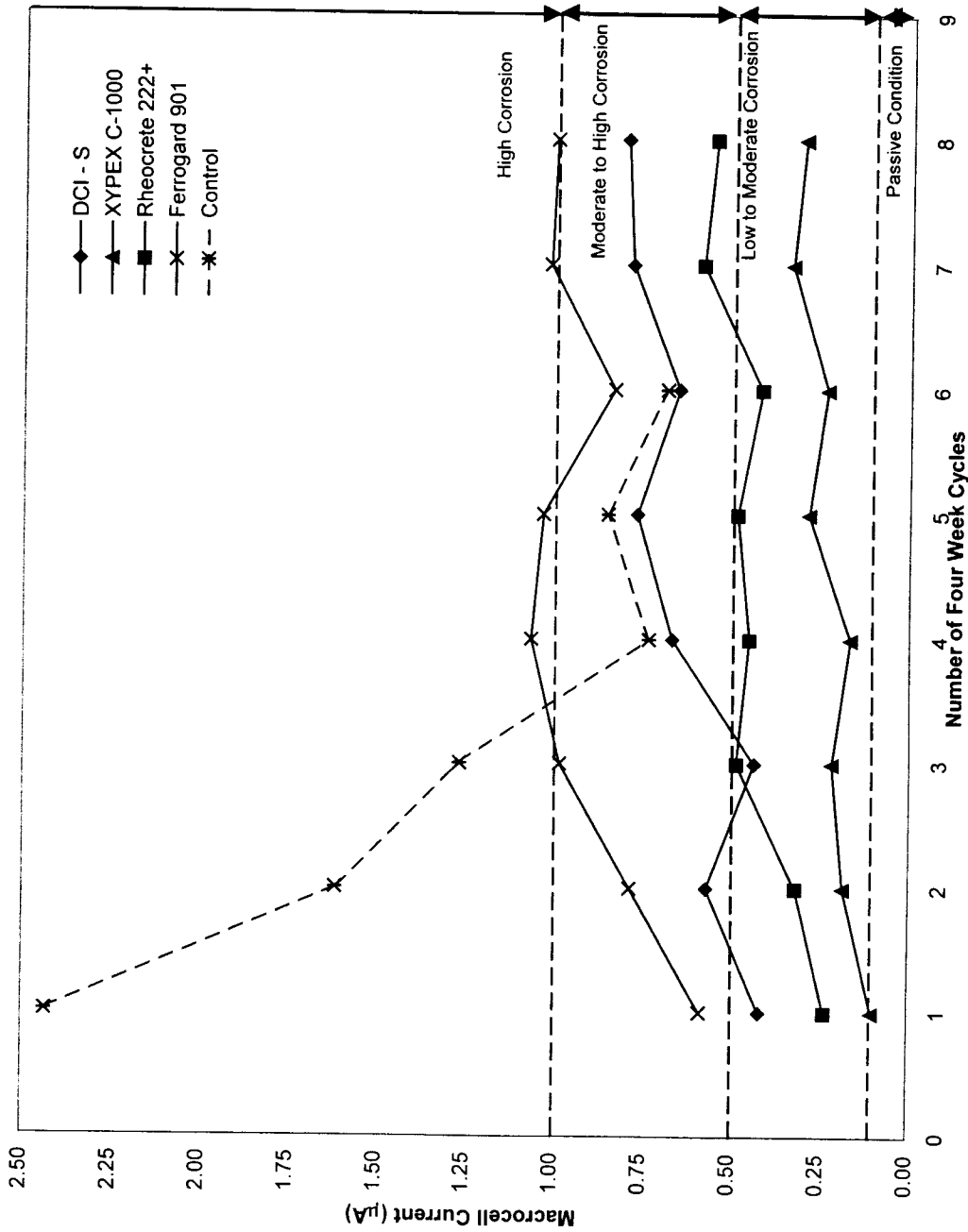


Fig. 4.36: Comparison of Corrosion Inhibitors Minideck Average Corrosion Rate Macrocell Current (µA)

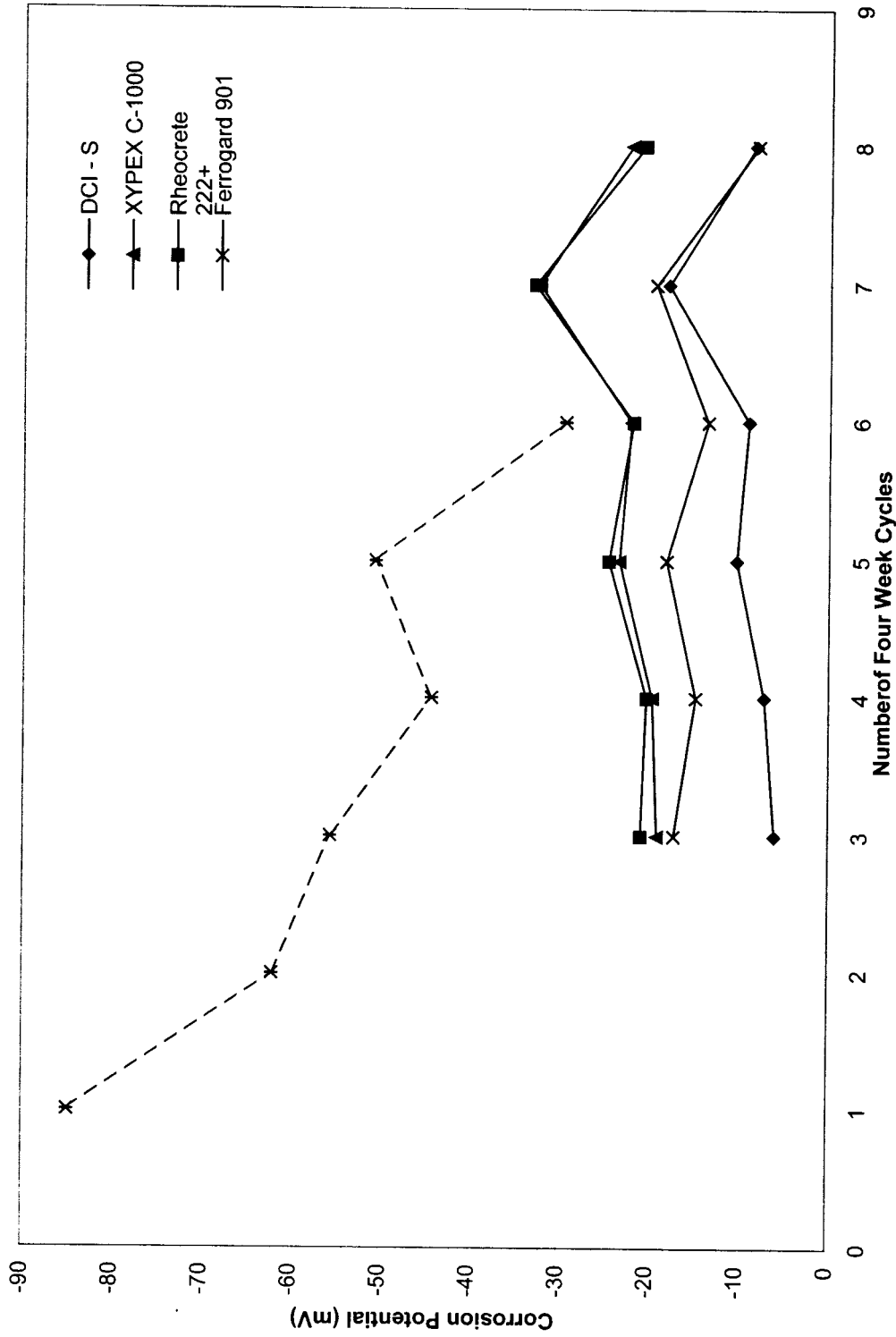


Fig. 4.37: Comparison of Corrosion Inhibitors Minideck Average Corrosion Potential (mV)

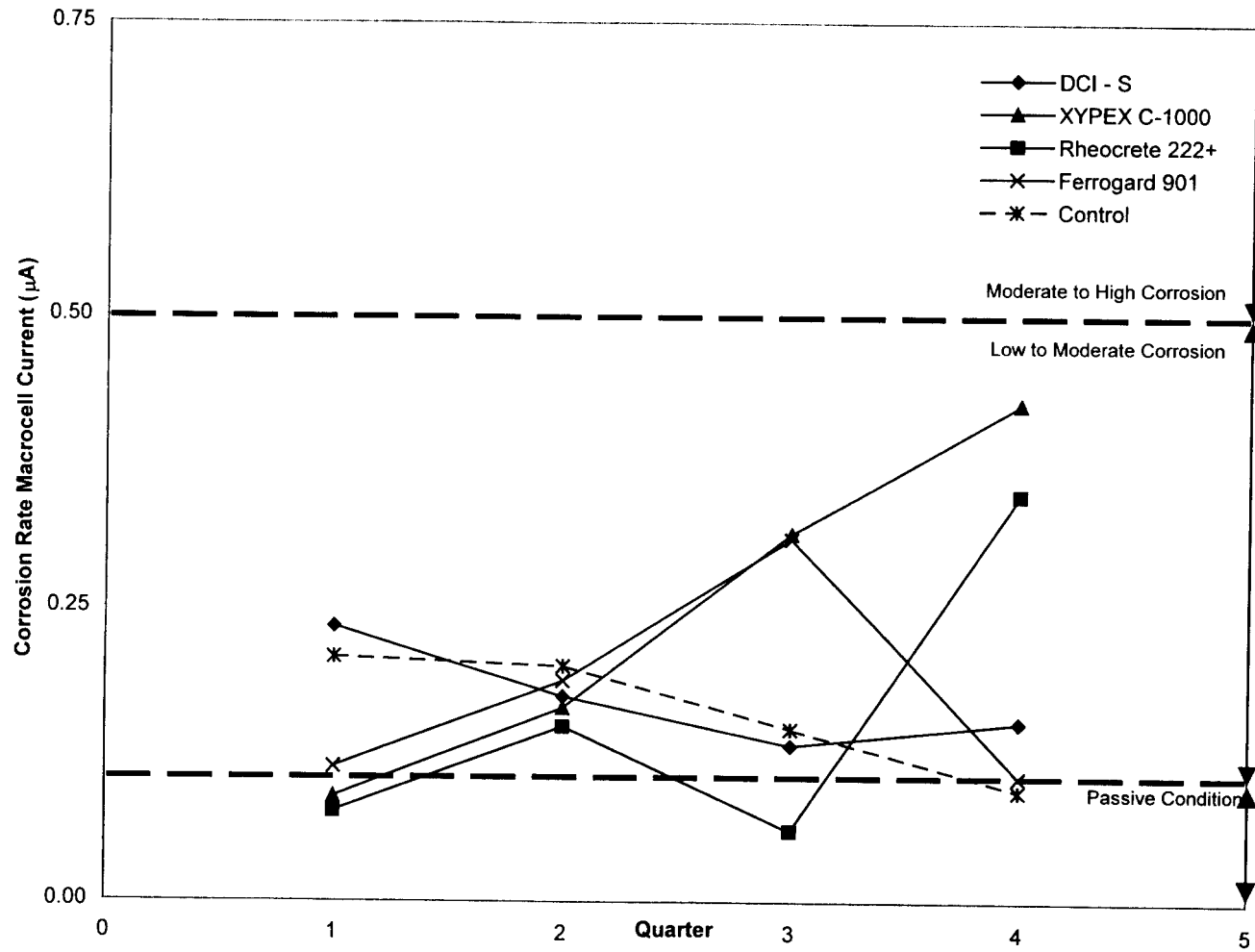


Fig. 4.38: Comparison of Corrosion Inhibitors GECOR 6 Average Corrosion Rate Macrocell Current (μA)

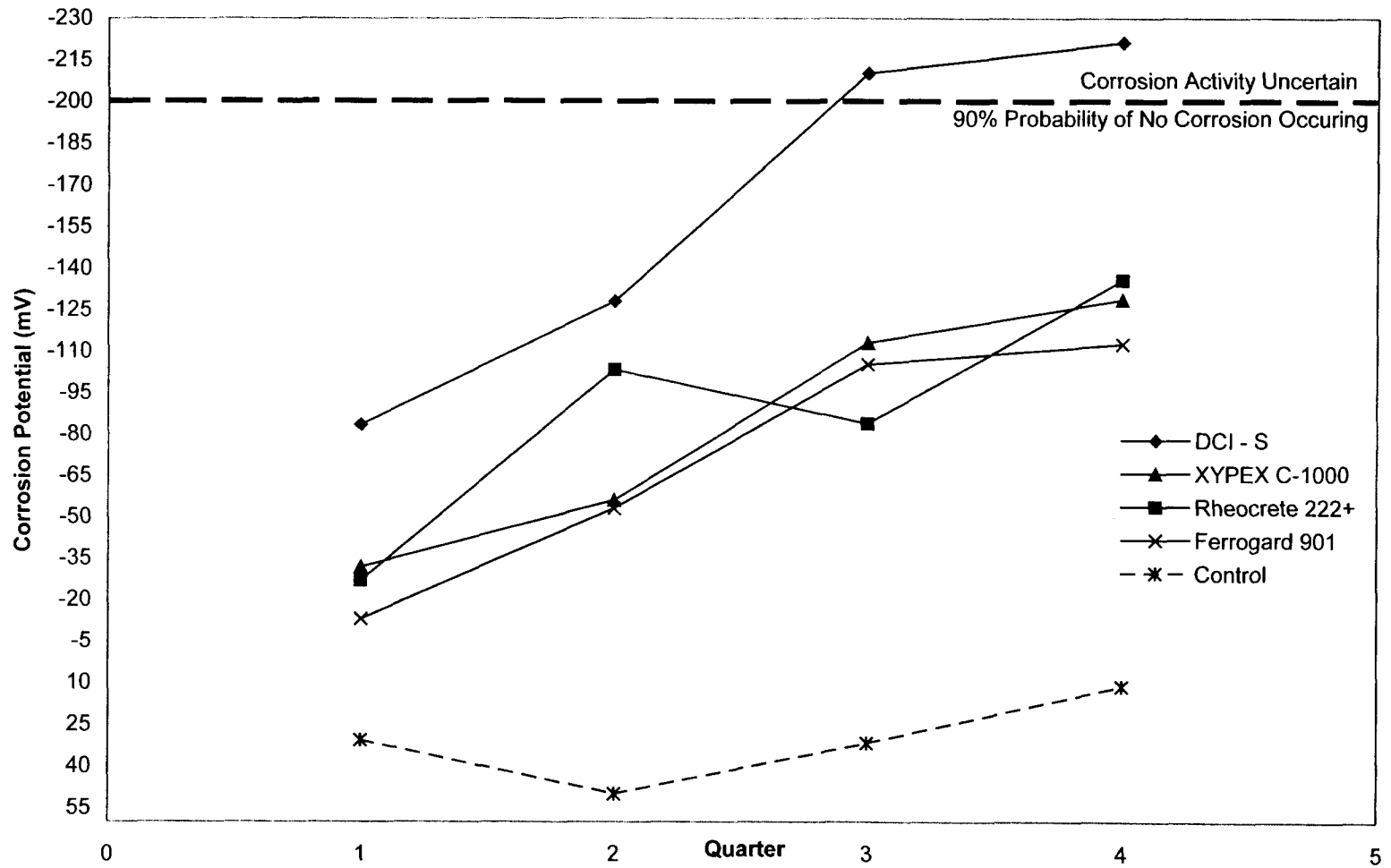


Fig. 4.39: Comparison of Corrosion Inhibitors GECOR 6 Average Corrosion Potential (mV)

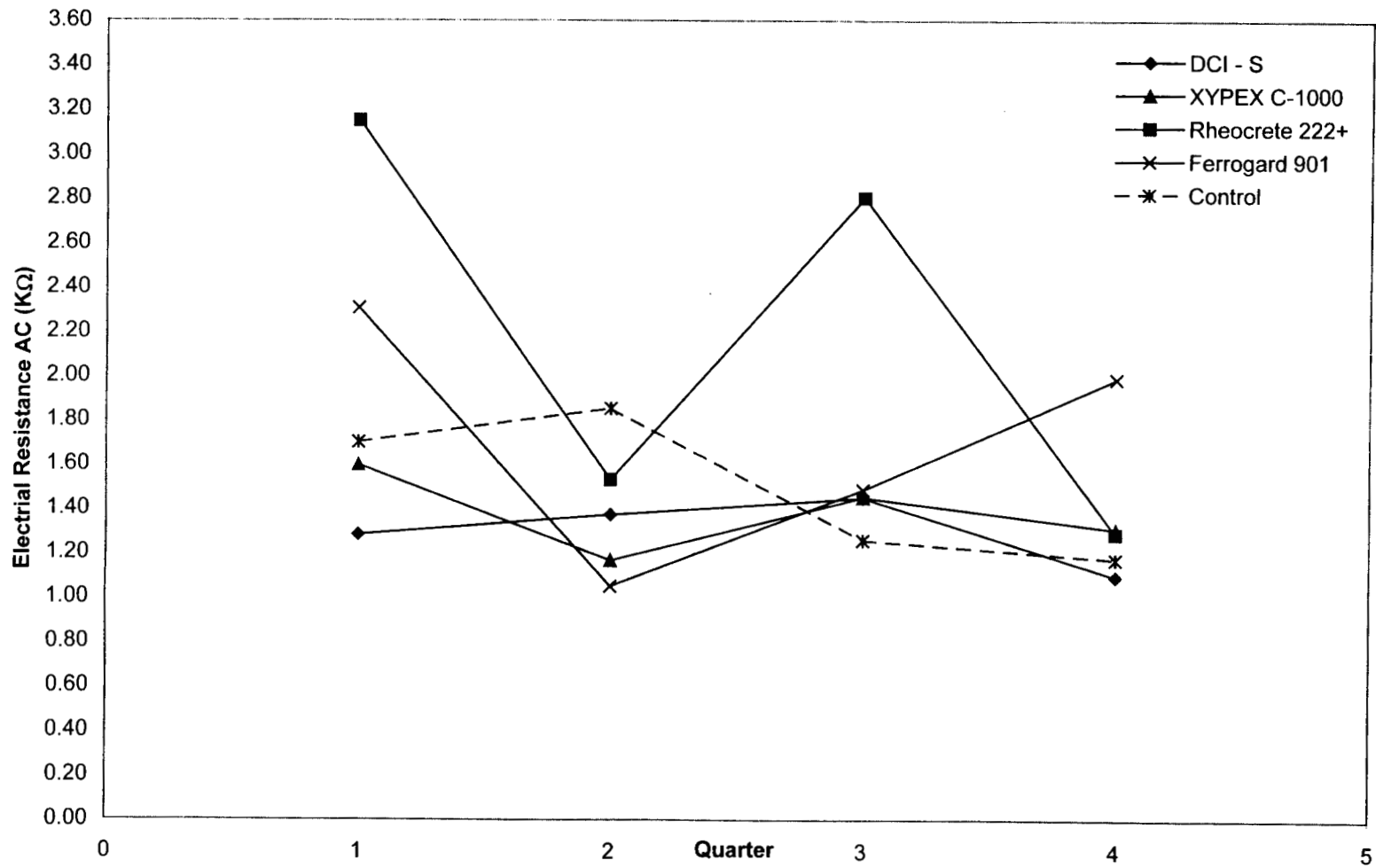


Fig. 4.40: Comparison of Corrosion Inhibitors GECOR 6 Average Electrical Resistance AC (KΩ)

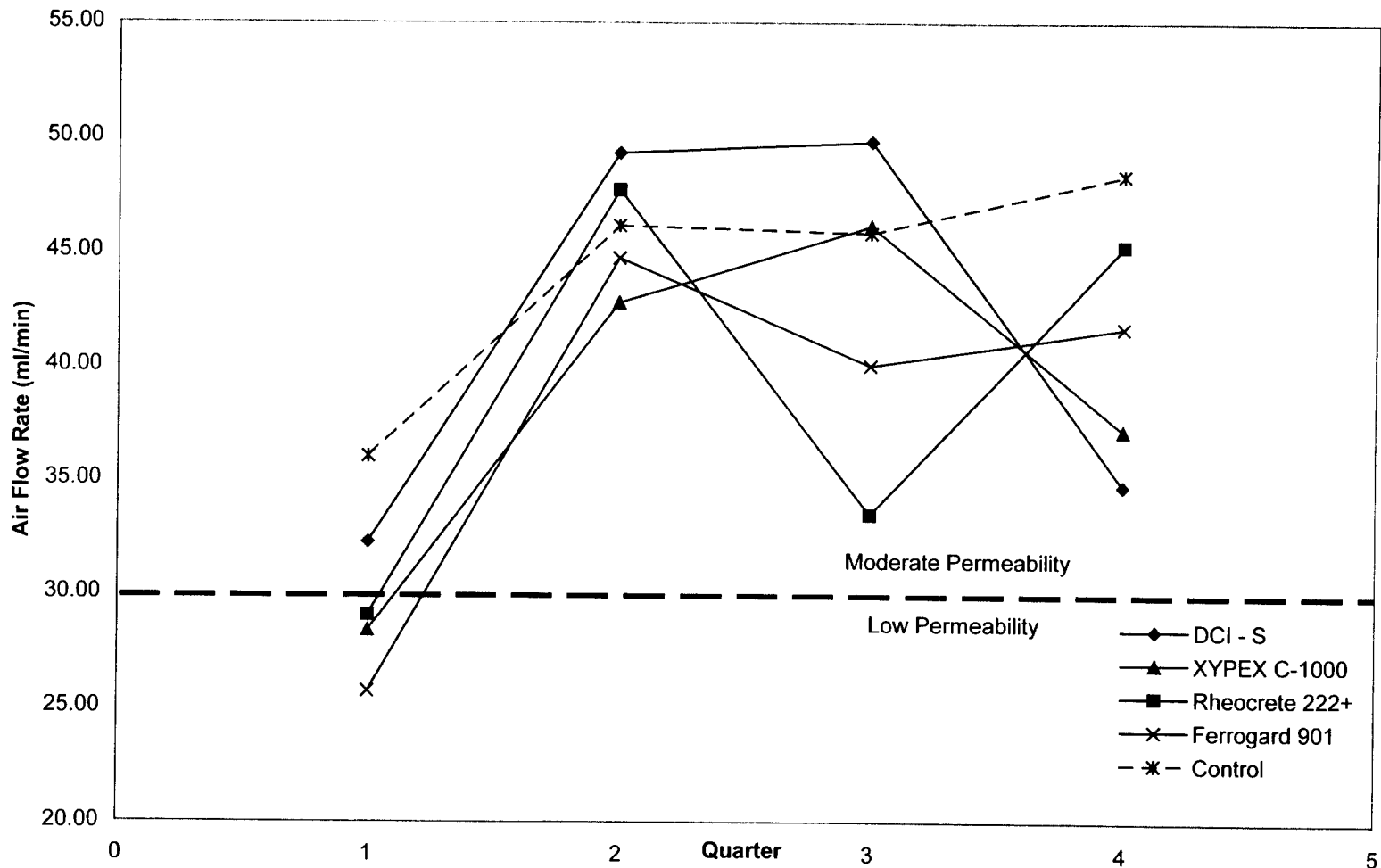


Fig. 4.41: Comparison of Corrosion Inhibitors Average Air Flow Rate (ml/min)

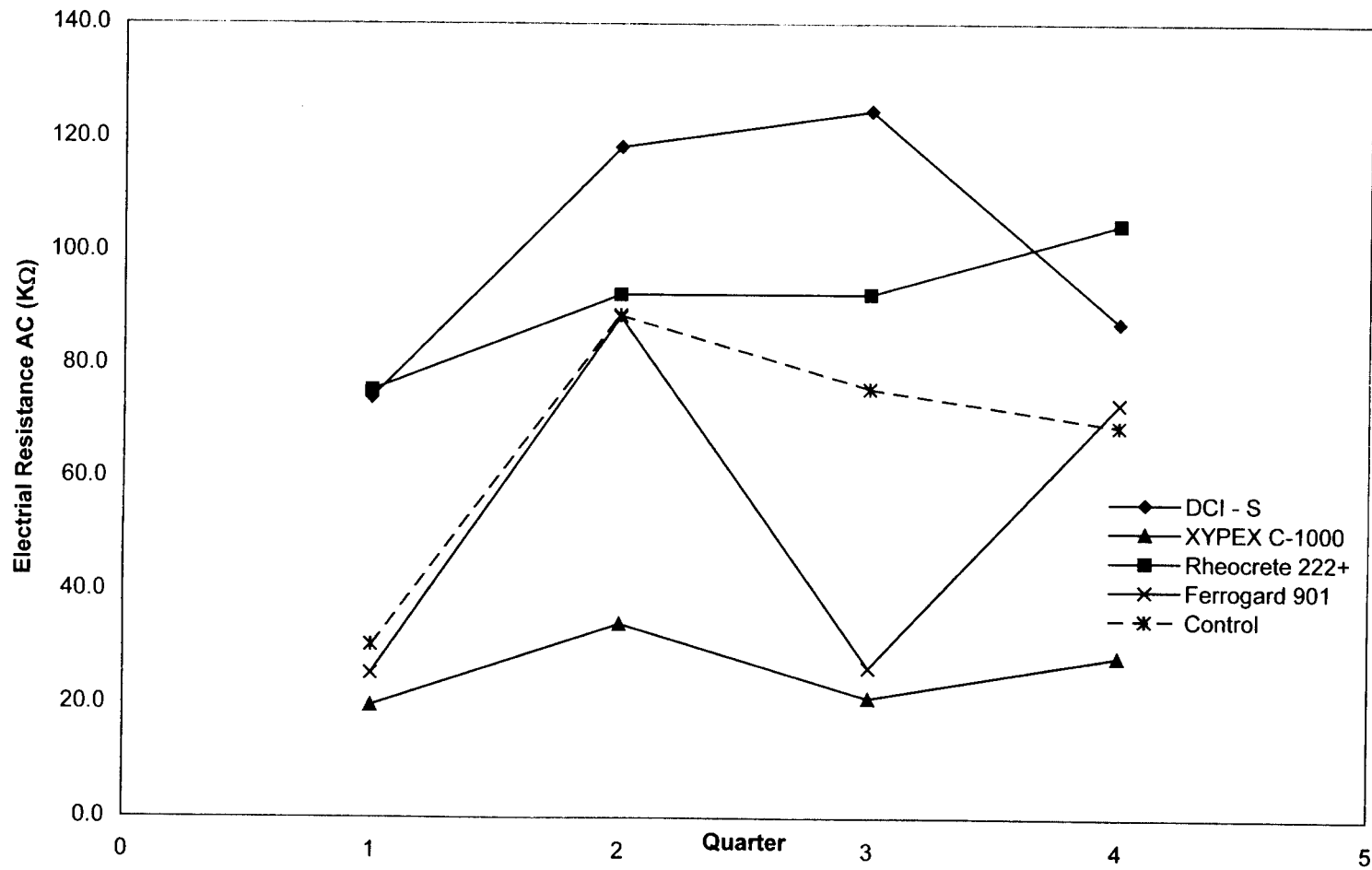


Fig. 4.42: Comparison of Corrosion Inhibitors Average Electrical Resistance AC (KΩ)

Many fluctuations can be seen in the trends contained in many of the previous figures in this chapter. In the laboratory tests, it has been determined that temperature and other ambient conditions significantly effects the readings (Beeby, A.W.). Atmospheric conditions such as humidity and temperature as well as the moisture content of the concrete from precipitation effect the results obtained from the field significantly. These variables found both in the field and laboratory can be neglected due to the fact that at the time of testing all the bridge decks and samples are under the same conditions Therefore for evaluation purposes, the error due to atmospheric and ambient conditions can be ignored.

It should be emphasized that the experiments are continuing. The discussion presented below pertain only to the results obtained thus far.

In Fig. 4.36: Comparison of Corrosion Inhibitors: ASTM G 109 Minideck Average Corrosion Rate Macrocell Current (μA) a steady rise in the macrocell current can be seen. XYPEX C-1000 kept the overall corrosion rate between the low and passive conditions. The other admixtures and the control were tested to have corrosion rates ranging from low to high corrosion. Initial corrosion in the control samples was very high and has stabilized in the moderate to high corrosion zone. Listed from best to worst performance in the Corrosion Rate Laboratory Test are as follows:

1. XYPEX C-1000
2. Rheocrete 222+
3. DCI - S
4. Ferrogard 901
5. Control

In Fig. 4.37: Comparison of Corrosion Inhibitors: ASTM G 109 Minideck Average Corrosion Potential (mV) the corrosion activity for the samples containing

DCI – S remained the lowest. Though nearly equal, XYPEX C-1000 performed slightly better than Rheocrete 222+. The initial corrosion for the control samples were found to be very high but decreased significantly. Listed from best to worst performance in the Corrosion Potential Laboratory Test are as follows:

1. DCI – S
2. Ferrogard 901
3. XYPEX C-1000
4. Rheocrete 222+
5. Control

In the author's opinion the results for the GECOR 6 Corrosion Rate Meter has been proven to be unreliable on the control deck Route 130 Westbound. This maybe due to the fact that the epoxy coated steel was used for the reinforcement of the bridge deck unlike the other bridge decks tested, which utilized uncoated steel reinforcement. Though the uncoated steel bars placed within the regular epoxy reinforcement should have overcome this problem, the meter nevertheless was unable to provide accurate readings. It is possible that the epoxy coating had interfered with the electrical continuity of the reinforcement. This would prevent the device from polarizing the reinforcement, which would lead to inaccurate readings. This discrepancy can be seen in the random results in Table 4.35, and Fig. 4.39 with the location of the control corrosion potential in the positive region. For this reason, the control will be excluded in the discussion of GECOR 6 Corrosion Rate, GECOR 6 Corrosion Potential, and the GECOR 6 Electrical Resistance. This will have no effect on the main purpose of the research program to evaluate the performance of the admixtures and to determine the overall best performer.

In Fig. 4.38: Comparison of Corrosion Inhibitors: GECOR 6 Average Corrosion Rate Macrocell Current (μA) the results fluctuate significantly. Further long term tests

should be performed to obtain an accurate evaluation of the performances of the admixtures. In the authors opinion, it can be inferred that DCI – S is the best performing admixture in this area. The results are steady and range in the low corrosion region. Rheocrete 222+ though initially remained in the low and passive corrosion region increased significantly approaching the moderate to high corrosion region. Listed in best to worst performance in Corrosion Rate Field Test, with the exception of the control as stated previously, are as follows:

1. DCI – S
2. Rheocrete 222+
3. XYPEX C-1000
4. Ferrogard 901

In Fig. 4.39: Comparison of Corrosion Inhibitors: GECOR 6 Average Corrosion Potential (mV) the inaccurate results of the tests on the control bridge deck Route 130 Westbound can easily be determined. The data series is located within the positive region of the chart. Most of the admixtures are tested to be within the range of 90% no corrosion occurring. According to tests, DCI – S has recently increased in corrosion activity. It is now located in the corrosion uncertain region. Listed from best to worst performing in Corrosion Potential Field Test, with the exception of the control as stated previously, are as follows:

1. Ferrogard 901
2. XYPEX C-1000
3. Rheocrete 222+
4. DCI – S

In Fig. 4.40: Comparison of Corrosion Inhibitors: GECOR 6 Average Electrical Resistance AC ($K\Omega$) it can be seen that the electrical resistance of the concrete with Ferrogard 901 is steadily increasing. Therefore it can be concluded that Ferrogard 901

may be more suitable in deterring the electrochemical processes of corrosion than the other admixtures tested. Listed in best to worst performing in GECOR 6 Electrical Resistance Test, with the exception of the control as stated previously, are as follows:

1. Ferrogard 901
2. Rheocrete 222+
3. XYPEX C-1000
4. DCI – S

In Fig. 4.41: Comparison of Corrosion Inhibitors: Average Air Flow Rate (ml/min) it can be seen that the readings fluctuate significantly but remain within the moderate permeability region. The increase in permeability is due to curing of the concrete and evaporation of the pore water. The results have been determined, during field testing, to be effected by the rough texture of the concrete bridge deck and the operator's applied pressure upon the sealing gasket. For this reason, the author suggests that though the results of the Surface Air Flow Field Permeability Indicator can be used for a rough evaluation and comparison of admixtures, it should not be used as an accurate means to determine air permeability. This finding was also stated in Participant's Workbook: FHWA – SHRP Showcase (Scannell, 1996) and in Chapter 3.2.2. Air flow rate for Ferrogard 901 has remained steadily in the moderate region while the admixtures including the control have ranged significantly above. Though Rheocrete 222+ had the lowest air flow rate during the 3rd quarter, the rate has steadily and significantly risen.

Listed in best to worst performance in Air Flow Rate Field Test are as follows:

1. Ferrogard 901
2. XYPEX C-1000
3. Rheocrete 222+
4. Control
5. DCI – S

In Fig. 4.42: Comparison of Corrosion Inhibitors: Average Electrical Resistance AC ($K\Omega$) it can be seen that there are significant differences between the admixtures. Though the surface electrical resistance of Rheocrete 222+ has recently decreased, its overall performance in this area has been significantly better than the other admixtures as well as the control. In the author's opinion, the GECOR 6 Corrosion Rate Meter provides a better electrical resistance reading than the Electrical Resistance Test for Penetrating Sealers. The GECOR 6 Corrosion Rate Meter's instrumentation and procedures are more controlled than that for the Electrical Resistance Test for Penetrating Sealers, which results in better, more reliable data. The interest of steel reinforcement corrosion also lies beyond the surface of the concrete which the GECOR 6 Corrosion Rate Meter can penetrate. Listed from best to worst performance in the Electrical Resistance Test for Penetrating Sealers are as follows:

1. DCI – S
2. Rheocrete 222+
3. Control
4. Ferrogard 901
5. XYPEX C-1000

Table 4.38: Ranked Results of Evaluation (Best – Worst)

	1st(5pts)	2nd(4pts)	3rd(3pts)	4th(2pts)	5th(1pt)
ASTM G 109 Corrosion Rate	XYPEX C-1000	Rheocrete 222+	DCI – S	Ferrogard 901	Control
ASTM G 109 Corrosion Potential	DCI – S	Ferrogard 901	XYPEX C-1000	Rheocrete 222+	Control
GECOR 6 Corrosion Rate	DCI – S	Rheocrete 222+	XYPEX C-1000	Ferrogard 901	N/A
GECOR 6 Corrosion Potential	Ferrogard 901	XYPEX C-1000	Rheocrete 222+	DCI – S	N/A
GECOR 6 Electrical Resistance	Ferrogard 901	Rheocrete 222+	XYPEX C-1000	DCI – S	N/A
Surface Air Flow Field Permeability Indicator	Ferrogard 901	XYPEX C-1000	Rheocrete 222+	Control	DCI – S
Electrical Resistance Test for Penetrating Sealers	DCI – S	Rheocrete 222+	Control	Ferrogard 901	XYPEX C-1000

Table 4.39: Points Evaluation of Corrosion Inhibiting Admixtures

	DCI – S	XYPEX C-1000	Rheocrete 222+	Ferrogard 901	Control
ASTM G 109 Corrosion Rate	3	5	4	2	1
ASTM G 109 Corrosion Potential	5	3	2	4	1
GECOR 6 Corrosion Rate	5	3	4	2	N/A
GECOR 6 Corrosion Potential	2	4	3	5	N/A
GECOR 6 Electrical Resistance	2	3	4	5	N/A
Surface Air Flow Field Permeability Indicator	1	4	3	5	2
Electrical Resistance Test for Penetrating Sealers	5	1	4	2	3
	23	23	24	25	N/A

Table 4.38 lists all the tests conducted during the course of the research program with admixtures ranked from best to worst for each test. From Table 4.39 it can be seen from the arbitrary point system of evaluation that Ferrogard 901 is the best performer though the differences in overall performance of the admixtures are not significant. In order to choose a corrosion inhibiting admixture, its purpose must be taken into consideration. Each has its benefits in certain areas of controlling corrosion though no individual is superior in all respects.

Continuation of the experiments is needed in this experimental program to fully evaluate the performance of the admixtures. As of the completion of this thesis, the construction for the new Route 133 Hightstown Bypass has not been finished. The bridge decks tested have not experienced heavy vehicular traffic during normal operation nor has road deicing salt been used during the course of this evaluation. Though the laboratory tests accelerate the corrosion process, more cycles are needed to corrode the imbedded reinforcing steel to an amount significant for measurement. The reinforcing steel losses have not been assessed. More data is needed to evaluate the long term performance of the admixtures.

5. Conclusions

Based on the experimental results and observations made during the fabrication and testing, the following conclusions can be drawn.

- There are no significant differences in the plastic and hardened concrete properties for the four admixtures evaluated.
- In the author's opinion, the results for the GECOR 6 Corrosion Rate Meter has been proven to be unreliable on the control deck Route 130 Westbound due to the epoxy coated reinforcement used for its construction.
- The author suggests that though the results of the Surface Air Flow Field Permeability Indicator can be used for a rough evaluation and comparison of admixtures, it should not be used as an accurate means to determine air permeability.
- In the author's opinion, the GECOR 6 Corrosion Rate Meter provides better electrical resistance reading than the Electrical Resistance Test for Penetrating Sealers.
- The best overall performing corrosion inhibiting admixture within the research program according to the points evaluation system is Sika Corporation: Ferrogard 901
- The best performing corrosion inhibiting admixture in the ASTM G 109 Corrosion Rate Test is the Quick Wright Associates, Inc.: XYPEX C-1000
- The best performing corrosion inhibiting admixture in the ASTM G 109 Corrosion Potential Test is the W.R. Grace: DCI – S
- The best performing corrosion inhibiting admixture in the GECOR 6 Corrosion Rate Test is the W.R. Grace: DCI – S
- The best performing corrosion inhibiting admixture in the GECOR 6 Corrosion Potential Test is the Sika Corporation: Ferrogard 901
- The best performing corrosion inhibiting admixture in the GECOR 6 Electrical Resistance Test is the Sika Corporation: Ferrogard 901
- The best performing corrosion inhibiting admixture in the Surface Air Flow Field Permeability Test is the Sika Corporation: Ferrogard 901
- The best performing corrosion inhibiting admixture in the Electrical Resistance Test for Penetrating Sealers in the W.R. Grace: DCI – S
- Continuation of the study is needed in this experimental program to fully evaluate the long term performance of the admixtures.

6. Appendix

Table 6.1: Interpretation of Corrosion Rate Data (Scannell, 1997)

I_{CORR} ($\mu A/cm^2$)	Corrosion Condition
Less than 0.1	Passive Condition
0.1 to 0.5	Low to Moderate Corrosion
0.5 to 1.0	Moderate to High Corrosion
Greater than 1.0	High Corrosion

Table 6.2: Interpretation of Half Cell (Corrosion) Potential Readings (ASTM C 876)

Half Cell Potential (mV)	Corrosion Activity
-200 >	90% Probability of No Corrosion Occurring
-200 to -350	Corrosion Activity Uncertain
< 350	90% Probability of Corrosion Occurring

Table 6.3: Relative Concrete Permeability by Surface Air Flow (Manual for the Operation of a Surface Air Flow Field Permeability Indicator, 1994).

Air Flow Rate (ml/minute)	Relative Permeability Indicated
0 to 30	Low
30 to 80	Moderate
80 >	High

7. References

1. ACI 222R-1996 Corrosion of Metals in Concrete, ACI Committee 222 American Concrete Institute 1997
2. ASTM G 109, Annual Book of ASTM Standards
3. ASTM C 876, Annual Book of ASTM Standards
4. ASTM C 94, Annual Book of ASTM Standards
5. ASTM C 150, Annual Book of ASTM Standards
6. Beeby, A.W., Development of a Corrosion Cell for the Study of the Influences of the environment and the Concrete Properties on Corrosion, Cement and Concrete Association, Slough, U.K.
7. Bentur, A., Diamond, S., Burke, N.S., Modern Concrete Technology Steel Corrosion in Concrete; Fundamentals and Civil Engineering Practice, E & FN Spoon, London, UK 1992
8. Berke, N.S., Hicks, M.C., Hoopes, R.J., Concrete Bridges in Aggressive Environments, "SP-151-3 Condition Assessment of Field Structures with Calcium Nitrate", American Concrete Institute 1995
9. Berke, N.S., Roberts, L.R. Concrete Bridges in Aggressive Environments, "SP 119-20 Use of Concrete Admixtures to Provide Long-Term Durability from Steel Corrosion", American Concrete Institute 1995
10. Berke, N.S., Weil, T.G., Advances in Concrete Technology, "World-Wide Review of Corrosion Inhibitors in Concrete" Published by CANMET, Canada 1997
11. Broomfield, John P., Corrosion of Steel in Concrete: Understanding Investigation and Repair, E & FN Spoon, London, UK 1997
12. DCI – S Corrosion Inhibitor, W.R. Grace and Co. 1997 <http://www.gcp-grace.com/products/concrete/summaries/dcis.html> and http://www.gcp-grace/pressroom/adva_nz.html
13. MacDonald, M., Sika Ferrogard 901 and 903 Corrosion Inhibitors: Evaluation of test Program, Special Services Division, Sika Corporation 1996
14. Manual for the Operation of a Surface Air Flow Field Permeability Indicator, Texas Research Institute Austin, Inc., Austin Texas, June 1994

15. Page, C.L., Treadway, K.W.J., Bamforth, P.B., Corrosion of Reinforcement in Concrete Society of the Chemical Industry, Symposium held at Warwickshire, UK 1990
16. Rheocrete 222+: Organic Corrosion Inhibiting Admixture, Master Builders, Inc. Printed in U.S.A 1995
17. Scannell, William T. Participant's Workbook: FHWA – SHRP Showcase, U.S. Department of Transportation, Conncorr Inc., Ashburn Virginia, July, 1996
18. Sennour, M.L., Wheat, H.G., Carrasquillo, R.L., The Effects of Chemical and Mineral Admixtures on the Corrosion of Steel in Concrete, University of Texas, Austin, Texas 1994
19. XYPEX Concrete Waterproofing by Crystallization, Quick-Wright Associates, Inc. <http://www.qwa.com/concrete.html>